

---

# LETTER FROM THE EDITOR

---

This is my 13th issue as Editor of *Mathematics Magazine*. That means I am officially halfway through my term of service, and I can think of no better way of marking the occasion than with the bumper crop of mathematical magnificence in this month's issue.

Sergei Koshkin and Isaiah Meyers get us started with a fascinating survey of oscillatory behavior in biology. They open with the classic Lotka–Volterra equations for modelling predator–prey interactions. In the model, the long-term population size of both predator and prey oscillates in a manner reminiscent of simple harmonic motion in physics. From this starting point, Koshkin and Meyers take us on a tour of virus dynamics, epidemiology, and plant dynamics, noting that each can be modeled via a “damped” version of the Lotka–Volterra model. Along the way, they introduce readers to several modern tools of mathematical modeling, especially the use of Lyapunov functions.

From there we move on to differential geometry. Kyle Celano, Vincent Coll, and Jeff Dodd investigate the geodesics on a torus. In their pithy definition, geodesics are curves that curve only because they must, meaning that they curve because the surface on which they reside is itself curved. Working out the geodesics on a given surface is a perennial problem in differential geometry. It is also frequently a very difficult problem, even for seemingly simple surfaces. As a result, this beautiful material is often found only in graduate-level textbooks and journal articles, where it is inaccessible to beginning students. Celano, Coll, and Dodd rectify that situation with a wonderfully readable presentation of this important topic.

The next two articles are for those who prefer discrete mathematics. Scott Andrew Herman investigates the game of Red-Blue Cherries, which has received considerable attention in the combinatorial game theory community. The game is played on a 2-colored graph, and involves players alternating turns by removing vertices of one or the other color. Herman greatly advances the theory of this game by constructing novel starting positions exhibiting various sorts of combinatorial behavior. Along the way he presents a very lucid introduction to this fascinating branch of mathematics.

Red-Blue Cherries might have been new to you, but I'm sure you're familiar with Yahtzee. Kathryn Kelly and Jeffrey Liese investigate optimal play in the game's solitaire version. Their novel approach makes it possible to compute precise probabilities and expectations of the optimal player's score, and this is an improvement over previous work, which involved numerical approximations.

It's back to physics for our final article. The catenary curve, formed by a chain mounted at its ends under its own weight, is a standard topic for a calculus class. It is well known that the curve is modeled by the hyperbolic cosine function. Subhranil De investigates the double catenary, which is formed by a circular chain mounted at two points under its own weight. The resulting analysis is a satisfying combination of multivariable calculus and physics.

As always, we close out the issue with Proofs Without Words, Problems, and Reviews.

Jason Rosenhouse, Editor

---

# ARTICLES

---

## Harmonic Oscillators of Mathematical Biology: Many Faces of a Predator-Prey Model

SERGIY KOSHKIN

University of Houston-Downtown

Houston, TX 77002

[koshkins@uhd.edu](mailto:koshkins@uhd.edu)

ISAIAH MEYERS

University of Texas at Austin

Austin, TX 78713

[isaiah.meyers@utexas.edu](mailto:isaiah.meyers@utexas.edu)

In the early 1920s, Lotka studied a system of two nonlinear differential equations for oscillating concentrations in a chemical reaction [12]. In 1926, Volterra used the same system to explain the rise in predatory fish populations in the Adriatic sea during World War I [16]. The Lotka-Volterra predator-prey model, as it came to be known, became a paradigmatic example of oscillatory behavior in biology, just as the harmonic oscillator is in physics. In 1927, Kermack and McKendrick applied a special case of it, now called the SIR model, to the spread of infection during epidemics [11]. Here the “predators” were infectious individuals, and those susceptible to the infection were the “prey.” Already in 1929, Soper needed a variation of it, with the inclusion of the natural birth rates of the susceptible population, to model measles epidemics in London [13]. Further variations and extensions of the Lotka-Volterra model are found in many other biological situations and are generically called predator-prey models [1, 3, 5, 8, 9].

We will study one model of this class that is especially closely related to the original. We call it the “*damped*” predator-prey model:

$$\begin{cases} \frac{dx}{dt} = \delta - \alpha x - \beta xy \\ \frac{dy}{dt} = \gamma xy - \sigma y. \end{cases} \quad (1)$$

When  $\beta = \gamma$  and  $\delta = 0$ , this is the classical Lotka-Volterra model, and when also  $\alpha = 0$ , it becomes the SIR model. In Soper’s model,  $\alpha = 0$ , but  $\delta > 0$ . Although system (1) has been extensively studied, its connection to the Lotka-Volterra model seems to have escaped attention. We will be able to characterize its behavior in detail by exploiting just this connection. The system, and its extensions, exhibit interesting dynamics that will allow us to introduce and use advanced modeling concepts and tools, such as phase portraits, invariant sets, first integrals, separatrices, trapping regions, omega-limit sets, domains of attraction, and bifurcations. But the main tool, exploited throughout the paper, will be Lyapunov functions that allow us to prove the global stability of solutions to the system, and even to obtain some estimates on them. Lyapunov functions are generalizations of energy functions in physics. We will show that for positive parameters system (1) behaves somewhat like a *damped* harmonic oscillator, an oscillator whose amplitudes decrease due to loss of energy. After a general analysis of the system and its study by means of Lyapunov functions, we will look

closely at some of its many applications. First, we will relate it to the classical Lotka-Volterra model and trace its bifurcation from damped oscillations to predator extinction. Then we will look at a basic model of virus dynamics [3], where the “predators” are virus-producing cells, and the “prey” are cells susceptible to the infection, and its modification that led to considering  $\beta \neq \gamma$ . Finally, in a more unexpected incarnation reminiscent of Lotka’s, we derive (1) from a simple model of plant growth dynamics, where  $x$  and  $y$  are concentrations of a nutrient and a growth hormone, respectively. The model itself is an interesting 3-dimensional extension of (1).

We feel that the “damped” predator-prey model makes for an excellent guided exploration project in a mathematical modeling or differential equations course. Its analysis helps introduce many techniques that are not typically seen in standard examples, and it can be easily modified to model more complicated behavior where these techniques are indispensable. Some variations, including models with limit cycles [8], 3-dimensional extensions of the virus dynamics model [3], and plant growth models that make different simplifying assumptions about water transport [2], can be used as a basis for student research projects.

## Equilibria and invariant regions

The first step when dealing with a system of differential equations like (1) is to find its equilibria, which are solutions that do not change with time. This means  $dx/dt = dy/dt = 0$ . We find two of them:  $(\delta/\alpha, 0)$  and  $(\sigma/\gamma, a/\beta)$ , where  $a := (\gamma\delta/\sigma) - \alpha$ . In addition to assuming that all parameters of the system are positive, we shall also assume for now that  $\gamma\delta > \sigma\alpha$ . This makes  $a > 0$ , and both equilibria are in the first quadrant. To get an idea of the overall behavior of the trajectories, i.e., of the *flow*, it is instructive to plot the right-hand side of (1) as vectors attached to points in the  $x$ - $y$  plane, the *vector field* of the system, as shown on top in Figure 1. Trajectories must be tangent to the slope field vectors at every point.

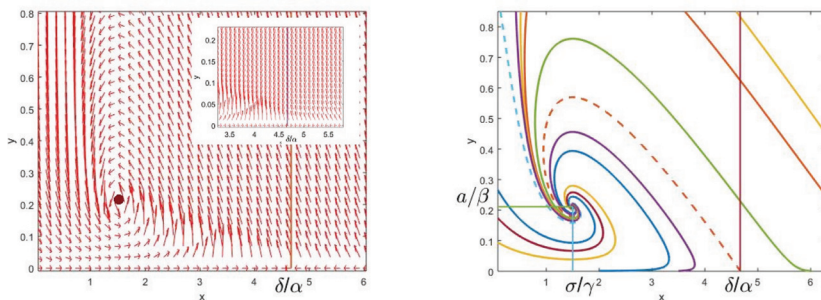


**Figure 1** (Top) Vector field of (1) for  $\delta > 0$  with inset figure of its behavior near  $(\delta/\alpha, 0)$ ; (Bottom) Flow of (1) in the first quadrant. Dashed lines are separatrices. Note that the online version of this article has color diagrams.

Note that the field restricted to the  $x$ -axis is  $(\delta - \alpha x, 0)$ . Therefore, it is parallel to the axis and points toward the equilibrium point  $(\delta/\alpha, 0)$ . Along the  $y$ -axis the field is  $(\delta, -\sigma y)$ , and it is either parallel to the axis (if  $\delta = 0$ ) or points inside the first quadrant (if  $\delta > 0$ ). Since trajectories are directed along the field vectors, they cannot leave the first quadrant if they start there. In general, regions that trajectories cannot leave are called *flow-invariant*. A closer look at the line  $x = \delta/\alpha$  for  $\delta > 0$  shows that the field

restricted to it,

$$\left(-\frac{\beta\delta}{\alpha}y, \left(\frac{\gamma\delta}{\alpha} - \sigma\right)y\right),$$

always points leftward. This means that the half-strip

$$H := \left\{(x, y) \in \mathbb{R}^2 \mid 0 \leq x \leq \frac{\delta}{\alpha}, y \geq 0\right\}$$

is also flow-invariant.

Moreover, for small  $y \neq 0$ , the vectors along the line  $x = \delta/\alpha$  point away from the equilibrium point  $(\delta/\alpha, 0)$ , which means that this equilibrium is *unstable*. Trajectories with  $y \neq 0$  will move away from it no matter how small  $y$  is. Conversely, the other equilibrium seems to be *stable*, more precisely, locally asymptotically stable, meaning nearby trajectories flow into it.

This simple analysis allows us to form a preliminary picture of the flow in the first quadrant, shown on the bottom of Figure 1. There is a family of trajectories entering  $H$  from the left through the  $y$ -axis, and another family entering it from the right through the line  $x = \delta/\alpha$ . By continuity, there has to be a special trajectory separating these two families. Such trajectories are called *separatrices*, and the behavior of the vector field along the  $y$ -axis suggests that this one should be asymptotic to it. There has to be another separatrix separating trajectories passing under the stable equilibrium and going up from those entering  $H$  from the right. This one seems to be “originating” (at  $t \rightarrow -\infty$ ) at the unstable equilibrium. The trajectories entering  $H$  from the right are squeezed between these two separatrices.

## Harmonic oscillator, damped and undamped

As compelling as the above picture is, it is only a picture. To move past mere illustrations, it will be helpful to look at the physical cousin of our model, the (damped) harmonic oscillator. To save space, from now on we will denote time derivatives by dots:

$$\dot{f} := \frac{df}{dt} \quad \text{and} \quad \ddot{f} := \frac{d^2f}{dt^2}.$$

The harmonic oscillator equation  $\ddot{y} + by = 0$ , and its damped version  $\ddot{y} + a\dot{y} + by = 0$ , are commonplace in mathematical physics, describing phenomena as diverse as springs, pendulums, RLC electric circuits, tuning forks, atoms in a solid, etc. [10]. Setting  $x := \dot{y}$  we present the oscillator as a 2-dimensional system

$$\begin{cases} \dot{x} = -ax - by \\ \dot{y} = x \end{cases} \quad (2)$$

It is instructive to visualize solutions  $(x(t), y(t))$  to this system as moving points in the  $x$ — $y$  plane called the *phase plane* of the system. When  $a = 0$ , equations of the curves they traverse can be found by dividing the second equation by the first, separating variables, and integrating:

$$\frac{dy}{dx} = \frac{\dot{y}}{\dot{x}} = -\frac{x}{by}.$$



The result, called the *first integral* of (2) with  $a = 0$ , is  $x^2 + by^2 = C$ . The curves it defines for  $C > 0$  are ellipses centered at the origin, and the points move along them counterclockwise. These ellipses are level sets of the function  $V(x, y) := x^2 + by^2$ , which represents the total energy of the oscillator.

When the damping coefficient  $a > 0$ , the oscillator is losing energy (say, to friction), and the phase trajectories spiral into the origin, always staying within every ellipse they enter, as shown on the top of Figure 2. The corresponding time behavior of the phase variables is shown on the bottom of Figure 2. Computing the derivative of energy  $V(x, y)$  along the trajectories of the damped system (2), we find:

$$\frac{d}{dt}V(x(t), y(t)) = \frac{\partial V}{\partial x}\dot{x} + \frac{\partial V}{\partial y}\dot{y} = -2ax^2 \leq 0.$$

As expected,  $V(x(t), y(t))$  is a decreasing function of time, and this is why the damped trajectories can enter the ellipses but never exit them. This is a prototypical example of a Lyapunov function for systems of differential equations.

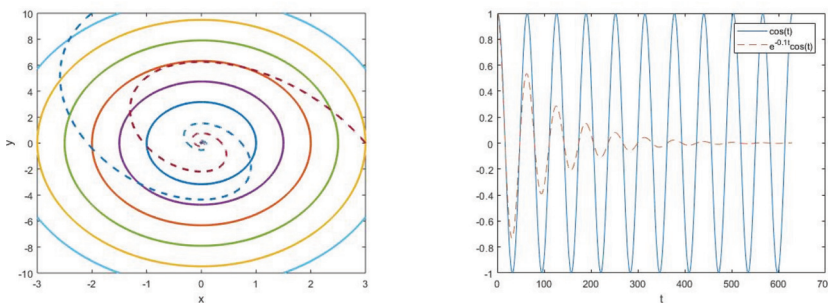


**Figure 2** The undamped (solid) and damped (dashed) trajectories of the harmonic oscillator: (Top) in the phase plane; (Bottom) as functions of time.

## Limit points and Lyapunov functions

To appreciate the utility of Lyapunov functions, it is instructive to imagine what can generally happen to trajectories. Going back to our model (1), let us abbreviate  $p(t) = (x(t), y(t))$  the solution starting at a point  $p_0 = (x_0, y_0)$  in the first quadrant. Our intuitive picture suggests that

$$p(t) \rightarrow p_* := \left( \frac{\sigma}{\gamma}, \frac{a}{\beta} \right)$$

when  $t \rightarrow \infty$ . But nothing we have said so far precludes  $p(t)$  from “escaping to  $\infty$ ” instead, e.g., moving up  $H$  indefinitely. Something yet more curious can happen. Rather than spiraling into  $p_*$ , our  $p(t)$  may get stuck cycling around it forever. This would mean having yet another separatrix, a closed curve that separates the inside and the outside trajectories. Such separatrices are called *limit cycles*. Limit cycles do indeed occur in some predator-prey models, like the Holling-Tanner system [8], see Figure 3. They correspond to solutions that display a pattern of sustained oscillations.

How do we detect (or rule out) such behavior? This is where Lyapunov functions come in. With their help, we can rule out escapes to  $\infty$  and limit cycles all at once. If trajectories escaped to  $\infty$ , then the Lyapunov function would eventually have to grow along them, which it can not. If there was a limit cycle, then its time derivative would have to vanish on it, and this can be checked.

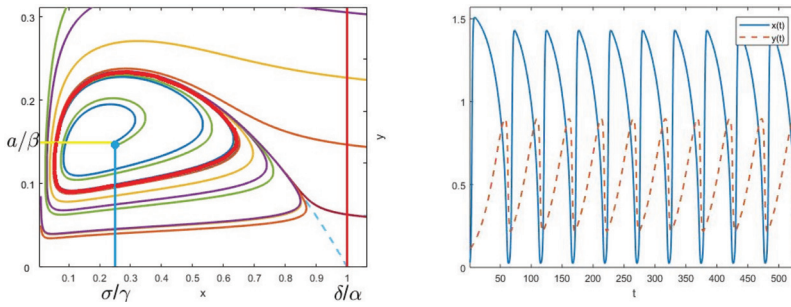


**Figure 3** Holling-Tanner system: (Top) limit cycle in the phase plane; (Bottom) phase variables as functions of time.

The asymptotic behavior of trajectories is reflected by their limit points. For a trajectory that starts at  $p_0$ , the set of such points is called the *omega-limit set* of  $p_0$  [9, 2.6]:

$$\omega(p_0) := \{q \in \mathbb{R}^2 \mid p(t_k) \rightarrow q \text{ for some } t_k \rightarrow \infty\}.$$

It is easy to show that  $\omega(p_0)$  is always closed, i.e., contains its own limit points, and is flow-invariant. It is nonempty if  $p(t)$  is bounded, and then it is itself bounded. If  $p(t)$  escapes to  $\infty$ , then this set will be empty. And if  $p(t)$  approaches a limit cycle, then  $\omega(p_0)$  will contain the whole cycle.

Suppose  $p(t)$  stays within some region  $U$  for all  $t \geq 0$ , a *trapping region*, and let  $V(p)$  be a function defined on  $U$ . Consider the time derivative of  $V$  along the trajectories of the system:

$$\dot{V}(x, y) := \nabla V \cdot (\dot{x}, \dot{y}) = \frac{\partial V}{\partial x} \dot{x} + \frac{\partial V}{\partial y} \dot{y}.$$

Then

$$\frac{d}{dt} V(p(t)) = \dot{V}(p(t)),$$

and if  $\dot{V}(p) \leq 0$  on  $U$ , then  $V(p(t))$  is nonincreasing along the trajectories. A version of the theorem due to Lyapunov [9, 2.6] tells us more.

**Theorem 1** (Lyapunov). *Let  $V$  be a continuously differentiable function defined on a region  $U$  such that  $\dot{V}(p) \leq 0$ . If  $p(t)$  stays within  $U$  for all  $t \geq 0$ , then  $\dot{V}$  vanishes on the limit points of  $p(t)$  that are within  $U$ , i.e.,*

$$\omega(p_0) \cap U \subseteq \dot{V}^{-1}(0).$$

In the classical case considered by Lyapunov,  $V$  was required to have a global minimum, a single point where  $\dot{V} = 0$  which also happens to be an equilibrium of the system. But these conditions are so demanding that not even the damped harmonic oscillator satisfies them all! Indeed,  $\dot{V} = -2ax^2 = 0$  on the entire line  $x = 0$ , not just at  $(0, 0)$ . We will call a function  $V$  a *Lyapunov function* if it simply satisfies  $\dot{V} \leq 0$ , i.e., if it does not increase along the trajectories. Figure 4 (Top) illustrates how Lyapunov functions work. It depicts a trajectory  $p(t)$  together with the value of  $V(p(t))$ , i.e., a trajectory lifted to the graph of  $V$ . The graph of  $V$  is bowl-shaped, and the fact that  $V$  decreases along the trajectories means that their lifts are funneled towards its bottom, ideally the global minimum.

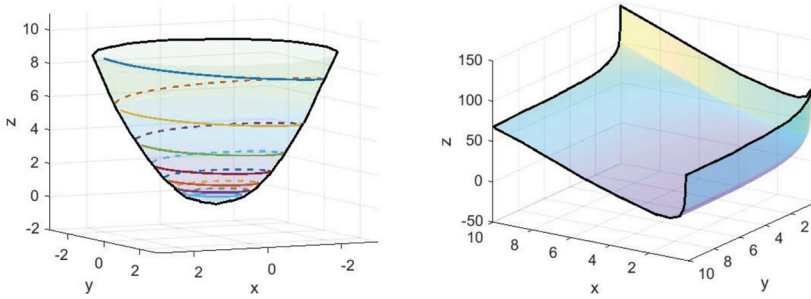


**Figure 4** (Top) Lyapunov lifted trajectory of the damped harmonic oscillator; (Bottom) Lotka-Volterra Lyapunov function.

### Lyapunov function for the “damped” predator-prey model

Let us start with the predator-prey model of Lotka-Volterra, a biological analog of the undamped harmonic oscillator:

$$\begin{cases} \dot{x} = ax - \beta xy \\ \dot{y} = \gamma xy - \sigma y. \end{cases} \quad (3)$$

Here  $x$  is the number of prey fish and  $y$  the number of their predator. The prey multiplies at the rate  $ax$ , proportional to the size of its population, and is consumed at a rate proportional to its encounters with the predator. It is a common assumption in population dynamics that these encounters are random and therefore proportional to the product of the population numbers  $xy$ . This is called the “mass action principle.” Conversely, the population of predators multiplies proportionally to  $xy$  and has death rate  $\sigma y$ . Unlike (2), this model is nonlinear, but we can still find the first integral by the same trick:

$$\frac{dy}{dx} = \frac{\gamma xy - \sigma y}{ax - \beta xy} = \frac{\gamma - \frac{\sigma}{x}}{\frac{a}{y} - \beta}.$$

Separating the variables and integrating, we compute:

$$\gamma x - \sigma \ln x + \beta y - a \ln y = C. \quad (4)$$

We assume that all the parameters are positive and only look at the positive values of  $x$  and  $y$  since neither populations nor concentrations can be negative. Then on the left we have a sum of two one-variable functions that, like parabolas, are convex down and have a global minimum. The resulting picture in the  $x$ - $y$  plane is topologically similar to Figure 2 (Top), but the ellipses are replaced by ovals confined to the first quadrant and the center is no longer at the origin. See Figure 5 (Top).

For our model (1), we shall take Lotka-Volterra’s first integral as a Lyapunov function template (such a template with free parameters is often called *ansatz*), but without specifying yet what  $a$  is:

$$V(x, y) = \gamma x - \sigma \ln x + \beta y - a \ln y. \quad (5)$$

Then we differentiate,

$$\nabla V = \left( \gamma - \frac{\sigma}{x}, \beta - \frac{a}{y} \right),$$

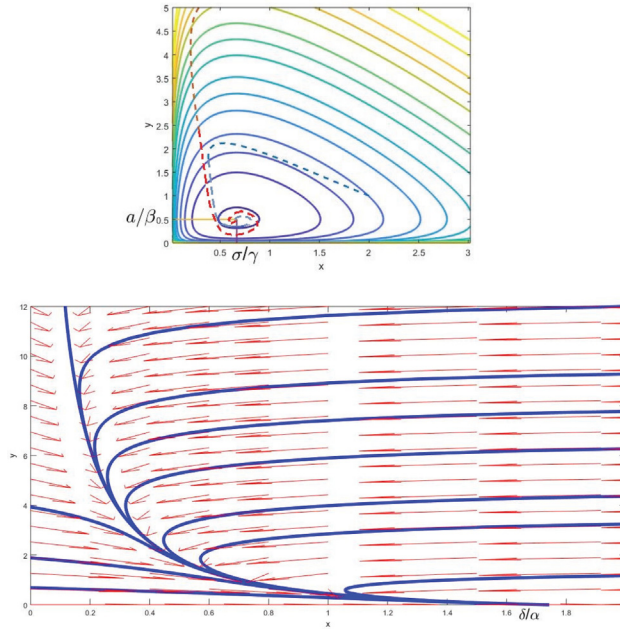


**Figure 5** Flows for (Top) the Lotka-Volterra model (solid) and its “damped” version (dashed) with  $a > 0$ ; (Bottom) predator extinction with  $a < 0$ .

and split the vector field of (1) as follows:

$$\begin{aligned} X &:= (\delta - \alpha x - \beta xy, \gamma xy - \sigma y) \\ &= (ax - \beta xy, \gamma xy - \sigma y) + (\delta - \alpha x - ax, 0) =: X_0 + Z. \end{aligned}$$

The first field  $X_0$  is from the Lotka-Volterra system (3). We know that  $\nabla V \cdot X_0 = 0$  because  $V$  is constant along its trajectories, so

$$\nabla V \cdot X = \nabla V \cdot Z,$$

and

$$\begin{aligned} \dot{V}(p) &= \nabla V \cdot Z = \left( \gamma - \frac{\sigma}{x} \right) (\delta - (a + \alpha)x) \\ &= -\frac{\gamma(a + \alpha)}{x} \left( x - \frac{\sigma}{\gamma} \right) \left( x - \frac{\delta}{a + \alpha} \right). \end{aligned}$$

Now it becomes clear how to select  $a$ , which we left indeterminate, to make  $V$  a Lyapunov function. If we set  $\sigma/\gamma = \delta/(a + \alpha)$ , and  $a > 0$ , then

$$\dot{V}(x, y) = -\frac{\gamma^2 \delta}{\sigma x} \left( x - \frac{\sigma}{\gamma} \right)^2 \leq 0. \quad (6)$$

This means that  $a := (\gamma\delta/\sigma) - \alpha$ , the same  $a$  we introduced when computing equilibria. With our additional restriction  $\gamma\delta > \sigma\alpha$ , we have  $a > 0$ . The graph of a Lyapunov function (5) for  $a > 0$  is shown in Figure 4 (Bottom). It is shaped more like a dustpan than a bowl, but like a bowl has a global minimum at the equilibrium. We will discuss what happens when  $a$  is negative shortly.

Note that moving from system (1) to (3) does not amount to simply setting a single “damping” coefficient to 0, as was the case for the harmonic oscillator. In this case,

the relation between the “damped” predator-prey system and its “undamped” version is more complicated. We should also mention that there are other ways of “damping” the Lotka-Volterra model [7].

## Global attraction

Now that we have a Lyapunov function, applying Theorem 1 requires the choice of a trapping region  $U$ . It is tempting to take the entire first quadrant as  $U$ , but this would not work for two reasons. First, we cannot include the axes since our  $V$  from (5) is not defined on them. Second, even without the axes  $U$  is unbounded, so we cannot rule out  $\omega(p_0)$  being empty. A resolution is to take as  $U$  the Lotka-Volterra oval from Figure 5 (Top) with  $p_0$  on its boundary, i.e.,

$$U_{p_0} := \{p \in \mathbb{R}^2 \mid V(p) \leq V(p_0)\}.$$

This region is closed and bounded, and  $p(t)$  stays within it for all  $t \geq 0$  since  $V(p(t))$  is nonincreasing. Now we can confirm our picture of the flow rigorously.

**Theorem 2.** *Suppose  $\alpha, \beta, \gamma, \delta, \sigma > 0$  and  $\gamma\delta > \alpha\sigma$ . Let  $p_* := (\sigma/\gamma, a/\beta)$  be the (stable) equilibrium of system (1) with  $a := (\gamma/\sigma)\delta - \alpha$ . Then for any  $p_0 = (x_0, y_0)$  with  $x_0, y_0 > 0$ , the trajectory starting at  $p_0$  converges to  $p_*$  at  $t \rightarrow \infty$ .*

*Proof.* Any  $p_0$  belongs to a Lotka-Volterra oval  $U_{p_0}$ . Since  $U_{p_0}$  is flow-invariant,  $p(t) \in U_{p_0}$  for all  $t \geq 0$ . Since it is closed and  $\omega(p_0)$  consists of limit points of  $p(t_k)$  we have  $\omega(p_0) \subseteq U_{p_0}$ . Hence, by the Lyapunov theorem, we have  $\omega(p_0) \subseteq \dot{V}^{-1}(0)$ . But

$$\dot{V}(p) = -\frac{\gamma^2\delta}{\sigma x} \left(x - \frac{\sigma}{\gamma}\right)^2,$$

so  $\dot{V}^{-1}(0)$  is the line  $x = \sigma/\gamma$ . But  $\omega(p_0)$  must be flow-invariant, while trajectories of (1) move off this line unless  $\dot{x} = 0$ , i.e., unless also  $y = a/\beta$ . Therefore,  $\omega(p_0) \subseteq \{p_*\}$ . Since  $U_{p_0}$  is bounded  $\omega(p_0)$  is nonempty, so  $\omega(p_0) = \{p_*\}$  and  $p_*$  is the limit of  $p(t)$ . ■

If trajectories originating from points of a certain region converge to an equilibrium, this area is called its *domain of attraction*. Our theorem says that the interior of the first quadrant is a domain of attraction of  $(\sigma/\gamma, a/\beta)$  when  $\gamma\delta > \alpha\sigma$ . Biologically, this means that the predator and the prey (or the infectious and the susceptible) populations stabilize at the equilibrium values.

## Bifurcation to predator extinction

As we saw, when  $\gamma\delta \leq \alpha\sigma$  function (5) ceases to be a Lyapunov function of the “damped” predator-prey system. This is not an artifact of its choice. As  $a = ((\gamma\delta - \alpha\sigma)/\sigma) - \alpha$  decreases, the stable equilibrium, the center of the ovals in Figure 5 (Top), moves to the  $x$ -axis and merges with the unstable one when  $a = 0$ . Then it moves below the  $x$ -axis when  $a < 0$  and is no longer relevant to the first quadrant. As a result, the geometry of the trajectories changes dramatically. According to the vector field, nearby trajectories now seem to approach the formerly unstable equilibrium  $(0, \delta/\alpha)$ . This kind of stability change under variation of parameter values is called *transcritical bifurcation* [14, pp. 50–51].

Since the  $x$ -coordinate of our suspected attracting equilibrium is 0 after the bifurcation, we will choose  $V(x, y) = \gamma x - b \ln x + \beta y$  as our Lyapunov function ansatz, with  $b$  to be determined. This is the first integral of a degenerate Lotka-Volterra system (3) with  $a = 0$  and  $\sigma = b$ . This system is of interest in its own right. It is called the SIR (for Susceptible-Infected-Removed individuals) model in epidemiology [4, 4.12], but we will not dwell on it here. Performing calculations as in the previous section, we find that  $b := (\delta/\alpha)\gamma$ , and then

$$\dot{V}(x, y) = -\frac{\alpha\gamma}{x} \left(x - \frac{\delta}{\alpha}\right)^2 - \beta \left(\sigma - \frac{\delta}{\alpha}\gamma\right) y \leq 0$$

in the first quadrant, whenever  $\gamma\delta \leq \alpha\sigma$ . The now familiar argument shows that the interior of the first quadrant is a domain of attraction of  $(\delta/\alpha, 0)$ . Figure 5 (Bottom) shows the vector field and the flow of the system after the bifurcation. Recall that the  $y$ -coordinate stands for the number of predators, and it is 0 at the attracting equilibrium. In biological terms, this means that the population of predators is driven to extinction. The growth and the death rates line up so that there is not enough prey to sustain it. This is also similar to the (heavily) damped harmonic oscillator, only there both variables are driven to 0.

## Virus dynamics

So far we have interpreted the variables of system (1) as the population numbers of either predators and prey or infected and susceptible individuals during epidemics. However, as with harmonic oscillators, there are many other interpretations. In this section we will interpret them as the numbers of virus-producing and susceptible-to-infection cells in an organism, rather than individuals. It will also give us an opportunity to illustrate how Lyapunov functions can help with more than just establishing global attraction.

In virus dynamics,  $\delta$  is the creation rate of susceptible (healthy) cells,  $\delta/\alpha$  is the stable density of cells in the absence of a virus,  $1/\sigma$  is the average life span of an infected cell, and  $\gamma$  determines the rate of infection. The ratio  $R = \gamma\delta/\alpha\sigma$  is then the average number of cells infected by a single virus-producing cell, and it is called the *basic reproductive ratio* [3]. As follows from our analysis in previous sections, if  $R \leq 1$  the virus is driven to extinction, and if  $R > 1$  the number of virus-producing cells eventually stabilizes at

$$\frac{a}{\beta} = \frac{\gamma}{\beta} \frac{\delta}{\sigma} \left(1 - \frac{1}{R}\right),$$

see Figure 6. In other words,  $R$  is a *bifurcation parameter*, with the bifurcation at  $R = 1$ .

But the basic reproductive ratio is also a measurable quantity taken as a measure of the viral load, the amount of virus present in the organism. In the original basic model of virus dynamics, it was assumed that  $\beta = \gamma$ , just as in the original Lotka-Volterra model, i.e., the number of susceptible cells decreased only due to infection (and natural dying off), and the number of infected cells increased by the same amount. However, this model predicted unrealistically low viral loads after virus inhibitor treatments that reduced  $\gamma$ . In one of the modifications proposed in [3],  $\beta = \gamma + q$ , where  $q$  is the rate of virus-induced killing of susceptible cells, e.g., due to the immune response. This gives exactly the “damped” predator-prey model.



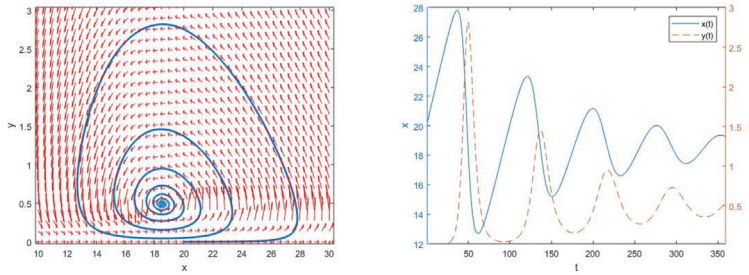


**Figure 6** (Left) Vector field and a trajectory of the basic virus dynamics model ( $R > 1$ ); (Right) Time evolution of susceptible and virus producing cells.

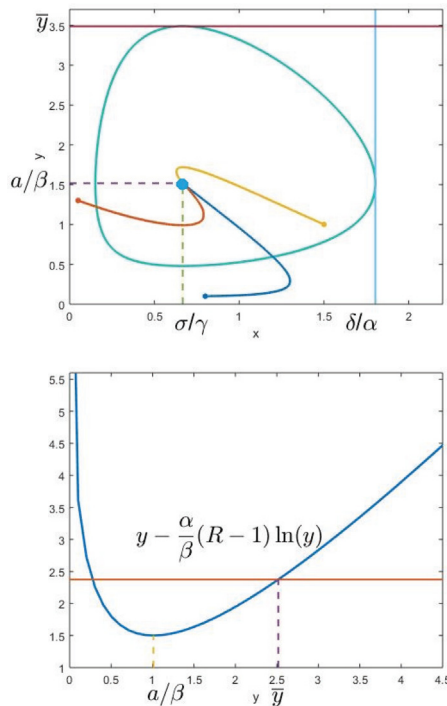


**Figure 7** (Left) Trapping oval for the “damped” predator-prey system; (Right) Solving for the upper bound  $\bar{y}$ .

Let us consider the following question: how much of an outbreak can we expect at the peak of infection after a small number of virus-producing cells is introduced into a susceptible population? To answer it, look at the oval depicted in Figure 7 (Left). It can be characterized by the condition that its right tip is tangent to the line  $x = \delta/\alpha$ . Since this oval is a level set of  $V$  from (5) the gradient of  $V$  is perpendicular to the  $y$ -axis at the point of tangency. This gives  $y = a/\beta$  for the  $y$  coordinate of that point, which is equal to the  $y$  coordinate of the stable equilibrium. Due to the direction of the field vectors, trajectories that pass to the left or under the oval must enter it since they cannot cross the  $x$ -axis, the  $y$ -axis, or the line  $x = \delta/\alpha$  outward. Once they enter it they cannot leave since  $V$  is a Lyapunov function. This means that  $y(t) \leq \bar{y}$ , where  $\bar{y}$  is the  $y$ -coordinate of the oval's top. Thus,  $\bar{y}$  gives the desired estimate on the peak number of virus producing cells.

To find it, note that the oval's equation is  $V(x, y) = C$ , where  $C$  can be found from the condition that the point  $(\delta/\alpha, a/\beta)$  lies on it, i.e.,  $C = V(\delta/\alpha, a/\beta)$ . Our  $\bar{y}$  is the larger solution to

$$V\left(\frac{\sigma}{\gamma}, y\right) = V\left(\frac{\delta}{\alpha}, \frac{a}{\beta}\right),$$

see Figure 7 (Right). We can express this equation more explicitly in terms of  $R$ :

$$y - \frac{\alpha}{\beta}(R-1) \ln y = \frac{\sigma}{\beta}(R-1 - \ln R) + \frac{\alpha}{\beta}(R-1) \left(1 - \ln \frac{\alpha}{\beta}(R-1)\right).$$

This is a transcendental equation for  $\bar{y}$  that can not be solved analytically, but numerical solutions can be found easily for specific parameter values. Now consider the limiting case of large infection rates, when  $\gamma \rightarrow \infty$  and

$$\frac{\gamma}{\beta} = \frac{\gamma}{\gamma + q} \rightarrow 1.$$

Then  $R \rightarrow \infty$  and

$$\frac{\alpha}{\beta}(R-1) \rightarrow \frac{\delta}{\sigma}.$$

The equation for  $\bar{y}$  simplifies to

$$y - \frac{\delta}{\sigma} \ln y = \frac{\delta}{\alpha} + \frac{\delta}{\sigma} \left(1 - \ln \frac{\delta}{\sigma}\right),$$

and gives a finite value. In other words, the maximal size of the outbreak remains bounded even for arbitrarily large infection rates!

## Plant growth

Let us switch from viral infections to growth of plants. Bessonov and Volpert proposed a model of early shoot growth from a seed that involves water flow transport of a nutrient to the top of the shoot, where a growth hormone regulates the creation of new cells [2]. After neglecting diffusion and making simplifying assumptions to eliminate the convection equation, the model can be reduced to a three-dimensional system:

$$\begin{cases} \dot{x} = \frac{1}{L}(v - \gamma xy) \\ \dot{y} = \gamma xy - \sigma y \\ \dot{L} = f(y). \end{cases} \quad (7)$$

Here,  $x$  and  $y$  are the nutrient and the hormone concentrations,  $L$  is the length of the shoot,  $v$  is the water flow speed,  $\gamma$  is the rate of hormone production and  $\sigma$  is the rate of its consumption. The  $1/L$  factor accounts for the dilution of the nutrient over the longer columns of water in longer shoots. The growth function  $f(y)$  is a nonnegative, monotone increasing, threshold function, i.e., it introduces a threshold level  $y_f$  the hormone concentration has to reach for the growth rate to be nonzero. See Figure 8 (Left). If  $y \leq y_f$ , then  $L$  is constant and the dynamics reduces to the first two equations. They are of the form (1) with  $\alpha = 0$ ,  $\beta = \gamma/L$ , and  $\delta = v/L$ . This reduced

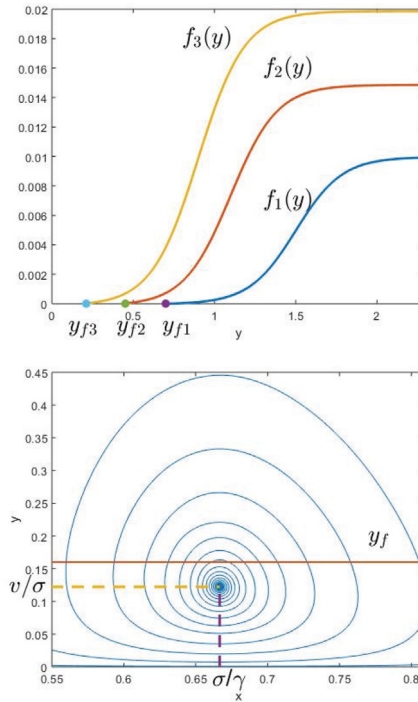


**Figure 8** (Left) Threshold functions for the plant growth model; (Right) Phase trajectory of (7) projected to the  $x$ - $y$  plane.

system has only one equilibrium in the first quadrant,  $(\sigma/\gamma, v/\sigma)$ . If  $v/\sigma \leq y_f$  then  $(\sigma/\gamma, v/\sigma, L_*)$  is an equilibrium of the full system (7) with any fixed  $L = L_*$ , see Figure 8 (Right). If not, the system has no equilibria.

Since  $L$  can grow without a bound, it is convenient to use  $z = 1/L$  as a variable instead, which converts (7) into

$$\begin{cases} \dot{x} = vz - \gamma zxy \\ \dot{y} = \gamma xy - \sigma y \\ \dot{z} = -f(y)z^2. \end{cases} \quad (8)$$

Now growth of  $L$  to infinity is replaced by convergence of  $z$  to 0, see Figure 9.

In three dimensions, dynamic behavior can be even more diverse than in the plane. In addition to escapes to infinity and limit cycles we can, in principle, encounter chaotic behavior with the omega-limit set being a fractal. This is what happens in the famous example of Lorenz's strange attractor [15], which also comes from simplifying convection equations. As before, to narrow down the range of possibilities we look for a Lyapunov function, but it takes an additional technique to find the right ansatz. From previous sections, we know a Lyapunov function (5) for the first two equations when  $z$  (and hence  $L$ ) are fixed:

$$V(x, y, z) := \gamma x - \sigma \ln x + \gamma z y - \gamma z \frac{v}{\sigma} \ln y. \quad (9)$$

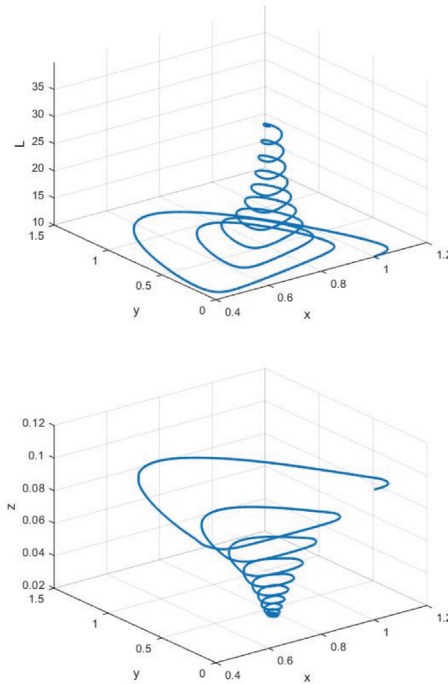


**Figure 9** Phase trajectories of: (a) system (7); (b) system (8).

But it may not be a Lyapunov function for the full system. Indeed, the derivative

$$\begin{aligned}\dot{V}(x, y, z) &:= \nabla V \cdot (\dot{x}, \dot{y}, \dot{z}) \\ &= -\frac{\gamma^2 v z}{\sigma x} \left(x - \frac{\sigma}{\gamma}\right)^2 - \gamma f(y) \left(y - \frac{v}{\sigma} \ln y\right) z^2\end{aligned}$$

may not be nonpositive in the entire first octant since the sign of  $y - (v/\sigma) \ln y$  changes there. Fortunately, the last equation in (8) and the shape of  $f(y)$  imply that the function  $W(x, y, z) := z$  is also a Lyapunov function! This just rephrases the fact that the length of the growing shoot never decreases. Since sums and positive multiples of non-positive derivatives are nonpositive positive linear combinations of Lyapunov functions, they are good candidates for Lyapunov functions. Adding  $m\gamma z$  to  $V$ , we obtain our new ansatz:  $V_m(x, y, z) := V(x, y, z) + m\gamma z$ , with  $m$  to be determined. Its derivative along the trajectories is

$$\dot{V}_m(x, y, z) = -\frac{\gamma^2 v z}{\sigma x} \left(x - \frac{\sigma}{\gamma}\right)^2 - \gamma f(y) \left(y - \frac{v}{\sigma} \ln y + m\right) z^2.$$

We can make it non-positive inside the entire first octant if we choose  $m$  so that

$$y - \frac{v}{\sigma} \ln y + m \geq 0$$

for all  $y > 0$ . This is possible because  $y - \frac{v}{\sigma} \ln y$  has a global minimum for  $y > 0$ . It is  $\frac{v}{\sigma}(1 - \ln \frac{v}{\sigma})$ , and we can simply take any  $\bar{m} > \frac{v}{\sigma}(1 - \ln \frac{v}{\sigma})$ .

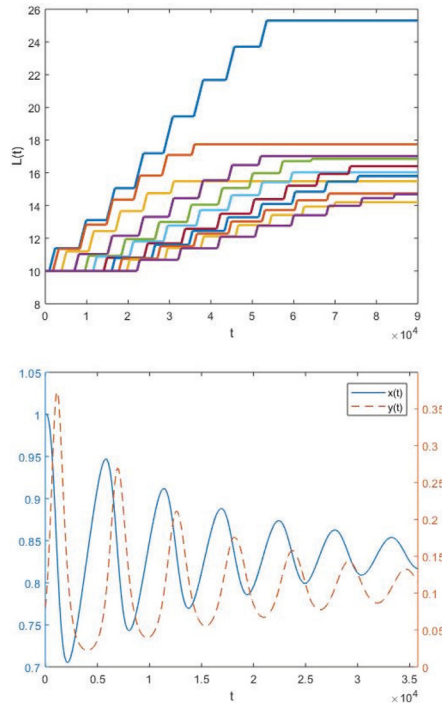


**Figure 10** Time evolution in (7): (Left) shoot length for different values of  $\sigma$ ; (Right) nutrient (solid) and hormone (dashed) concentrations.

With this function, and a trapping region bound by its level set, the Lyapunov theorem tells us that the omega-limit set of a point inside the first octant is contained in

$$\dot{V}_m^{-1}(0) = \{(x, y, z) \mid z = 0 \text{ or } x = \frac{\sigma}{\gamma}, f(y) = 0\}.$$

Since  $z(t) \geq 0$  is monotone decreasing we also know that  $z(t) \rightarrow z_* \geq 0$ . The case  $z_* = 0$  means that  $L(t) \rightarrow \infty$ , and this is the only option if  $v/\sigma > y_f$ , which is unbiological. But if  $v/\sigma < y_f$  and  $z_* > 0$ , then we can say more.

**Theorem 3.** Suppose  $v/\sigma < y_f$  and  $x_0, y_0, L_0 > 0$ . Then either  $L(t) \rightarrow \infty$  (unbounded growth), or there is a stopping time  $T_* > 0$  and a final length  $L_*$  such that  $L(t) = L_*$  is constant for  $t \geq T_*$ . In the latter case the nutrient and the hormone concentrations approach the equilibrium values  $\sigma/\gamma, v/\sigma$ , respectively.

*Proof.* If  $z_* > 0$  then  $L(t) \leq L_* := 1/z_*$ . Moreover, since the trajectories approach  $(\sigma/\gamma, v/\sigma, z_*)$ , and  $v/\sigma < y_f$ , their  $x$ - $y$  projections must for large  $t > 0$  stay in a disk contained entirely under the threshold  $y_f$ . When this is so,  $L(t)$  is constant since  $f(y) = 0$ . Therefore, there is a smallest time  $T_*$  after which the growth stops, and then  $L_* = L(T_*)$  is the final length. After  $T_*$ , the dynamics of  $x(t), y(t)$  is determined by the first two equations of (7) with  $z = z_*$ . Since  $\gamma\delta - \alpha\sigma = \gamma v z_* > 0$ , Theorem 2 applies to them. ■

Figure 10 shows the growth pattern for different values of parameters, and typical behavior of the nutrient and the hormone concentrations.

As one can see, the growth occurs in spurts interrupted by quiet periods. The system may spend a long time in a quiet period before resuming growth again. To make sure in simulations that the growth stops for good, we can use the Lyapunov function again.

For every fixed value of  $L$  (and  $z$ ), the function  $V_m(x, y, z)$  defines a family of Lotka-Volterra ovals in the  $x$ - $y$  plane. Consider the oval that touches the threshold line  $y = y_f$  at the upper tip. Its equation can be determined from the fact that  $(\sigma/\gamma, y_f)$  lies on it. If in the course of a simulation

$$V_m(x, y, z) \leq V_m\left(\frac{\sigma}{\gamma}, y_f, z\right),$$

then growth can never resume, and  $L_* = 1/z$  is the final length ( $m$  may be set to 0 if  $y_m < 1$ ).

This pattern was predicted also by the full Bessonov-Volpert model. Simulations show that for realistic initial values (small lengths and hormone concentrations) the growth does eventually stop. This raises many interesting questions, like finding explicit estimates for the final length and the stopping time in terms of the initial values. But answering them would probably require techniques beyond the use of Lyapunov functions.

**Technology Used** Simulations and figures were made in MATLAB. The *pde45* function was used to solve systems of differential equations numerically. The *plot* function was used for the 2D plots, the 3D plots were made with *surf* (for surfaces) and *plot3* (for trajectories). The vector fields in Figures 1 (Top), 5 (Bottom), and 6 (Top) were plotted with the *vectfieldn* package.

**Acknowledgments** The research for this paper was completed during the Research Experiences for Undergraduates (REU) program held at the University of Houston-Downtown in the summer of 2018. We would like to thank our fellow REU participants Dr. Youn-Sha Chan, Dr. Michael Tobin, Tomas Bryan, Roberto Hernandez and Michael Zhang for their helpful insights. This work was supported by NSF grant #1560401.

## REFERENCES

- [1] Berryman, A. (1992). The origins and evolution of predator-prey theory. *Ecology*. 73(5): 1530–1535. [doi.org/10.2307/1940005](https://doi.org/10.2307/1940005)
- [2] Bessonov, N., Volpert, V. (2006). *Dynamical Models of Plant Growth*. Paris: Publibook.
- [3] Bonhoeffer, S., Coffin, J., and Nowak, M. (1997). Human immunodeficiency virus drug therapy and virus load. *J. Virol.* 71(4): 3275–3278. [doi.org/10.1128/JVI.71.4.3275-3278.1997](https://doi.org/10.1128/JVI.71.4.3275-3278.1997).
- [4] Braun, M. (1983). *Differential Equations and their Applications*. New York: Springer-Verlag.
- [5] Chauvet, E., Paillet, J., Previte, J., Walls, Z. (2002). A Lotka-Volterra three-species food chain. *Math. Mag.* 75(4): 243–255. [doi.org/10.2307/3219158](https://doi.org/10.2307/3219158).
- [6] Cohen, M. (2012). *Classical Mechanics: A Critical Introduction*, pp. 155–172. [www.physics.upenn.edu/sites/default/files/Classical\\_Mechanics\\_a\\_Critical\\_Introduction\\_0.0.pdf](http://www.physics.upenn.edu/sites/default/files/Classical_Mechanics_a_Critical_Introduction_0.0.pdf)
- [7] Garrett, T. (2012). Modes of growth in dynamic systems. *Proc. Royal Soc. A.* 468(2145): 2532–2549. [doi.org/10.1098/rspa.2012.0039](https://doi.org/10.1098/rspa.2012.0039).
- [8] Gasull, A., Kooij, R., Torregrosa, J. (1997). Limit cycles in the Holling-Tanner model. [doi.org/10.5565/37888](https://doi.org/10.5565/37888)
- [9] Hofbauer, J., Sigmund, K. (1998). *Evolutionary Games and Population Dynamics*. Cambridge: Cambridge University Press.
- [10] Jha, D. K. (2005). *Textbook of Simple Harmonic Motion and Wave Theory*. Discovery Publishing.
- [11] Kermack, W., McKendrick, A. (1927). A contribution to the mathematical theory of epidemics. *Proc. Royal Soc. A.* 115(772): 700–721. [doi.org/10.1098/rspa.1921.0118](https://doi.org/10.1098/rspa.1921.0118).
- [12] Lotka, A. J. (1920). Undamped oscillations derived from the law of mass action. *J. Amer. Chem. Soc.* 42(7): 1595–1599. [doi.org/10.1021/ja01453a010](https://doi.org/10.1021/ja01453a010)
- [13] Soper, H. E. (1929). The interpretation of periodicity in disease prevalence. *J. Roy. Statist. Soc.* 92(1): 34–73. [doi.org/10.2307/2341437](https://doi.org/10.2307/2341437)
- [14] Strogatz, S. (1999). *Nonlinear Dynamics and Chaos: with Applications to Physics, Biology, Chemistry, and Engineering*. New York: Perseus Books.



- [15] Viana, M. (2000). What's new on Lorenz strange attractors? *Math. Intell.* 22(3): 6–19.
- [16] Volterra, V. (1926). Variazioni e fluttuazioni del numero d'individui in specie animali conviventi. *Mem. Accad. Lincei* 6: 31–113. doi.org/10.1038/11855a0. Reprinted in: *Opere matematiche*, vol. 5, Accademia nazionale dei Lincei, Roma (1962).

**Summary.** We show that a number of models in virus dynamics, epidemiology and plant biology can be presented as “damped” versions of the Lotka-Volterra predator-prey model, by analogy to the damped harmonic oscillator. The analogy deepens with the use of Lyapunov functions, which allow us to characterize their dynamics and even make some estimates.

**SERGIY KOSHKIN** (MR ID 656404) received his first Ph.D. in mathematics from the National Technical University of Ukraine, and second one from Kansas State University. Currently he is an associate professor of mathematics at the University of Houston-Downtown. His research ranges from functional analysis and differential geometry to mathematical modeling in mechanics and biology. He is also fond of history of mathematics, and good literature and film.

**ISAIAH MEYERS** received a Bachelor's degree in mathematics from the University of Texas at Austin. His research interests include numerical analysis, mathematical modeling and neural networks, but more generally he is fascinated by the interface of theory and computation. Outside of mathematics, he enjoys visiting museums, reading, and coding.

# A Few Ripe Red-Blue Cherries

SCOTT ANDREW HERMAN

Choate Rosemary Hall and  
University of Pennsylvania  
Philadelphia, PA 19104  
[scherman@sas.upenn.edu](mailto:scherman@sas.upenn.edu)

Let's play a game or two of Red-Blue Cherries.\* We are given an arbitrary graph with vertices colored red or blue, not both, as shown, for example, in Figure 1A. (Our graphs are always finite, undirected, and unweighted, with neither self-loops nor multiple edges between the same two vertices. They may or may not be connected.)

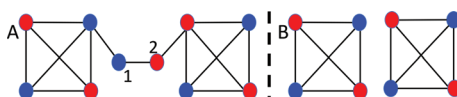


**Figure 1** (A) Starting position of a game of Red-Blue Cherries on a 10-vertex graph, and (B) the same game after one move by each player.

You choose one color and I get the other. We take turns, deleting vertices of our own color and all the edges incident to them. The first of us who cannot move *loses*. But here's the catch: only vertices of *minimum degree* over the entire graph, that is, with the fewest remaining edges incident to them, may be deleted. Thus, in Figure 1A, only the cherries at vertices labeled 1 and 2 of degree 2 are ripe for picking. The other eight vertices have degree three or degree four. You may choose a color and go first.

Let's say you choose blue. You must delete the vertex labeled 1. After your first move, the graph is disconnected, but this does not matter, play continues. I must now delete the vertex labeled 2, which, after your first move, now has minimum degree 1. We arrive at Figure 1B: your turn. All four choices for your second move lead to rearrangements of the same picture, and play unfolds as in Figure 2. The last cherry is red and mine. You lose.

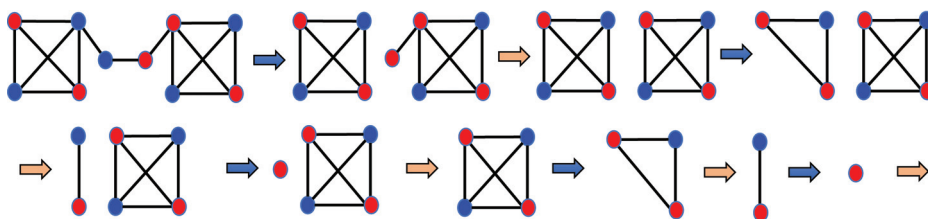


**Figure 2** A complete game of Red-Blue Cherries on a 10-vertex graph.

Would you rather start by choosing red vertices instead of blue? Not if you have already noticed that the position in Figure 1A is symmetric (i.e., has a color-preserving graph isomorphism) with one that has colors reversed. Whoever goes first loses, and

\*Note that the online version of this article has color diagrams.

no one wants to make the first move in this game. But games are supposed to be fun and require some strategy for winning.

Let's try something a bit different. We are given the new game in Figure 3A. You may choose a color and even require me to start this time. Say you choose red. I must take 1, you must take 2, and then I am careful to take 3, not 3', and arrive at Figure 3B, not Figure 3C. Your turn. You must take 4, I take 5, and I win. Would you rather choose blue? Again, the starting position is symmetric with one that has colors reversed, and I still win. This is different from the first game: each of us wants to go first and get to pick a winning second move. We will see shortly that the two games we just played are in different *outcome classes*.

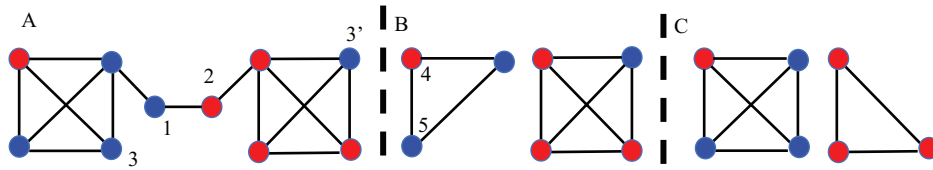


**Figure 3** Positions from a game of Red-Blue Cherries on a 10-vertex graph: (A) Starting position and first moves, picking a blue cherry first, (B) Position after a good move at 3, and (C) Position after a poor move at 3'.

All that had been published about Red-Blue Cherries before 2019 was a paragraph in the “Unsolved Problems” chapter of *Games of No Chance 4* [7, p. 285]. (A different but related game simply called Cherries is mentioned in *Winning Ways*, vol. 3, 2nd ed. [4, p. 757].) Nowakowski describes Red-Blue Cherries and states that Albert, McCurdy, Grossman, Nowakowski, and Wolff [1] (AMGNW) show that if the game’s graph has a leaf, then the value is an integer. He adds that they ask: Is every Red-Blue Cherries position an integer? We will soon say a lot more about these “values” and what it means for a game to be called an integer. We will examine these claims and learn what is true, false, and perhaps surprising about Red-Blue Cherries.

## Intuitive notion of values

*Values* indicate who is winning and by how much. They show us what happens when we combine games and compare results. Both players should be indifferent if games with equal values are substituted for each other in any context, even if the games have different forms. Look at the four games in Figure 4. Game *A* is a balanced position in which the first player loses. It has value 0 and is called a *zero game*.

In combinatorial games such as Red-Blue Cherries, the players are usually called *Left* and *Right*. In our game, Left deletes *her* *bLue* cherries, and Right deletes *his* *Red* cherries. Positive values indicate Left is winning, and negative values indicate Right is winning. Game *B* has value +1 (Left is one move ahead of a zero game), and game *C* has value +2. They belong to the same outcome class (Left can win no matter who plays first), but they have different values. Game *D* has value −1, and it is natural to say  $D = -B$ . We get the *negative* of a game by “switching places,” or, in our game, “reversing colors,” so, for example,  $A = -A$  and  $-(-B) = B$ .

We play the *sum* of a finite number of games by requiring each player, alternately, to make one move in any one of the summands he or she chooses. Indeed,  $A + B$  has value  $0 + 1 = 1$ , because, after each player has made four moves in  $A + B$ , one blue cherry remains. Simply counting cherries also shows that  $A + A + A$  has value

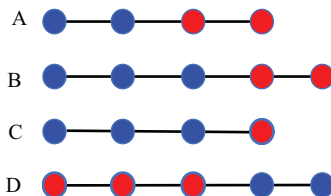


**Figure 4** Four simple games of Red-Blue Cherries.

0,  $A + D$  has value  $-1$ ,  $2C \equiv C + C$  has value 4, and  $B + B - C \equiv B + B + (-C)$  has value 0.

Counting cherries also shows that the game in Figure 1A is a zero game. Because we want to make the last move, we usually view moving as disadvantageous and expect values to decrease after Left moves and increase after Right moves. But there are exceptions! Counting cherries does *not* work for the game in Figure 3B. It does *not* have value  $-1$ , and it is *not* the sum of its two components regarded as separate games. It is, in fact, a zero game. That is what makes things interesting. After we define all of this more precisely, we will see:

- Why the above claim about values on graphs with a leaf is wrong, and how to fix it
- Games with values  $n$ ,  $n + \frac{1}{2}$ ,  $\frac{1}{2^n}$ , and  $1 - \frac{1}{2^n}$  for all integers  $n$
- Games with values that are *not* numbers

## Outcome classes and values

We need to complement our intuitive grasp of what values tell us about our game with a mathematical understanding of them. Values simultaneously (1) have a formal definition in terms of sets, (2) allow us to calculate and manipulate them as though they were numbers, and (3) characterize when positions in our game are essentially the same or different. By identifying games with their values, we can explain what was meant above by calling a “game” an “integer.” After this preparation, we obtain our results listed above by applying two theorems from AMGWN [1] about games on graphs that are trees and paths.

Every game  $G$  has a first player and second player, winner and loser—it ends in finitely many moves. Thus,  $G$  belongs to exactly one of four *outcome classes* of games:

- $\mathcal{P}$  The second (or previous) player can always win, as illustrated in Figure 1A.
- $\mathcal{N}$  The first (or next) player can always win, as illustrated in Figure 3A.
- $\mathcal{L}$  Left can always win, no matter who plays first, as in game  $B$  of Figure 4.
- $\mathcal{R}$  Right can always win, no matter who plays first, as in game  $D$  of Figure 4.

Combinatorial game theory captures our intuitive notion of values by defining *games* and *numbers* in terms of sets. We sketch the rudiments of this theory, which is needed to define and compute the values of our games of Red-Blue Cherries. You can find the missing details in a textbook [2], a treatise with many examples [3], or a mathematical monograph [5]. See also the paper by Conway [6] for an introduction to combining and evaluating games.

In any game (or, equivalently, in any game position)  $G$ , Left and Right each have a set of moves or *options*,  $\mathcal{G}^L$  and  $\mathcal{G}^R$ , respectively, which are sets of (other) games. We define the *value* of the game  $G$  to be the ordered pair of sets of Left’s and Right’s

options, written  $G = \{\mathcal{G}^L \mid \mathcal{G}^R\}$ . (This equating of games with their values is our first abuse of notation, which requires justification.) The simplest set of options is the empty set, so for  $\mathcal{G}^L = \mathcal{G}^R = \emptyset$ , we define  $0 := \{\emptyset \mid \emptyset\} = \{\mid\}$ . Note that  $0 \in \mathcal{P}$ , i.e., 0 is a zero game. (We violate set theoretic notation by writing the sets of games in Left's and Right's options as lists and the empty set of options as nothing at all.)

Armed with two sets of options,  $\emptyset$  and 0, we construct and define  $1 := \{0 \mid\} \in \mathcal{L}$ ,  $-1 := \{\mid 0\} \in \mathcal{R}$ , and  $*$   $:= \{0 \mid 0\}$  (called *star*)  $\in \mathcal{N}$ . We continue, one step after another, inductively, constructing all exponentially many new values possible. At the next step, for example, among many other possibilities, we find  $2 := \{1 \mid\}$ . We define  $n + 1 := \{n \mid\}$  and  $-n - 1 := \{\mid -n\}$  for  $n = 1, 2, \dots$ . We can verify that if  $G$  has  $k$  vertices, all blue, then  $G = k$ , and if  $H$  has  $l$  vertices, all red, then  $H = -l$ , for any positive integers  $k$  and  $l$ . (We subtly use  $k$  and  $l$  here in two senses, and we freely replace games by their corresponding values. The justification comes from the fact that values are equivalence classes of an equivalence relation preserved by all of the usual arithmetic operations and order properties we will define on them.)

## Negatives and sums

We saw that the negative of a game  $G = \{\mathcal{G}^L \mid \mathcal{G}^R\}$  corresponds to our intuitive notion of “switching places.” Your options in  $-G$  are exactly the negatives of my options in  $G$ , and *vice versa*, as illustrated by the games labeled  $G$  and  $-G$  in Figure 5. Thus, we define  $-G := \{-\mathcal{G}^R \mid -\mathcal{G}^L\}$ . The foundation of this inductive definition is that the empty set of options is its own negative.

We can verify by induction that the definition of negative integers given in this paragraph is consistent with the one given above. First, we observe that  $-0 = -\{\emptyset \mid \emptyset\} = \{-\emptyset \mid -\emptyset\} = \{\emptyset \mid \emptyset\} = 0$ . If, by the induction hypothesis, our definitions agree for  $-k$ , then  $\{\mid -k\} = -\{k \mid\}$ , and  $-k - 1 = \{\mid -k\} = -\{k\} = -(k + 1)$ .

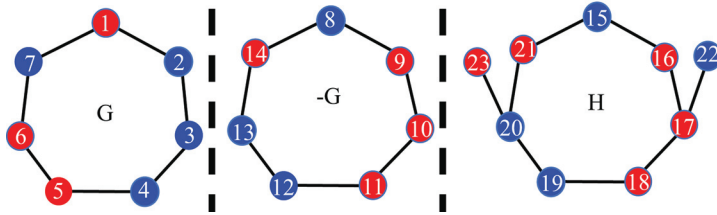


**Figure 5** Examples illustrating a game  $G$ , its negative  $-G$ , and a game  $H$  where  $G + H$  is a zero game. The numbers are labels used only for reference.

For games  $G$  and  $H$ , we agreed that the *sum*  $G + H$  is the game in which each of us, alternately, at each turn, makes a single allowable move in either game of our own choosing. Let's check that  $G + (-G)$  in Figure 5 is a zero game, that is, the first player loses. If I start, you can reply to every move  $n$  with  $n + 7 \pmod{14}$  and thereby get the last move. This same copy-cat argument works for  $G + (-G)$  in general.

What about  $G + H$  in Figure 5? Let's show that this is also a zero game. Suppose Left plays first in  $G + H$ . If Left's first move is in  $G$ , Right takes 23 at his first turn and then follows along in  $G$ , until Left chooses to take 22 (by her fifth move at the latest). Then, Right immediately takes 17, and wins as soon as Left's moves in  $G$  are exhausted. If Left's first move is 22, Right takes 23 and then wins by copying Left's moves in the other component. Suppose Right plays first in  $G + H$ . If Right's first move is in  $G$ , Left takes 22 and then replies with 20 as soon as Right is forced to take

23 (by his fourth move at the latest). Then, Left cannot be prevented from getting all eight moves and winning. If Right's first move is 23, Left takes 22 and then wins by copying Right's moves in the other component. So,  $G + H$  is a loss for the first player, a zero game.

Formally, we define

$$G + H := \{G + \mathcal{H}^L, \mathcal{G}^L + H \mid G + \mathcal{H}^R, \mathcal{G}^R + H\}.$$

We also write  $G - H$  for  $G + (-H)$ . One caution about these sums: we saw in our first two examples that a single game of Red-Blue Cherries is allowed to be played on a disconnected graph. As pointed out in AMGWN [1] and as seen in Figure 3B, a single game of Red-Blue Cherries on a disconnected graph is different from the sum of games on the components, because, in the former case, the minimum degree constraint applies globally, whereas, in the latter case, it applies locally to each game.

Now, we can define equality and an order relation for our game values, which include our newly defined numbers. We define  $G = H$  whenever, for all games  $X$ ,  $G + X$  and  $H + X$  are in the same outcome class. Then we can prove that  $G = H$  if and only if  $G - H \in \mathcal{P}$  (i.e.,  $G - H$  is a zero game). Next, we define  $G \geq H$  to mean  $G - H \in \mathcal{L} \cup \mathcal{P}$ . This is only a partial order. For example,  $0 \not\geq *$  and  $* \not\geq 0$ .

Verifying that everything is well-defined, that these conventional abuses of notation cause no problems, and that numbers as defined here have all of the expected properties is a lengthy process. However, in the end, we obtain a powerful way to compute and manipulate values of games.

## Additional examples

Next, we want to summarize the simplest games of Red-Blue Cherries and see a couple of new examples. The omitted proofs are straightforward.

**Proposition 1.** *A single blue vertex has value 1, and a single red vertex has value  $-1$ .*

**Proposition 2.** *Any game with only isolated (i.e., degree 0) vertices has value equal to the number of blue vertices minus the number of red vertices.*

**Proposition 3.** *Any two-vertex game has value equal to the number of blue vertices minus the number of red vertices.*

**Proposition 4.** *Any three-vertex games has a value equal to the number of blue vertices minus the number of red vertices, except for the game in Figure 6A and its negative, which have value 0.*

*Proof.* In a game with one or two vertices, all vertices have minimal degree. Thus, in the three-vertex case, the value can differ from the number of blue vertices minus the number of red vertices only if the player with the majority of vertices cannot move, that is, when all of the majority color vertices fail to have minimal degree. The only such possibility is the game in Figure 6A and its negative. ■

**Proposition 5.** *There exists a game on a connected graph with four vertices, for which it is not the case that the game value equals the number of blue vertices minus the number of red vertices.*

*Proof.* See the game in Figure 6B. The number of blue vertices minus the number of red vertices is 2. Left to move loses immediately, and Right to move loses after one move by each player, so the game's value is 0. ■



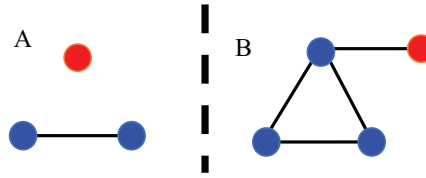


**Figure 6** Games with (A) three and (B) four vertices. Both have value 0.

In the next two examples, we see that some moves, called *dominated options*, are distinctly worse than some other move and should be avoided.

**Proposition 6.** *The six-vertex game in Figure 7A has value  $*$  =  $\{0 \mid 0\}$ .*

*Proof.* Whoever moves first can produce a zero game and win by avoiding his or her dominated options marked “D.” Other first moves lose. ■

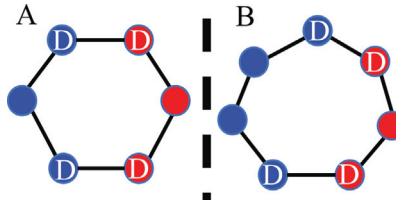


**Figure 7** Games with values (A)  $*$  =  $\{0 \mid 0\}$  and (B)  $\{1 \mid 0\}$ . “D” marks dominated options.

**Proposition 7.** *The seven-vertex game in Figure 7B has value  $\{1 \mid 0\}$ .*

*Proof.* Left can avoid either of her dominated options and still be a move ahead of a zero game, whereas Right can avoid his dominated options and leave a zero game. We will give a formal proof that other first moves are less advantageous below. ■

The two games in Figure 7 are in  $\mathcal{N}$ . We also noted that the game in Figure 3A is in  $\mathcal{N}$  and has value  $\{0 \mid 0\} = *$ . All games in  $\mathcal{N}$  have values, but their values are *not* numbers. Although  $*$  is not a number, we can still apply our definitions of negatives and sums to it. For example, we can compute

$$* + * = \{* + 0 \mid * + 0\} = \{* \mid *\} = 0.$$

Games with values  $\{m \mid n\}$ , where  $m > n$ , are called *switch games* because of their inherent first move advantage. The game in Figure 7B with value  $\{1 \mid 0\}$  is an example of a switch game.

## Rational values, dominated options, and simplicity

In addition to creating all of the integers, our inductive definition of numbers also creates all *dyadic rationals* (i.e., those of the form  $a/2^b$  for integers  $a$  and  $b$ ). One

can justify this by showing that  $\{0 \mid 1\} + \{0 \mid 1\} \geq 1$  and  $\{0 \mid 1\} + \{0 \mid 1\} \leq 1$ , so it is correct to *define*  $\frac{1}{2} := \{0 \mid 1\}$ , after which,  $\frac{1}{4} := \{0 \mid \frac{1}{2}\}$ , and, in general,

$$\frac{2n+1}{2^{m+1}} := \left\{ \frac{n}{2^m} \mid \frac{n+1}{2^m} \right\}.$$

The dyadic rationals are the only numbers that occur in our inductive process after *finitely* many steps. All of our games have finite length and sets of options, so, *if* they have numbers as values, then the values are dyadic rationals. (However, these numbers are dense in  $\mathbb{R}$ , so this construction obtains all of  $\mathbb{R}$ , among other things, at “step  $\omega$ .”)

The removal of *dominated options* corresponds to our intuitive notion of “making the best move.” If  $g_1^L$  and  $g_2^L$  are two options in  $\mathcal{G}^L$ , and if  $g_1^L > g_2^L$ , we can ignore  $g_2^L$  and get a game of the same value. We use a standard technique to prove this result: let  $G$  be any game with both options  $g_1^L$  and  $g_2^L$ , and  $H$  be the same game with the dominated option  $g_2^L$  omitted; show that  $G - H$  is a zero game and  $G = H$  by giving a copy-or-improve strategy that wins for the second player (where, in the missing case, the reply to  $g_2^L$  in  $G$  is  $-g_1^L$  in  $H$ ). Similarly, if  $g_1^R$  and  $g_2^R$  are two options in  $\mathcal{G}^R$ , and if  $g_1^R < g_2^R$ , we can ignore  $g_2^R$  and get a game of the same value. This result tells us that Left can never do better than choosing an option with the greatest value, and Right can never do better than choosing an option with the smallest value. It also tells us that if  $m < n$ , then

$$\{m \mid \mathcal{G}^R\} \leq \{n \mid \mathcal{G}^R\} \quad \text{and} \quad \{\mathcal{G}^L \mid m\} \leq \{\mathcal{G}^L \mid n\}.$$

With one more result, we will have everything we need about values of games. Let  $m$  and  $n$  be numbers with  $m < n$ . We define  $s$  to be the *simplest number* between  $m$  and  $n$  in the following sense:

1. If an integer lies between  $m$  and  $n$ , then  $s$  is the unique integer of smallest absolute value in the open interval number  $(m, n)$ .
2. Otherwise,  $s$  is the unique fraction  $a/2^b$  with odd integer  $a$  and smallest integer  $b > 0$  in the open interval  $(m, n)$ .

**Theorem 1** (Simplicity Theorem). *If  $m$  and  $n$  are numbers,  $m < n$ , and  $s$  is the simplest number between  $m$  and  $n$ , then  $\{m \mid n\}$  is a number, and  $s = \{m \mid n\}$ .*

*Proof.* See Albert, Nowakowski, and Wolfe [2, pp. 110–112]. ■

This result illustrates that numbers defined in terms of game values have multiple names. We defined  $2 := \{1 \mid\}$  above, but we also have  $2 = \{1 \mid 5\} = \{\frac{3}{2} \mid 4\}$ . This resembles our conventional knowledge that, for example,  $\frac{1}{4} = \frac{3}{12} = (-\frac{1}{2})^2$ . You may find it counter-intuitive that, e.g.,  $\{1 \mid 5\} = 2$  or  $\{\frac{3}{8} \mid 1\} = \frac{1}{2}$ , but the number we chose for  $\{m \mid n\}$  was created in our inductive definition of numbers at an earlier step than any other number in  $(m, n)$ . Thus, when we “chase all the way down the game tree” from  $m$  on the left and  $n$  on the right, we “land on” the first spot created.

## Games on trees

We need to agree on some terminology about graphs. A *leaf* is a vertex of degree one. A *cycle* is a connected graph with three or more vertices, all of degree two. A *path* is a graph produced by removing one vertex from a cycle. The resulting two leaves in a path are called its *end vertices*. A connected subgraph of a path that includes an end vertex is an *end segment*. A *tree* is a connected graph for which no subgraph is a cycle.

It is convenient to regard an isolated vertex as a path with equal end vertices, and to include the empty graph as a path or tree of size 0.

It is claimed in AMGWN [1] that all games with a leaf have integer values. However, their proof is by induction on the number of vertices, denoted  $|V(G)|$ , and the induction in their proof fails. If the last remaining leaf is removed, but the graph is still nonempty, as happens, for example, with the graph labeled  $H$  in Figure 5, the induction hypothesis cannot be applied. We will soon see why the value of  $H$  in Figure 5 is not an integer. Meanwhile, their proof does work when the graph is a tree because removing a leaf from a tree always results in a smaller tree. The proof below is exactly the one given by AMGWN, but the theorem applies only to trees, not to an arbitrary graph with a leaf.

**Theorem 2.** *The value of any game of Red-Blue Cherries on a graph that is a tree is an integer.*

*Proof.* The proof is an induction on  $n = |V(G)|$ . A single blue vertex has value  $\{0\} = 1$ ; similarly, a single red vertex has value  $\{0\} = -1$ . Now suppose the statement is true for game positions on a tree with  $n = t - 1$ . Consider a game  $G$  with  $G = \{\mathcal{G}^L \mid \mathcal{G}^R\}$  and with  $|V(G)| = t$ . We will show that

$$\mathcal{G}^L \leq G - 1 \quad \text{and} \quad \mathcal{G}^R \geq G + 1,$$

which implies that  $G$  is an integer. If  $\mathcal{G}^L$  or  $\mathcal{G}^R$  is empty, the claim is clear by the Simplicity Theorem for game values. So, suppose that both  $\mathcal{G}^L$  and  $\mathcal{G}^R$  are nonempty.

First, we will show that  $\mathcal{G}^L \leq G - 1$ . Since  $\mathcal{G}^L \neq \emptyset$ ,  $G$  has a blue leaf. Then  $\mathcal{G}^L$  is  $G$  with a blue leaf removed. We will show that the sum of  $\mathcal{G}^L$  and  $G - 1$  is a Right win when Left starts, or  $\mathcal{G}^L - (G - 1) \leq 0$ . It is enough to give a winning strategy for Right when Left starts. First, note that  $-(G - 1)$  is the game  $-G + 1$ , which is  $-\mathcal{G}^L$  with a red leaf attached along with an isolated blue vertex. If Left first elects to play in  $-(G - 1)$  by taking the isolated vertex, Right responds by taking the red leaf in the same game. From then on, Right plays a copy-cat strategy, mirroring Left's moves in  $\mathcal{G}^L$  with the corresponding ones in  $-\mathcal{G}^L$  playing in  $\mathcal{G}^L$  when left plays in  $-\mathcal{G}^L$ . Right wins by taking the last vertex. If Left's first move is to play in  $\mathcal{G}^L$ , then Right will copy her move in  $-\mathcal{G}^L$ , unless Left takes the vertex in  $\mathcal{G}^L$  that has been exposed by removal of the blue leaf of  $G$ . In this case, Right takes the red leaf attached to  $-\mathcal{G}^L$  and then continues the mirroring strategy by replying in  $-\mathcal{G}^L$  whenever Left plays in  $\mathcal{G}^L$  and vice versa. If Left continues to take blue vertices newly exposed in  $\mathcal{G}^L$  whose partners in  $-\mathcal{G}^L$  have not been exposed due to the presence of the extra leaf, Right is guaranteed moves in  $-\mathcal{G}^L$  since he is one vertex behind: Left's previous such play in  $\mathcal{G}^L$  is Right's play in  $-\mathcal{G}^L$ . This continues until Left takes the isolated vertex, to which Right responds by taking the extra red vertex in  $-\mathcal{G}^L$ . By using this copying and one behind strategy, Right can guarantee that he is the last to play whenever Left starts.

Next, we show that  $\mathcal{G}^R \geq G + 1$ . Since  $\mathcal{G}^R \neq \emptyset$ ,  $G$  has a red leaf. So represent  $G$  as  $\mathcal{G}^R$  with a red leaf attached. Then to prove  $\mathcal{G}^R - (G + 1) \geq 0$  we need to give a winning strategy for Left when Right starts in the game  $\mathcal{G}^R - (G + 1)$ . The strategy is identical to that above, with the colors and Left and Right reversed.

Finally, since  $\mathcal{G}^L$  and  $\mathcal{G}^R$  have integer game values by the hypothesis, and since we have shown that  $\mathcal{G}^L \leq G - 1$  and  $\mathcal{G}^R \geq G + 1$ , the value for  $G$  is, by the Simplicity Theorem, also an integer. ■

**Corollary 1.** *A game of Red-Blue Cherries on a tree with  $n > 0$  vertices, all blue, has value  $n$ , and a game on a tree with  $n > 0$  vertices, all red, has value  $-n$ .*

*Proof.* A single blue (red) vertex has value 1 ( $-1$ ). The result then follows immediately from the inductive definition of integers. ■

**Corollary 2.** *For any integer  $n$ , a game of Red-Blue Cherries on a connected graph with value  $n$  exists.*

*Proof.* For  $n = 0$ , see game  $A$  in Figure 4. For  $n \neq 0$ , apply Corollary 1. ■

## Games on paths

For finding nonintegral values, the Simplicity Theorem tells us that we will need to look at graphs with embedded cycles. Cycles become paths when one vertex is removed, so if we knew how to compute the values of games on paths, we could compute the values of games on cycles. We could evaluate the paths resulting from each first move, discard dominated options, and apply the Simplicity Theorem. But we are in luck, because AMGNW [1] describe three steps, called Rule-1, Rule-2, and Rule-3 here, which, when applied in order, compute the value of any path  $P$ :

Rule-1: Contract the longest end segments of  $P$  consisting of vertices of the same color to a single such vertex, and call the result  $P'$ . Let  $D_b$  and  $D_r$  be the total numbers of blue and red vertices removed by these contractions, respectively.

Rule-2: Contract the longest end segments of  $P'$  consisting of consecutive Red-Blue pairs or of consecutive Blue-Red pairs to a single such pair, and call the result  $P''$ .

Rule-3: Compute the value of  $P$  as follows:

- (a) If  $P''$  has length 4 or less, the value of  $P$  is  $D_b - D_r$ , plus 1 for every blue vertex in  $P''$ , and minus 1 for every red vertex in  $P''$ .
- (b) If  $P''$  has length greater than 4, match its end segments (or those of its negative) to one of the six pairs of end segments shown in Figure 8. The value of  $P$  is  $D_b - D_r$  plus (or minus) the adjustment shown on the right.

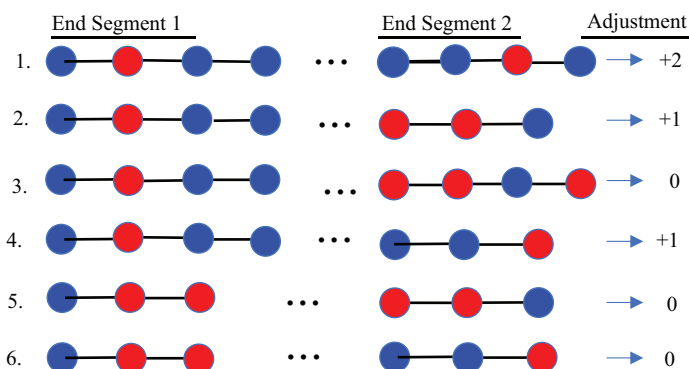


**Figure 8** Computing the Rule-3b adjustment in the path algorithm for paths  $P''$  longer than four. The end vertex of End Segment 1 is the leftmost. The end vertex of End Segment 2 is the rightmost.

Let's look at an example. For the path  $P$  shown in Figure 9, Rule-1 tells us to contract  $P$  to the path  $P'$ , set  $D_b = 2$ , and set  $D_r = 1$ . Rule-2 tells us to contract  $P'$  to the path  $P''$ . Rule-3b tells us to match  $P''$  with case 4 in Figure 8 and find the adjustment +1 on the right. Thus,

$$P = D_b - D_r + 1 = 2 - 1 + 1 = 2.$$

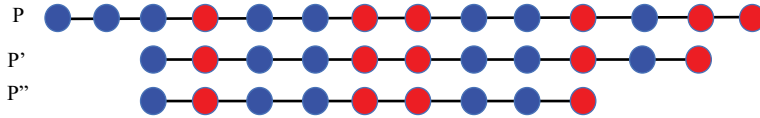


**Figure 9** Example used to illustrate the path algorithm.

**Theorem 3** (Albert, McCurdy, Grossman, Nowakowski, and Wolff). *Applying Rule-1, Rule-2, and Rule-3, in order, correctly computes the value of any path  $P$ .*

This result is proved in AMGWN [1] as follows. A path is a tree, so it has integral value, as discussed above and proved in Theorem 2. For Rule-1, suppose  $n + 1$  blue vertices in  $P$  are contracted to a single blue vertex in  $P'$ . They show that  $P - P' - n$  is a zero game. Similarly, if  $m + 1$  red vertices are contracted to 1, they show that  $P - P' + m$  is a zero game. For Rule-2, they show that  $P' - P''$  is a zero game. Then, they show that the six cases in Figure 8, their negatives, and a few strings of length less than 5 exhaust all remaining possibilities, and they compute the values of these cases directly. For example, in Figure 8, the second player has straightforward wins in cases 3, 5, and 6, and the other cases reduce to zero games after Left makes 1 or 2 moves.

To become more familiar with the path algorithm, let's check what is claimed about Figure 7B by computing the values of the paths resulting from all first moves. If Left removes a dominated option, we get  $+2 - 2 = 0$  from Rule-1 and an adjustment of 0 for value 0. If Left removes a nondominated option, we get 1 from Rule-1 and an adjustment of 0 for value 1. If Right removes a dominated option, we get  $+3 - 1 = 2$  from Rule-1 and an adjustment of 0. If Right removes his nondominated option, we get nothing from Rule-1 and an adjustment of 0. So the game has value  $\{0, 0, 1, 1 \mid 2, 2, 0\} = \{1 \mid 0\}$  as claimed. This completes the proof of Proposition 7.

### Games with values $\frac{1}{2}$ and $\frac{3}{2}$

The first game for which we will compute a fractional value is the seven-cycle shown in Figure 10A. Next to each vertex is the value of the resulting game when that vertex is removed, as computed with the path algorithm. This game is a win for Left because, if Left moves first, Left can take vertex 3 and win immediately, whereas, if Right moves first, Right cannot prevent Left from potentially making all four moves. For example, if Right takes vertex 6 and Left takes vertex 7, Right must take vertex 1 or vertex 5, after which Left has more moves than Right.

We prove that this game has value  $\frac{1}{2} = \{0 \mid 1\}$  by computing the values of all of the paths after each vertex is taken, eliminating dominated options, and applying the Simplicity Theorem. Table 1 shows the steps and results of applying the path algorithm to the paths that result from each possible first move. Removing vertex 6 produces the path with smallest value among Right's options. The resulting path has value 1. The largest path value after a blue vertex is removed is 0. This occurs after the removal of vertex 2, 3, or 4. By the Simplicity Theorem, the cycle has value

$$\{0, 0, 0, -1 \mid 2, 2, 1\} = \{0 \mid 1\} = \frac{1}{2}.$$

One may be able to grasp this result more intuitively by checking directly that the sum of two copies of the game in Figure 10A and a single red vertex is a zero game. This approach, however, rapidly gets harder as the graphs get bigger.

Figure 10B shows our second fractional game, a game with value  $\frac{3}{2}$ . Next to each vertex is the value of the resulting game when that vertex is removed first, again com-

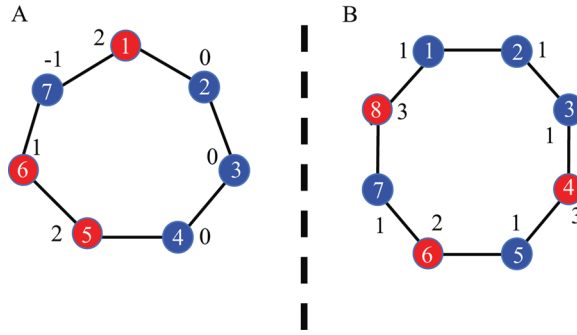


**Figure 10** (A) A game with value  $\frac{1}{2}$  and (B) a game with value  $\frac{3}{2}$ . A number inside a vertex is a label. A number outside shows the value of the resulting game after deleting that vertex.

First Move	Rule-1 Removals; Result	Rule-2 Removals	Rule-3 Adjustment	Path Value
Vertex 1 (Red)	vertices 2, 3; +2	—	0	2
Vertex 2 (Blue)	vertex 3; +1	—	-1	0
Vertex 3 (Blue)	none; 0	vertices 1, 2	0	0
Vertex 4 (Blue)	vertices 3, 5; +1, -1	vertices 6, 7	0	0
Vertex 5 (Red)	vertices 3, 4; +2	vertices 6, 7	0	2
Vertex 6 (Red)	none; 0	—	1	1
Vertex 7 (Blue)	vertex 6; -1	—	0	-1

TABLE 1: Applying the Path Algorithm to the games resulting from Figure 10A.

puted with the path algorithm. Because any move by Left produces a game with value 1, and any move by Right produces a game of value 2 or greater, the original game has value

$$\{1, 1, 1, 1, 1 \mid 2, 3, 3\} = \{1 \mid 2\} = \frac{3}{2}.$$

### Games with values $n + \frac{1}{2}$

It would be nice to have a single family of games with values  $n + \frac{1}{2}$  for all  $n > 0$ , but the games in Figure 10 with values  $\frac{1}{2}$  and  $1\frac{1}{2}$  do not generalize easily to values  $2\frac{1}{2}, 3\frac{1}{2}, \dots$ . Also, the family of cycles of length  $2n + 5$  in Figure 11 attaining these larger values does not contract to values  $\frac{1}{2}$  or  $1\frac{1}{2}$ . Thus, we get our result by combining cases.

**Lemma 1.** *For every integer  $n > 1$ , there exists a game of Red-Blue Cherries played on a cycle with value  $n + \frac{1}{2}$ .*

*Proof.* Figure 11 displays a cycle of length  $2n + 5$ ,  $n > 1$ . We show that it has value  $n + \frac{1}{2}$  by computing the values of all of Left's and Right's options with the path algorithm, eliminating dominated options, and applying the Simplicity Theorem. If Right plays at R1, R2, or R3, his options have values  $n + 2$ ,  $n + 1$ , and  $2n$ , respectively, so



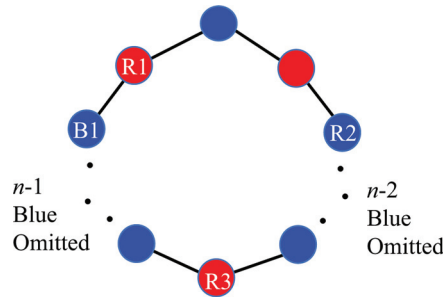


**Figure 11** A cycle of length  $2n + 5$ . Eight vertices are shown and  $(n - 1) + (n - 2) = 2n - 3$  vertices are unpictured. It has value  $n + \frac{1}{2}$ ,  $n > 1$ .

he will choose R2. For example, Figure 12A shows the path that remains after Right's first move at R2. Applying the path algorithm to Figure 12A results in contributions of  $n - 1$  from Rule-1 and  $+2$  from Rule-3b, so the result is  $n - 1 + 2 = n + 1$ . If Left plays at the single blue vertex, the string of  $n$  blue vertices, or the string of  $n + 1$  blue vertices, her options have values  $0$ ,  $n - 1$ , and  $n$ , respectively, so she will choose the last of these. For example, Figure 12B shows the path that remains after Left's first move at B1. Applying the path algorithm to Figure 12B results in a contribution of  $n - 1$  from Rule-1, removal of one pair according to Rule-2, and a contribution of  $+1$  from Rule-3b, so the result is  $n - 1 + 1 = n$ . It is straightforward to check that all other Left options are no better. Thus, we have verified that the value of this game is

$$\{0, n - 1, n \mid n + 2, n + 1, 2n\} = \{n \mid n + 1\} = n + \frac{1}{2}.$$

■

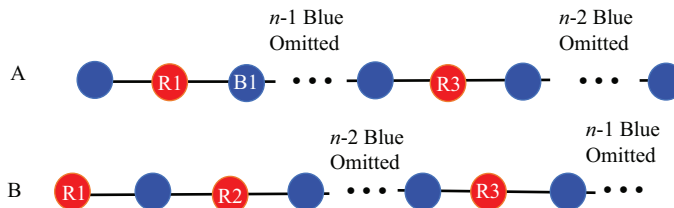


**Figure 12** Paths from Figure 11: (A) after removing R2 and (B) after removing B1

**Theorem 4.** For every integer  $n$ , there exists a game of Red-Blue Cherries played on a cycle with value  $n + \frac{1}{2}$ .

*Proof.* It is sufficient to show the result for  $n + \frac{1}{2} > 0$ , because interchanging all red and blue vertices negates the value of the game. We constructed examples with values  $\frac{1}{2}$  and  $1 + \frac{1}{2}$  shown in Figure 10 and with values  $n + \frac{1}{2}$ ,  $n > 1$  shown in Figure 11. ■

### A game with value $\frac{1}{2}$ on a graph with a leaf

Did you notice that the game in Figure 10A and the game labeled  $G$  in Figure 5 are the same game, which we now know has value  $\frac{1}{2}$ ? Because  $G + H = 0$  in

Figure 5, we now also know that the game labeled  $H$  has value  $-\frac{1}{2}$ , and, therefore,  $-H = \frac{1}{2}$ . This single example simultaneously refutes the assertion about values of games with a leaf and answers the open question about integer values presented in Nowakowski [7].

## Games with values $\frac{1}{2^n}$ and $1 - \frac{1}{2^n}$

**Theorem 5.** *For every integer  $n$ , there exists a game of Red-Blue Cherries on a connected graph with value  $\frac{1}{2^n}$ .*

*Proof.* We have already covered all cases for  $n \leq 1$ . For  $n > 1$  we proceed by induction. The base case is  $n = 2$ .

We show that the game in Figure 13A has value  $\frac{1}{2^2} = \frac{1}{4}$ . If Left plays first at vertex U, Left loses, but Left can play first at vertex Q or R, which produces a zero game, and Left wins. If Right starts at vertex T or V, the next two moves are forced, after which Left is a move ahead, so both of these first moves for Right leave a position of value 1. But Right can do better, because we know that the position after removing vertex 2 has value  $\frac{1}{2}$ . Therefore, the game has value

$$\left\{ -1, 0, 0 \mid \frac{1}{2}, 1, 1 \right\} = \left\{ 0 \mid \frac{1}{2} \right\} = \frac{1}{4} = \frac{1}{2^2}$$

by the removal of dominated options and the Simplicity Theorem.

The induction hypothesis is that the game in Figure 13B has value  $\frac{1}{2^k}$ , where the ellipses indicate that vertices  $3, \dots, k-1$  adjacent to vertices P and S are not shown. For the induction step, we need to show that the game in Figure 13C has value  $\frac{1}{2^{k+1}}$ . In Figure 13C, the analysis of initial moves at vertices Q, R, T, U, and V is exactly the same as that for Figure 13A. However, by starting at vertex  $j$ , Right has the option to create the game in Figure 13B of value  $\frac{1}{2^k}$ , and any other first move at  $2, \dots, k$  results in a position symmetric to Figure 13B. Therefore, the game in Figure 13C has value

$$\left\{ -1, 0, 0 \mid \frac{1}{2^k}, 1, 1 \right\} = \left\{ 0 \mid \frac{1}{2^k} \right\} = \frac{1}{2^{k+1}}$$

by the removal of dominated options and the Simplicity Theorem. ■

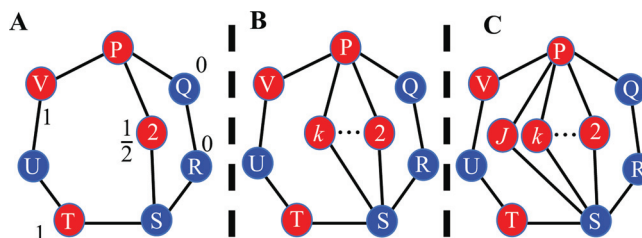


**Figure 13** Games with values (A)  $\frac{1}{2^2} = \frac{1}{4}$ , (B)  $\frac{1}{2^k}$ ,  $k \geq 2$ , and (C)  $\frac{1}{2^{k+1}}$ , where  $j = k + 1$  and  $k \geq 2$ . A symbol inside a vertex is a label. A number outside shows the value of the game after deleting that vertex.

**Theorem 6.** For every integer  $n$ , there exists a game of Red-Blue Cherries on a connected graph with value  $1 - \frac{1}{2^n}$ .

*Proof.* We have already covered all cases for  $n \leq 1$ . For  $n > 1$  we proceed by induction. The base case is  $n = 2$ .

We show that the game in Figure 14A has value  $1 - \frac{1}{2^2} = \frac{3}{4}$ . If Right moves first at vertex T or V, the resulting game has value 1, because, after Left replies at vertex U, we reach a zero game: Left has no move, but after Right's forced move, Left can play at R and win. If Left moves first at vertex U, Right can reply at vertex V and reach the same zero game, so this Left option has value  $-1$ . Left can do better by starting at vertex 2 and creating the winning position of value  $\frac{1}{4}$  we saw in Figure 13A. But now we are experts, and Left's expert first move is at vertex R, which denies Right the possibility of replying at vertex W. After this move, Right's best options have value 1 (at vertices T and V), and Left's have value 0 (at vertices 2 and Q), so playing first at vertex R leaves a value of  $\{0|1\} = \frac{1}{2}$ . Therefore, the game in Figure 14A has value

$$\left\{-1, \frac{1}{4}, \frac{1}{2} \mid 1, 1\right\} = \left\{\frac{1}{2} \mid 1\right\} = \frac{3}{4} = 1 - \frac{1}{2^2}.$$

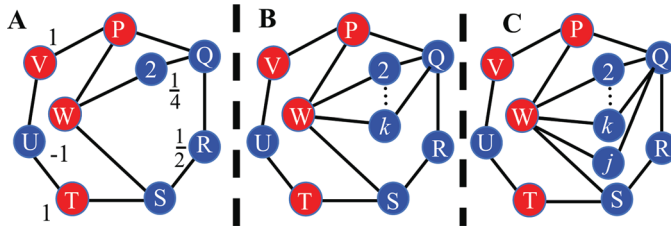


**Figure 14** Games with values (A)  $1 - \frac{1}{2^2} = \frac{3}{4}$ , (B)  $1 - \frac{1}{2^k}$ ,  $k \geq 2$ , and (C)  $1 - \frac{1}{2^{k+1}}$  for  $j = k + 1$ ,  $k \geq 2$ . A symbol inside a vertex is a label. A number outside shows the value of the game after deleting that vertex.

The induction hypothesis is that the game in Figure 14B has value  $1 - \frac{1}{2^k}$ , where the ellipses indicate that vertices  $3, \dots, k - 1$  adjacent to vertices W and Q are not shown. For the induction step, we need to show that the game in Figure 14C has value  $1 - \frac{1}{2^{k+1}}$ . In Figure 14C, Right, again, has options of value 1 at vertices T and V, because Left's reply at vertex U leaves a zero game. But in this game Left can play first at vertex  $j$  and produce the game in Figure 14B of value  $1 - \frac{1}{2^k}$ . Playing first at vertex R or any of  $2, \dots, k$  transposes into the same result, and playing first at vertex U is clearly inferior, so this game has value

$$\left\{1 - \frac{1}{2^k} \mid 1\right\} = 1 - \frac{1}{2^{k+1}}.$$

■

## One more game

Let's show that the game in Figure 15 is in  $\mathcal{L}$  and has value

$$\left\{0, 0 \mid *, *, \{1 \mid 0\}, \frac{1}{8}\right\} = \{0 \mid *\} := \uparrow.$$



which we call  $\uparrow$ . We know that  $\uparrow \in \mathcal{L}$ , so  $0 < \uparrow$ , but we can also show that for any positive number  $x$ ,  $0 < \uparrow < x$ . Indeed, for all positive integers  $n$ ,  $\ast < 2^{-n}$ , so

$$\uparrow = \{0 \mid \ast\} \leq \{0 \mid 2^{-n}\} = 2^{-(n+1)} < 2^{-n}.$$

The values  $\uparrow$  and  $-\uparrow := \{\ast \mid 0\}$  are not isolated curiosities, but merely the first encountered in multiple infinite hierarchies of infinitesimal values.

## Epilogue

We answered the question about integer game values and corrected the claim about values of games with a leaf in Nowakowski [7] (as noted in Nowakowski [8]). All of our results are direct constructions that follow from (1) our definitions of games, values, numbers, negatives, sums, equality, and order; and (2) the elimination of dominated options, the Simplicity Theorem, and the path algorithm. We needed the theorem that a game on a graph that is a tree has integral value to prove certain claims in the path algorithm. We took the path algorithm and proof of the theorem on trees directly from AMGNW [1].

Although all of our results have been demonstrated from first principles, the CGSuite software written by Aaron Siegel and described in Albert, Nowakowski, and Guy [2] was augmented with a script to play Red-Blue Cherries and used to verify (a finite subset of) the game values in this article.

We have seen many examples, but a complete analysis of this game seems to be a long way off. One major difficulty, encountered already in our second example, is that when, during play, a game splits into components, the single game on the resulting components is *not* the same as the sum of distinct games on these components. We finish by listing four open questions about Red-Blue Cherries:

- **Question 1:** Do single games with dyadic rational values other than  $n$  or  $n \pm \frac{1}{2^m}$  exist? Perhaps start by trying to find a game with value  $\frac{3}{8} = \{\frac{1}{4} \mid \frac{1}{2}\}$ .
- **Question 2:** Can the games in  $\mathcal{N}$ , or at least some of them, which are wins for the first player, be systematically categorized?
- **Question 3:** What additional games or families of games with infinitesimal values exist?
- **Question 4:** What upper or lower bounds exist for the sizes of the graphs needed to obtain certain game values? For example, are the games in Figures 16 and 15 the smallest with fractional and positive but infinitesimal values, respectively?

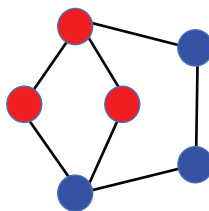


**Figure 16** A 6-vertex game with value  $\frac{1}{2}$ .

**Acknowledgments** Matthew Bardoe pointed out this problem to me, helped to compute fractional game values, and reviewed a draft of this paper. Joseph Shipman, Peter Winkler, the referees, and the editor offered many helpful comments. Richard Nowakowski graciously provided the unpublished paper [1] along with words of encouragement.

## REFERENCES

- [1] Albert, M. H., McCurdy, S. K., Grossman, J. P., Nowakowski, R. J., Wolfe, D. A note on picking ripe cherries at waist height. (Unpublished paper).
- [2] Albert, M. H., Nowakowski, R. J., Wolfe, D. (2019). *Lessons in Play: An Introduction to Combinatorial Game Theory*. 2nd ed. Boca Raton, FL: CRC Press.
- [3] Berlekamp, E. R., Conway, J. H., Guy, R. K. (2003). *Winning Ways for Your Mathematical Plays*. Vol. 1. Natick: A. K. Peters.
- [4] Berlekamp, E. R., Conway, J. H., Guy, R. K. (2003). *Winning Ways for Your Mathematical Plays*. Vol. 3. Natick: A. K. Peters.
- [5] Conway, J. H. (2001). *On Numbers and Games*. 2nd ed. Natick: A. K. Peters.
- [6] Conway, J. H. (1978). A gamut of game theories. *Math. Mag.* 51(1): 5–12. [doi.org/10.1080/0025570X.1978.11976668](https://doi.org/10.1080/0025570X.1978.11976668)
- [7] Nowakowski, R. J. (2015). Unsolved problems in combinatorial games. In: Nowakowski, R. J., ed. *Games of No Chance 4*. New York: Cambridge University Press, pp. 279–308.
- [8] Nowakowski, R. J. (2019). Unsolved problems in combinatorial games. In: Larsson, U., ed. *Games of No Chance 5*. New York: Cambridge University Press, pp. 125–168.

**Summary.** We construct games of “Red-Blue Cherries” with values  $n$ ,  $n + \frac{1}{2}$ ,  $\frac{1}{2^n}$ , and  $1 - \frac{1}{2^n}$  for all integers  $n$ . We also show games with values that are *not* numbers, specifically games with a value called *star*, an example of a *switch game*, and a game with a value called *uparrow*. We prove that games on trees always have integer values, and we present a previously discovered but unpublished algorithm to compute values of games on paths efficiently. These results correct a claim and answer an open question posed about this game.

**SCOTT ANDREW HERMAN** is in the class of 2023 at the University of Pennsylvania, where he is a member of the lightweight rowing team. In 2019, he graduated from Choate Rosemary Hall, where he first got interested in combinatorial games.

# Let's Get Rolling! Exact Optimal Solitaire Yahtzee

KATHRYN KELLY

California Polytechnic State University  
San Luis Obispo, CA 93407  
[katylynnkelly@gmail.com](mailto:katylynnkelly@gmail.com)

JEFFREY LIESE

California Polytechnic State University  
San Luis Obispo, CA 93407  
[jliese@calpoly.edu](mailto:jliese@calpoly.edu)

If you happen to be a strategy game aficionado, chances are that you have played (or at least heard of) Yahtzee®. It was introduced in the 1940s by Milton Bradley (now owned by Hasbro), and has provided many hours of entertainment in our families and many others alike. The game is played in a sequence of rounds, and in each round, a player rolls five dice. He or she then makes decisions about which dice to keep and which to reroll, which ultimately ends up with five dice that can no longer be rerolled. The player then selects a category from their scorecard (which is divided into an upper section and a lower section) in which to score this hand based on the numbers that are showing. The rules of scoring are more thoroughly explained in the next section. The best possible hand in Yahtzee is five of a kind, and this hand is called a yahtzee, the name of the game. Those who have indulged in a game realize immediately that the best strategy is not intuitively obvious. As a challenge to those who have played, grab a pencil and jot down which dice you would elect to keep if your opening roll was any one of the four shown in Table 1. The optimal choices will be shared in the final section, so no peeking.





















Roll 1:					
Roll 2:					
Roll 3:					
Roll 4:					

TABLE 1: Four first rolls to challenge your skills.

We wondered how one might play Yahtzee optimally and hoped the game was simple enough to analyze by brute-force. Unfortunately, with multiple players this type of analysis becomes extremely computationally expensive. The reason for the complexity of the multiplayer game is that when other players are introduced, the players' goals shift from trying to maximize their scores to trying to maximize their probability of winning. While these two objectives seem like they should be aligned, this is not always the case. For example, if your opponent was lucky enough to score a yahtzee in the first round, you would need to play more aggressively in an attempt



to win. This strategy would actually reduce the expected value of your score, but would increase the probability of victory. In the multiplayer situation, an optimal strategy would not only depend on the scorecard of a player, but also on the scorecard of his or her opponents. Even with only two players the number of combinations is too large to handle with an inexpensive workstation. So, we decided to focus on the solitaire game using the official rules, i.e., the rules that currently come with the game if you were to purchase it today.

Our definition of an optimal player is one whose decisions always maximize his or her expected score. Here were some of our questions: Under optimal play, how many points would one expect to score? How do the individual scoring categories contribute to the total? What are the standard deviations of the scores by category? At what point during a game should particular categories be scored? A quick search on the Internet revealed, perhaps not surprisingly, that many others before us had asked and answered the same types of questions about solitaire Yahtzee and have published some numerical results [1, 2]. Therefore, some of the contents of this article will duplicate (confirm) results that have been highlighted elsewhere. Of particular interest, Tom Verhoeff has provided an online implementation [3] of the optimal solitaire Yahtzee player as well as a web application [4] where you can roll dice, make selections and be graded against the optimal selection.

However, what was truly surprising about our search was that we were unable to find exact answers to our questions, only numerical approximations. Additionally, we had questions whose answers were not readily available upon a simple Internet search. So we set out on a quest to find exact answers and implemented the optimal solitaire Yahtzee player in Mathematica®. One of our main results is the expected score of the game as a rational number under optimal play. This article consists of a partial analysis of our efforts. Let's get rolling!

## Rules of the game

The official rules can be found online in a variety of places, such as Hasbro's official website [5]. We will merely provide a brief explanation of the rules in this section.

Upper section	How to score
Aces (Ones)	Total of aces only
Twos	Total of twos only
Threes	Total of threes only
Fours	Total of fours only
Fives	Total of fives only
Sixes	Total of sixes only
Lower section	
3 of a kind	Total of all 5 dice
4 of a kind	Total of all 5 dice
Full house (3 of a kind and 2 of a kind)	25 points
Small straight (4 consecutive dice)	30 points
Large straight (5 consecutive dice)	40 points
Yahtzee (5 of a kind)	50 points
Chance	Total of all 5 dice

TABLE 2: A Yahtzee scorecard with scoring rules.

The game is played with some number of players in a sequence of 13 rounds. In each round, the players take turns completing a roll. During a roll, a player begins by rolling

five dice at which point he or she can decide the roll is over or make a *modification*. A modification allows the player to select a subset of their five dice to keep and to re-roll the unselected dice. During a roll, the player can perform a maximum of two modifications at which point he or she is left with five dice called a *hand*. To complete a roll, the player may score the hand in any one of 13 fixed categories on his or her scorecard that has not been previously scored. There are some simple rules about how many points a hand is worth in each category.

The scorecard is divided up into two sections, the *upper section* and *lower section*, which are shown in Table 2 along with explanations about how each category is scored. It is worth noting that a player can score in a category where the criteria for scoring is not met for zero points. In fact, the optimal solitaire player will choose to score a category for zero points in certain situations.

There are three additional special rules that exist in the official Yahtzee rules that have not yet been addressed. First, there is the *upper section bonus*. If, at the end of the game, a player has achieved a score of 63 points or more in the upper section, then he or she would achieve a 35-point bonus onto the final score. Second, there is another type of bonus called the *yahtzee bonus*, which is designed to reward a player who obtains multiple yahtzees during a game. If a player rolls a yahtzee and has previously scored in the yahtzee category with 50 points (meaning he or she has already obtained at least one yahtzee) then the player earns a 100-point bonus onto the final score. Lastly, there is the notion of a *joker*, which is again designed to reward a player obtaining multiple yahtzees by allowing a yahtzee to be scored in additional categories for full credit. If a yahtzee is rolled and the corresponding upper section category has already been filled in, the player must score in any open lower section category under the following rules given in Table 3. If the corresponding upper section category has already been filled in and the lower section is entirely filled, then the player must score a zero in one of the open upper section categories. We are using a strict interpretation of the official rules, which is sometimes referred to as the *forced joker rule*.

Lower section	
3 of a kind	Total of all 5 dice
4 of a kind	Total of all 5 dice
Full house	25 points
Small straight	30 points
Large straight	40 points
Chance	Total of all 5 dice

TABLE 3: The yahtzee joker values for the lower section.

## Probability generating polynomials

Given a discrete random variable  $X : \Omega \rightarrow \mathbb{N}$  with probability function  $P$ , we denote the probability that  $X$  is equal to the natural number  $n$  [i.e.,  $P(X = n)$ ] by  $p_X(n)$ . We can also define the *probability generating function* of  $X$ , by

$$G_X(x) := \sum_{n=0}^{\infty} p_X(n)x^n.$$

In other words,  $G_X$  is a power series in  $x$  centered at 0 whose coefficient of  $x^n$  is the probability that the random variable  $X$  is equal to  $n$ . If  $\Omega$  is finite, then  $G_X$  is simply

a polynomial, and we call it a *probability generating polynomial*. For the application of Yahtzee, there are only a finite number of outcomes of a game and thus we will be working purely with probability generating polynomials. Manipulating these polynomials can be quite useful. For one, note that

$$p_X(n) = \frac{G_X^{(n)}(0)}{n!},$$

and thus one can easily extract probabilities from the probability generating polynomial. Also, given a random variable  $S$  which is a sum of independent random variables  $X_1, X_2, \dots, X_n$ , say

$$S = \sum_{i=1}^n X_i, \text{ then } G_S = \prod_{i=1}^n G_{X_i}.$$

For example, suppose  $X$  is the discrete random variable corresponding to the roll of a single die. Then

$$p_X(n) = \begin{cases} 1/6 & 1 \leq n \leq 6 \\ 0 & \text{otherwise,} \end{cases}$$

and the probability generating polynomial is given by

$$G_X = \frac{x^6}{6} + \frac{x^5}{6} + \frac{x^4}{6} + \frac{x^3}{6} + \frac{x^2}{6} + \frac{x}{6}.$$

If we let  $X_1$  and  $X_2$  each represent the roll of a particular die, then we can model the roll of two dice by the random variable  $Y = X_1 + X_2$ . Conveniently, the fact mentioned in the previous paragraph tells us that

$$\begin{aligned} G_Y &= G_{X_1} \cdot G_{X_2} = G_X^2 \\ &= \frac{x^{12}}{36} + \frac{x^{11}}{18} + \frac{x^{10}}{12} + \frac{x^9}{9} + \frac{5x^8}{36} + \frac{x^7}{6} + \frac{5x^6}{36} + \frac{x^5}{9} + \frac{x^4}{12} + \frac{x^3}{18} + \frac{x^2}{36}. \end{aligned}$$

From this, one can quickly determine that the probability of obtaining a 7 when rolling two dice is exactly  $1/6$ .

Another advantage of working with probability generating polynomials is that one can easily determine the expectation, variance and standard deviation (as well as other moments). In particular, the expectation of  $X$  (denoted by  $E(X)$  or  $\mu_X$ ) is given by  $E(X) = G'_X(1)$ . Similarly, the variance of  $X$  is given by

$$\text{Var}(X) = G''_X(1) + G'_X(1) - [G'_X(1)]^2$$

and the standard deviation of  $X$  denoted by  $\sigma_X = \sqrt{\text{Var}(X)}$ .

Returning to our dice examples, one can easily compute that

$$G'_X(x) = x^5 + \frac{5x^4}{6} + \frac{2x^3}{3} + \frac{x^2}{2} + \frac{x}{3} + \frac{1}{6}$$

and

$$G''_X(x) = 5x^4 + \frac{10x^3}{3} + 2x^2 + x + \frac{1}{3}.$$

Thus,

$$E(X) = G'_X(1) = 1 + \frac{5}{6} + \frac{2}{3} + \frac{1}{2} + \frac{1}{3} + \frac{1}{6} = \frac{7}{2} = 3.5$$

and

$$\begin{aligned} \text{Var}(X) &= G''_X(1) + G'_X(1) - [G'_X(1)]^2 \\ &= \frac{35}{3} + \frac{7}{2} - \left(\frac{7}{2}\right)^2 = \frac{35}{12} \approx 2.91667. \end{aligned}$$

For two dice, one could perform similar calculations to obtain that  $E(Y) = 7$  and  $\text{Var}(Y) = 35/6 \approx 5.83333$ .

## Analyzing Yahtzee

This section describes the idea behind our algorithm, but it does not completely describe every aspect of the implementation. It mostly consists of technical details, so feel free to skip to the next section if you are more interested in the results.

As mentioned, there are 15 categories that contribute to a Yahtzee score, the 13 scoring categories and the two bonus categories. To simplify things, let us label them: Ones, Twos, Threes, Fours, Fives, Sixes, Three of a kind, Four of a kind, Full house, Small straight, Large straight, Yahtzee, Chance, Upper section bonus, and Yahtzee bonus with the integers from 1 to 15, respectively. Let  $X_i$  denote the random variable corresponding to the  $i$ th category on this list. With this setup, the final score can be regarded as a random variable  $Y := \sum_{i=1}^{15} X_i$ . Using Mathematica, we wrote an algorithm to compute the probability generating polynomials  $G_{X_i}(x)$ . With these polynomials one can easily compute the exact expectation and variance of each category. Since

$$E(Y) = \sum_{i=1}^{15} E(X_i),$$

we can also obtain the exact expectation of the game. Unfortunately, we were unable to obtain  $G_Y(x)$  due to computational limitations and thus we do not have the exact variance of the final game score. Note that it is not the case that

$$G_Y = \prod_{i=1}^{15} G_{X_i}$$

as the  $X_i$ 's are certainly not independent. For example, it is impossible to earn a yahtzee bonus without first obtaining a yahtzee.

A *game state* is a triple  $(B, y, n)$  consisting of a subset  $B$  of  $\{1, 2, \dots, 12\}$ , an integer  $0 \leq y \leq 2$  and an integer  $0 \leq n \leq 63$ . The subset  $B$  tracks whether the categories 1 through 12 are still available on a scorecard ( $i \in B$  means that the  $i$ th category has previously been scored),  $y$  represents the yahtzee category (0 means available, 1 means this category has previously been scored with a zero, 2 means this category has previously been scored with fifty points) and lastly  $n$  tracks the number of points needed in the upper section to achieve the upper section bonus. In short, a game state indicates what a scorecard looks like directly before a new round begins. The starting state is  $(\emptyset, 0, 63)$ . Basic combinatorics tells us that the number of game states is equal to

$$2^{12} \times 3 \times 64 = 786,432.$$

However, many of these states are unreachable from the starting state. For example, the state  $(\{7, 9, 10, 12\}, 2, 20)$  is unreachable since it would be impossible to have all six categories in the upper section available, but only need 20 points to achieve the upper section bonus. It turns out that there are only 2794 ways to have the upper section filled out along with a specific number of points required to achieve the upper section bonus so of these 786,432, only

$$2794 \times 2^6 \times 3 = 536,448$$

are *reachable game states*.

Consider the directed graph  $G$  whose vertices are the reachable game states, with a directed edge between two vertices  $g_1$  and  $g_2$  if it is possible to start in state  $g_1$  and reach state  $g_2$  by playing a single round. An example of an edge in  $G$  is shown below. Try to determine what was scored to move from the state on the left to the one on the right.

$$(\{1, 3, 4, 7, 9, 12\}, 1, 41) \rightarrow (\{1, 2, 3, 4, 7, 9, 12\}, 1, 33)$$

To each reachable state  $g$ , one can assign a sequence of generating polynomials of length 15,  $\{G_{X_i^g}\}_{i=1}^{15}$ , where  $X_i^g$  represents the random variable for that particular category given that a player is currently at state  $g$  (that is, it represents the random variable for points to come in the future). All scoring categories  $i$  which have already been used must then have  $G_{X_i^g} = 0$ . One can simply differentiate these polynomials and evaluate at 1 to obtain the expected additional points in each open category from this state forward, and summing these expectations yields the total expected additional points, denoted simply by  $E_g$ . Certainly all states  $g$  which have no available categories will satisfy  $E_g = 0$ , as the expected additional points to be achieved after a scorecard is already full is 0. When  $g$  is the starting state, we have that  $X_i^g = X_i$  defined in the second paragraph of the section. The remainder of this section explains how our algorithm calculates these generating polynomials for an arbitrary game state.

Similar to game states, one can introduce a roll state. Suppose a player is at a fixed game state  $g$ . A *roll state* is a pair consisting of a subset of the multiset  $\{1^5, 2^5, \dots, 6^5\}$  having cardinality 5, which represents the dice in front of the player at a current moment (either kept or rolled from a previous decision), and an integer  $0 \leq n \leq 2$  indicating how many modifications could be made from this point forward. To allow a player to keep his or her current hand, we will extend the idea of a modification to include keeping every die and rerolling none. Basic combinatorics tells us that there are  $3\binom{10}{5} = 756$  such roll states associated with this particular game state. Similarly, one can construct a directed graph  $R$  whose vertices are the roll states, with a directed edge between two vertices  $r_1$  and  $r_2$  if one can make a modification at roll state  $r_1$  and reach roll state  $r_2$ . To each roll state  $r$ , one can again assign a sequence of generating polynomials of length 15,  $\{G_{X_i^{g,r}}\}_{i=1}^{15}$  where  $X_i^{g,r}$  represents the random variable for that particular category given that the player is currently at game state  $g$  and roll state  $r$  (so, just as before, it represents the random variable for points to come in the future). Again, all scoring categories  $i$  which have already been used must then have  $G_{X_i^{g,r}} = 0$ .

Imagine a Yahtzee player currently at the game state  $g$ . Let  $W_g$  denote the set of game states  $w$  such that it is possible to reach  $w$  from  $g$  by playing a single roll, and assume that  $E_{X^w}$  is known for every  $w \in W_g$ . Note that each  $w \in W_g$  will have one fewer empty category than  $g$ .

Suppose further that the player has just completed a roll from this game state  $g = (B, y, n)$  and needs to score his or her hand (i.e., he or she is at a roll state  $r$  such that no more manipulations can be made). At this point, if the player were to score in the

open category  $j \in B^c$  to arrive at the game state  $w \in W_g$ , there would be a contribution to their score from this category, denoted by the integer  $s_j$ , and a contribution from the future in all open categories, denoted by  $E_w$ . The algorithm maximizes  $s_j + E_w$  over all  $j \in B^c$  and sets

$$G_{X_i^{g,r}} = \begin{cases} G_{X_i^w} & i \neq j, \\ x^{s_j} & i = j \end{cases}$$

for the optimal  $j$ . Some care must be taken here for the yahtzee bonus category (being the only category that can be scored in multiple rounds), so instead of replacing the  $j$ th part, we add onto it.

Instead, suppose that the player is in the middle of a roll. In other words, he or she is at the game state  $g$  and a roll state  $r$  where modifications need to be made. Let  $V_r = \{v_1, \dots, v_n\}$  denote the set of roll states  $v$  such that it is possible to reach  $v$  from  $r$  by making a single modification. Each  $v_i$  will allow one fewer modification than  $r$ . Of course, while playing a roll, a player gets to choose which modification to make and thus has influence on the probabilities that they land in state  $v_j$  after making a modification. The algorithm simply optimizes over all possible choices and once this optimal modification is found, there is a probability associated with each  $v_j$ ,  $P(r \rightarrow v_j)$  which denotes the probability that the player will transition from state  $r$  to state  $v_j$  after making the optimal modification. The algorithm then sets

$$G_{X_i^{g,r}} = \sum_{j=1}^n P(r \rightarrow v_j) \cdot G_{X_i^{g,v_j}}.$$

When rolling five dice, the probability that one rolls the subset

$$S = \{1^{m_1}, 2^{m_2}, \dots, 6^{m_6}\}$$

is exactly

$$\frac{1}{6^5} \binom{5}{m_1, \dots, m_6}.$$

Thus, this also corresponds to the probability that one will land in the roll state having subset  $S$  with two remaining modifications after the first five dice are thrown during a player's roll. This allows us to obtain the probability generating polynomials for the game state  $g$ , by setting

$$G_{X_i^g} = \sum_r \frac{1}{6^5} \binom{5}{m_1, \dots, m_6} G_{X_i^{g,r}},$$

where the sum is over all games states  $r$  with subset  $S$  having 2 modifications.

In case you missed it, we just sneaked a proof by double induction past you showing that we can correctly compute  $G_{X_i^g}$  for an arbitrary game state  $g$  and all  $1 \leq i \leq 15$ . Now on to the fun stuff!

## Distributions by category

**Upper section and yahtzee bonus** Figure 1 shows the probability function for the random variable  $X_i$  described in the previous section for  $1 \leq i \leq 6$ , as a bar chart. These  $i$  correspond to the categories in the upper section of the scorecard. The  $x$ -axis

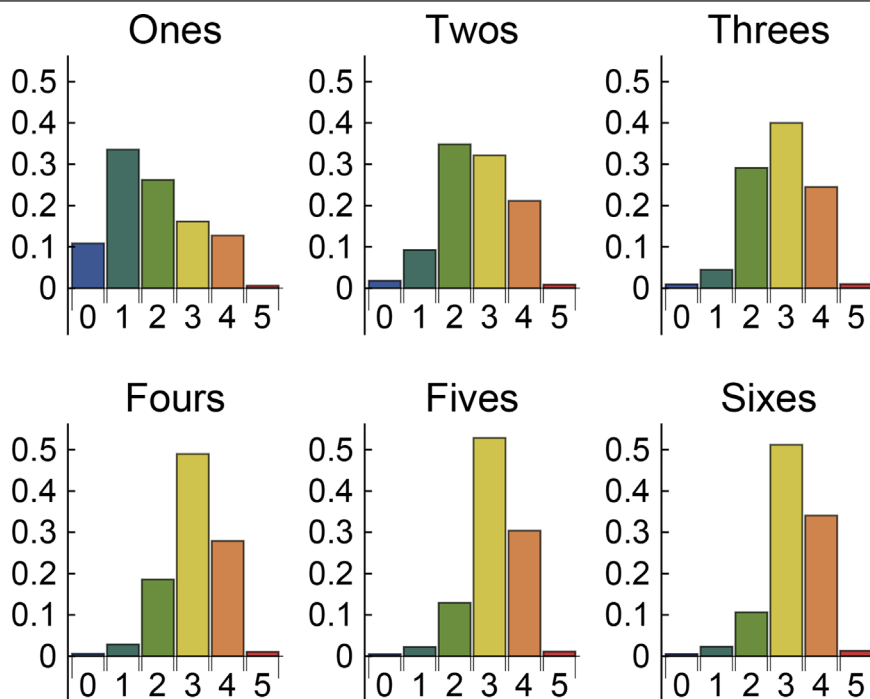


**Figure 1** The probability distributions for the upper section. Note that the online version of this article contains color diagrams.

represents the number of dice that get scored in the category and the y-axis represents the probability of scoring said number of dice. Notice that as  $i$  increases the area shown in these graphs tend to shift right. This should make intuitive sense as 6's are more valuable than 1's when scoring and will allow a player to more easily achieve the upper section bonus. An optimal player chooses to score a 0 in the ones category approximately 10% of the time, which is quite high considering how easy it is to roll at least a single 1 during a roll. The conclusion here is that the ones category is often used as a throw-away category, meaning that one would choose to score zero points in it to allow more valuable categories to remain open.

As for the yahtzee bonus, it sounds very enticing to a player, but it turns out not to have a significant impact on the final score. Figure 2 contains a bar chart representing the probability distribution for the yahtzee bonus category. In this chart, the x-axis represents the number of yahtzee bonuses a player earns throughout the game, and the y-axis represents the logarithm (base 10) of the probability. The probability that one earns 4 yahtzee bonuses during a game is approximately 0.00008; the probability of obtaining a yahtzee on every roll of a game is approximately  $4 \cdot 10^{-19}$ , which is about as likely as winning the Powerball lottery twice in a row.

**Three of a kind, four of a kind and chance** These categories are unique in the sense that when scoring them, the value of the score is the sum of the dice in the hand (assuming that the requirements for the particular category are met). Thus, in Figure 3 we again provide a bar chart where the y-axis represents probability, but the x-axis represents the sum of the dice. This sum will either be interpreted as 0 (if one fails to meet the requirements), or anywhere from 5 to 30. It is very natural to expect unimodality of these probabilities (meaning that the probabilities increase to a point and then decrease), but only chance has that property. Three of a kind is extremely



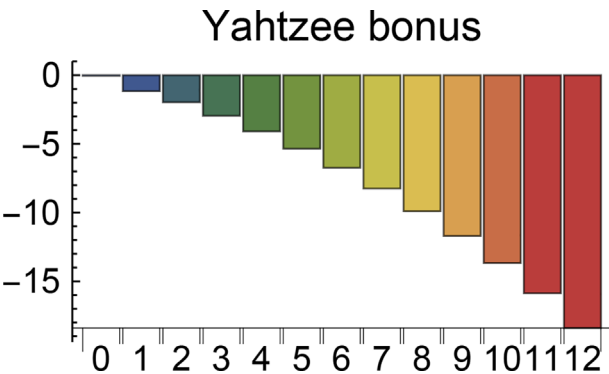


Figure 2 The semilog plot of the probability distribution for yahtzee bonus.

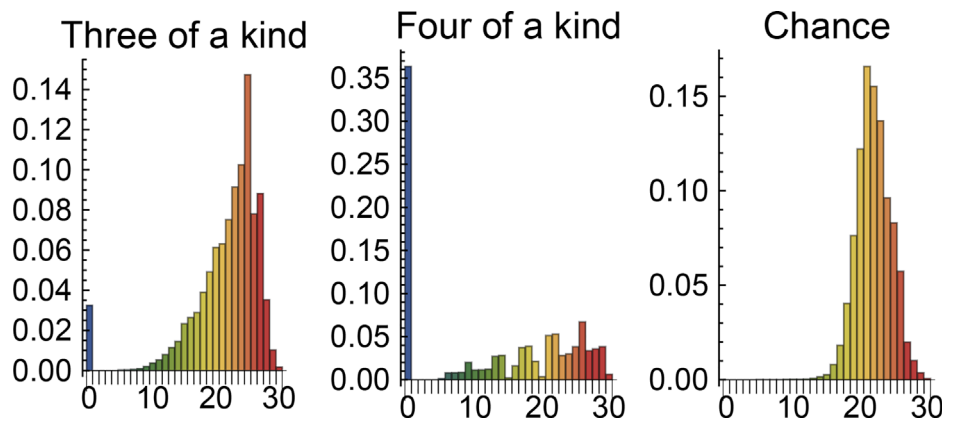


Figure 3 The probability distributions for three of a kind, four of a kind and chance.

close to having this property, but indeed fails. Observe in Figure 3 that one is more likely to score either 25 or 27 than 26 in the three of a kind category.

**Full house, small straight, large straight, yahtzee and upper section bonus** These categories are also unique, but due to the fact that when scoring them, one either scores a prescribed fixed number of points or 0 points. For these categories we present Table 4, a table of probabilities. This table indicates the probability that one achieves a nonzero score in each particular category. A quick glance at the table reveals that under optimal play, a player would obtain a yahtzee in approximately one out of every three games. It’s also worth noting that the upper section bonus is achieved in approximately 68% of games, indicating that achieving the upper section bonus is an important aspect of optimal play!

Category	Approximate probability of nonzero score
Full house	.90
Small straight	.98
Large straight	.82
Yahtzee	.34
Upper section bonus	.68

TABLE 4: Probabilities of nonzero scores in several categories

### Expectation and standard deviation by category

The expectation of each category can be calculated easily, with the results shown by category in Figure 4. After a quick inspection, one notices that the large straight category contributes the greatest number of expected points to the final score. We can also compute the standard deviations by category, which are shown in Figure 5. The yahtzee and yahtzee bonus categories have a high standard deviation associated with them. However this should not come as a surprise; they are extremely valuable, yet difficult to obtain.

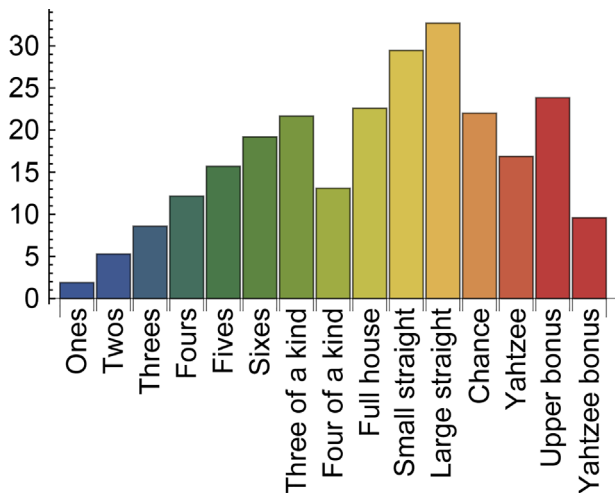


Figure 4 Expectations by category.

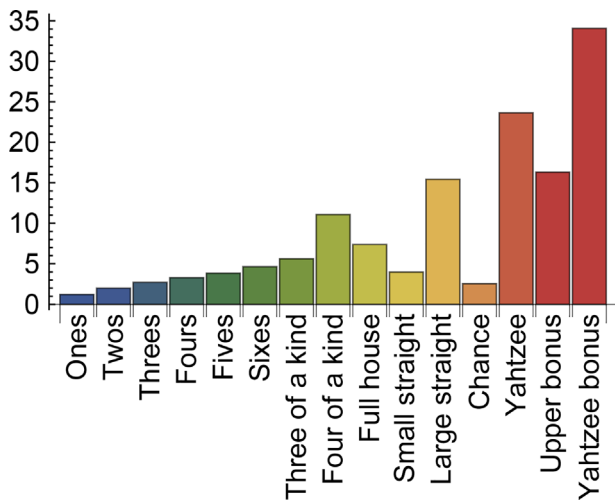


Figure 5 Standard deviations by category.

### The expectation of solitaire Yahtzee

As mentioned before, we do have exact values for all of these probabilities and expectations shown in the preceding figures. To obtain the exact expectation of the game,

we simply to need to sum the expectations over each category. However, there is quite a bit of complexity in obtaining these values so it may not be surprising to learn that as a rational number in reduced form, the numerator and denominator of the expectation of Yahtzee are extremely large integers. It is displayed below with the rational number squeezed onto a single line.

The expectation of solitaire Yahtzee

43536532669975279571401097355946939059234156583005999913383601664372459155214344537914532874552492952166140138260533289185022066152462308875  
171007977825115837834062572448245920361235544505613986900067885349858677143969201052156905351994680233805986447857466552932518189372276736

The numerator of this rational number has 140 digits and the denominator has 138. It is approximately equal to 254.58772873449589123, which matches the results of Verhoeff [2] to two decimal places. One reason for this discrepancy could be to a different interpretation of the joker rules. Unfortunately due to computational limitations, we were unable to obtain the exact standard deviation of the game (although Verhoeff [2] provides numerical estimates).

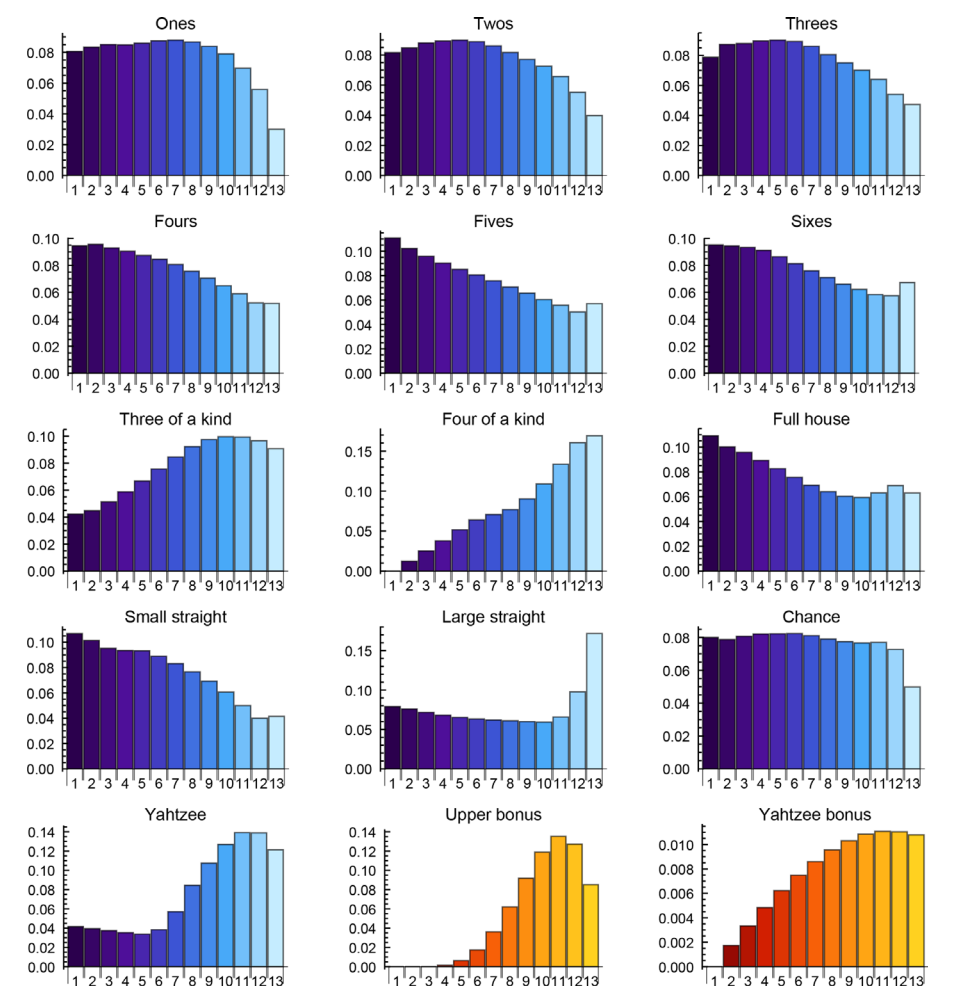


Figure 6 Probability distributions by round.

## Results by round

After obtaining the probability generating polynomial for the random variable  $X_i^g$  for each game state  $g$  and category  $1 \leq i \leq 15$ , we chose to investigate the round in which a particular category is scored. Thus, for each scoring category,  $1 \leq i \leq 13$  we introduce a new random variable,  $R_i$  which corresponds to the round in which the player enters a score into the  $i$ th category.

Figure 6 depicts the probability function for the random variable  $R_i$  as a bar chart. The two remaining scoring categories (upper section bonus and yahtzee bonus) do not have a corresponding random variable. The reason for this is that a player may never achieve an upper section bonus, and in the case of the yahtzee bonus, he or she may earn it multiple times. These two categories are treated separately and their corresponding bar charts do not reflect probability functions, but are very similar (hence the different color in Figure 6). For the upper section bonus, the bar heights represent the probability that one achieves the upper section bonus in the corresponding round. As mentioned, it closely resembles a probability function, but the area will not sum to one. For the yahtzee bonus, the bar heights represent the probability that one earns a yahtzee bonus in the corresponding round. The first column of the chart corresponding to the yahtzee bonus is of height zero as it is impossible to earn this bonus in the first round (a player must first have scored a yahtzee before it can be earned).

Decision to score	Exp. score	Decision to score	Exp. score
50 in Yahtzee	320.831	4 in Ones	248.065
24 in Sixes	268.232	6 in Twos	247.600
20 in Fives	264.483	30 in Small straight	246.555
40 in Large straight	261.531	26 in Chance	245.958
16 in Fours	261.048	3 in Ones	245.324
12 in Threes	257.401	25 in Chance	244.958
28 in Three of a kind	253.957	24 in Chance	243.958
25 in Full house	253.909	23 in Chance	242.958
8 in Twos	253.268	2 in Ones	242.384
27 in Three of a kind	252.957	22 in Chance	241.958
26 in Three of a kind	251.957	4 in Twos	241.753
25 in Three of a kind	250.957	21 in Chance	240.958
18 in Sixes	250.526	20 in Chance	239.958
15 in Fives	249.982	6 in Threes	239.951
12 in Fours	249.415	1 in Ones	239.629
9 in Threes	248.725	19 in Chance	238.958

TABLE 5: The ranked decisions at the end of the first roll.

- Here is a short list of observations that we found interesting:
1. It is never appropriate to score in the four of a kind category during the first round.
  2. The large straight category is significantly more likely to be scored in the last round than any other.
  3. The yahtzee category is typically scored late in the game, meaning that it is not in a player's best interest to use this as a throw-away category early on.
  4. It is extremely likely that during the course of a game one will obtain a full house and a small straight. Their probability distributions indicate that they are more likely to be scored in the early rounds.
  5. The probability of earning a yahtzee bonus in any particular round is at most approximately 1%.

Rank of hands at the end of first round

In Table 5, we provide a full list of the possible approximate expected scores (from best to worst) that the optimal player might end up with after completing a roll in round one. If you were wondering where the optimal player would score a particular hand on

Open category	Expected value		Standard deviation	
Ones	$455/216 \approx$	2.10648	$25\sqrt{91}/216 \approx$	1.10410
Twos	$455/108 \approx$	4.21296	$25\sqrt{91}/108 \approx$	2.20819
Threes	$455/72 \approx$	6.31944	$25\sqrt{91}/72 \approx$	3.31229
Fours	$455/54 \approx$	8.42593	$25\sqrt{91}/54 \approx$	4.41639
Fives	$2275/216 \approx$	10.5324	$125\sqrt{91}/216 \approx$	5.52048
Sixes	$455/36 \approx$	12.6389	$25\sqrt{91}/36 \approx$	6.62458
Three of a kind	$\frac{114845383}{7558272} \approx$	15.1947	$\frac{\sqrt{6163759578782159}}{7558272} \approx$	10.3872
Four of a kind	$\frac{56548607}{10077696} \approx$	5.61126	$\frac{\sqrt{9480311223232511}}{10077696} \approx$	9.66162
Full house	$\frac{11530925}{1259712} \approx$	9.15362	$\frac{35875\sqrt{178847}}{1259712} \approx$	12.0437
Small straight	$\frac{1676190395}{90699264} \approx$	18.4807	$\frac{5\sqrt{70050512568832895}}{90699264} \approx$	14.5906
Large straight	$\frac{6497333405}{612220032} \approx$	10.6127	$\frac{25\sqrt{187034504366754983}}{612220032} \approx$	17.6601
Chance	$70/3 \approx$	23.3333	$\sqrt{10} \approx$	3.16228
Yahtzee	$\frac{8697425}{3779136} \approx$	2.30143	$\frac{125\sqrt{100338713255}}{3779136} \approx$	10.4774

TABLE 6: Expected score and standard deviation on the final round of the game (ignoring bonuses) by open category.

their scorecard in this round, he or she would make the best decision on this list that is compatible with their hand. Every possible hand will be compatible with at least one decision on this list and any decision that does not appear would not be optimal. Many conclusions can be drawn from this data. For example, if one ends up with a full house, he or she would always score it as 25 points in the full house category except for in one specific situation. A player finishing the first round with the hand



should instead score this hand as 28 points in the three of a kind category. It is also worth noting how valuable obtaining a yahtzee is in the first round. A player needs to end up with either a large straight, a four of a kind (with 3's or higher), or a yahtzee to be “ahead” after the first round.

Expectation and standard deviation on the final round

In the previous section we examined the ranking of the hands for scoring in the first round. Now let us examine the other extreme, the final round of the game. In this round, the player will have exactly one open scoring category remaining and thus the strategy for the player is to maximize the points in that specific category. Because of the simplicity of these calculations, the probabilities as rational numbers are the quotient of integers that are reasonably sized for print. In Table 6, we provide the exact (and approximate) expectation and standard deviation for the number of points to be scored in the final round for each scoring category. These values assume that the player cannot obtain points from either the upper section bonus or the yahtzee bonus.

Roll 1:	
Dice kept	Exp. score
	251.131
	250.420
	249.879
	249.874
	249.607

Roll 2:	
Dice kept	Exp. score
	249.936
	249.729
	249.711
	249.607
None	249.472

Roll 3:	
Dice kept	Exp. score
	249.936
	249.828
	249.729
	249.711
	249.607

Roll 4:	
Dice kept	Exp. score
	259.646
	256.219
	253.935
	253.909
	251.706

TABLE 7: Expected scores for the top 5 decisions in each of the challenge rolls.

## Solutions to challenge

At the beginning of the article in Table 1, we proposed four possible opening rolls (shown again below) and asked which dice should be kept. In Table 7, we present, for each roll, the best five decisions and the player's approximate expected score upon making each decision. How did you fare?

## REFERENCES

- [1] Woodward, P. (2003). Yahtzee : The solution. *CHANCE* 16(1): 18–22.  
[doi.org/10.1080/09332480.2003.10554833](https://doi.org/10.1080/09332480.2003.10554833)
- [2] Verhoeff, T. (1999). How to maximize your score in solitaire Yahtzee (unfinished).  
[www.win.tue.nl/~wstomv/publications/yahtzee-report-unfinished.pdf](http://www.win.tue.nl/~wstomv/publications/yahtzee-report-unfinished.pdf).
- [3] Optimal Solitaire Yahtzee Player Application. (1999).  
[www-set.win.tue.nl/~wstomv/misc/yahtzee/osyp.php](http://www-set.win.tue.nl/~wstomv/misc/yahtzee/osyp.php)
- [4] Yahtzee Proficiency Test with Detailed Feedback. (1999).  
[www-set.win.tue.nl/~wstomv/misc/yahtzee/ypdt.php](http://www-set.win.tue.nl/~wstomv/misc/yahtzee/ypdt.php)
- [5] Hasbro Yahtzee Instructions. (1996).  
[www.hasbro.com/common/instruct/Yahtzee.pdf](http://www.hasbro.com/common/instruct/Yahtzee.pdf)

**Summary.** Yahtzee is a popular dice game that involves a combination of chance and decision making. We implemented a brute-force algorithm to understand optimal play for a solitaire version of Yahtzee using Mathematica. The novelty in our approach is that we were able to compute probabilities and expectations of the optimal player's score *exactly* as rational numbers. Previous work involved only numerical approximations. We give an overview of our approach and analyze some of the data generated by our implementation. The figures provided in the article should give an insight as to how a game under optimal play would typically unfold.

**KATHRYN KELLY** is a data scientist at Adobe in San Francisco, CA. She graduated from California Polytechnic State University with a B.S. in Applied Mathematics and an M.S. in Business Analytics. She now loves to apply her skills in mathematics and statistics to predict and improve future outcomes for the business.

**JEFFREY LIESE** (MR Author ID: [829937](https://orcid.org/0000-0001-9145-3443)) is a professor of mathematics at California Polytechnic State University, whose research interests lie mainly in enumerative and algebraic combinatorics, game theory and discrete probability theory. He loves to participate in competitive strategy games, especially games involving dice.



# The Curious Case of the Double Catenary

SUBHRANIL DE  
Indiana University Southeast  
New Albany, IN 47150  
[subde@ius.edu](mailto:subde@ius.edu)

During a visit home in India, one winter morning, I was playing with a chain of beads that belongs to my mother, whimsically holding the chain to make shapes like the one shown in Figure 1. I had been fascinated by the catenary since my college days, and to play with a shape that was made of two catenaries coming from one single chain was just a little addictive.



**Figure 1** Playing with the chain to make a double catenary shape.

Then, suddenly, a mechanics question came to mind that relates to the stability of the double catenary shape. Before getting into the details of that question, let us briefly go over the pertinent basics.

A uniform, inextensible, ideal chain (or rope, or cable, whatever one prefers to call it), when hanging at rest under gravity, forms a catenary shape described by the equation of the form (see Douglas [2])

$$y^* = a^* \cosh \left( \frac{x^* - b^*}{a^*} \right) + c^* \quad (1)$$

where  $x^*$  and  $y^*$  are the dimensional horizontal and vertical coordinates, respectively. In general, quantities denoted by asterisks are dimensional. The constant  $a^*$  is equal to the radius of curvature of the catenary at its vertex and is a measure of the “size” of the catenary. The constants  $b^*$  and  $c^*$  are arbitrary and do not change the shape of the catenary, but rather dictate the horizontal and vertical positions of its vertex.

Let us consider a single closed chain of fixed length  $L^*$  that is draped over two frictionless pointlike pins fixed in place at the same vertical height, separated by a horizontal distance  $D^*$ . When the chain has attained its equilibrium configuration, we should have two catenaries as shown in the schematic in Figure 2, with one having, say, length  $l_1^*$ , and the other one having length  $l_2^* = (L^* - l_1^*)$ .

The question that came to my mind, and the one that happens to be the essence of this paper, is as follows: What configuration of the double catenary shape will be one of *stable equilibrium*? We start by focusing our attention on the configuration that

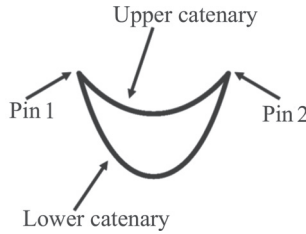


**Figure 2** A configuration of two catenaries formed by draping a single chain around two smooth pins located at the same vertical height.

consists of *two identical catenaries of the same length*, since it is somewhat straightforward to show that it is an equilibrium configuration. However, will it be *stable* or *unstable*? If it is unstable, what configuration will pertain to stable equilibrium in that case?

We first need to remind ourselves that at any equilibrium configuration, the gravitational potential energy of the system will be at a local *extremum* (see Taylor [4]). Depending on if the equilibrium is stable or unstable, the potential energy is at a local *minimum* or a *maximum*, respectively, (see Taylor [4]).

Before delving deeper into the analysis, let us first derive the mathematical dependence of the gravitational potential energy  $p^*$  as a function of the length  $l^*$  of a single catenary hanging from the two pins since that will be an important component of our calculations.

### The dependence of the gravitational potential energy as a function of length for a single catenary

Without loss of generality, let us take the coordinates of the two pins to be  $(-\frac{D^*}{2}, 0)$  and  $(\frac{D^*}{2}, 0)$ , respectively. Then, from equation (1), we obtain:  $b^* = 0$  and  $c^* = -a^* \cosh(\frac{D^*}{2a^*})$ , so that the equation of any catenary hanging from the two pins becomes

$$y^* = a^* \cosh\left(\frac{x^*}{a^*}\right) - a^* \cosh\left(\frac{D^*}{2a^*}\right). \quad (2)$$

Now, a length element  $ds^*$  is given by

$$ds^* = \sqrt{dx^{*2} + dy^{*2}} = \sqrt{1 + (dy^*/dx^*)^2} dx^*.$$

Hence, the length  $l^*$  of the catenary in question will be

$$l^* = \int_{-D^*/2}^{D^*/2} \sqrt{1 + (dy^*/dx^*)^2} dx^*. \quad (3)$$

However, from equation (2), we get after differentiating:

$$\frac{dy^*}{dx^*} = \sinh\left(\frac{x^*}{a^*}\right). \quad (4)$$

Making use of the identity (see Weisstein [5])

$$\cosh^2 \theta - \sinh^2 \theta = 1, \quad (5)$$

and then completing the integration for (3) using the standard integral (see Weisstein [6])

$$\int \cosh \theta \, d\theta = \sinh(\theta) + C_1, \quad (6)$$

we obtain:

$$l^* = 2a^* \sinh\left(\frac{D^*}{2a^*}\right). \quad (7)$$

It is worth noting that  $a^*$  happens to be a monotonically decreasing function of  $l^*$ , with

$$\lim_{l^* \rightarrow D^*} (a^*) = \infty \quad \text{and} \quad \lim_{l^* \rightarrow \infty} (a^*) = 0.$$

Now, the gravitational potential energy  $dp^*$  of a length element  $ds^*$  is given by (see Serway [3])

$$dp^* = \lambda^* (ds)^* g^* y^* = \lambda^* g^* y^* \sqrt{1 + (dy^*/dx^*)^2} \, dx^*$$

where  $\lambda^*$  is the uniform linear mass density of the chain, and  $g^*$  is the acceleration of gravity.

Hence, the gravitational potential energy  $p^*$  of the whole length  $l^*$  of the catenary is obtained through:

$$p^* = \int_{-D^*/2}^{D^*/2} \lambda^* g^* y^* \sqrt{1 + (dy^*/dx^*)^2} \, dx^*. \quad (8)$$

Using the identity  $\cosh(2\theta) = 2 \cosh^2 \theta - 1$  [5], along with the integral in equation (6) we can derive the integral:

$$\int \cosh^2 \theta \, d\theta = \frac{1}{4} \sinh(2\theta) + \frac{\theta}{2} + C_2. \quad (9)$$

Using the expression of  $y^*$  from equation (2) and  $(dy^*/dx^*)$  from equation (4), identity equation (5), along with the integrals in equations (6) and (9), we complete the integration in equation (8) to obtain, after some rearranging:

$$p^* = \lambda^* g^* \left\{ \frac{D^* a^*}{2} - \frac{a^{*2}}{2} \sinh\left(\frac{D^*}{a^*}\right) \right\}. \quad (10)$$

At this point, without loss of generality, we define some pertinent dimensionless quantities:

$$\begin{aligned} x &= x^*/D^* & y &= y^*/D^* \\ a &= a^*/D^* & l &= l^*/D^* \\ p &= p^*/(\lambda^* g^* D^{*2}), \end{aligned}$$

where we choose  $D^*$  to be the natural length scale of the system since it is the same for both catenaries.

From equation (7), we can now write, for the dimensionless length of the catenary,

$$l = 2a \sinh\left(\frac{1}{2a}\right), \quad (11)$$

whereas, from equation (10), we write, for the dimensionless potential energy,

$$p = \frac{a}{2} - \frac{a^2}{2} \sinh\left(\frac{1}{a}\right). \quad (12)$$

Equations (11) and (12) together give the implicit dependence of  $p$  versus  $l$  through the parameter  $a$  since  $p$  cannot be expressed as a function of  $l$  in an explicit, closed-form manner.

Now, utilizing the chain rule, we can write:

$$\frac{dp}{dl} = \frac{dp/da}{dl/da}. \quad (13)$$

From equation (11), we derive:

$$\frac{dl}{da} = 2 \sinh\left(\frac{1}{2a}\right) - \frac{1}{a} \cosh\left(\frac{1}{2a}\right), \quad (14)$$

and from equation (12), we derive:

$$\frac{dp}{da} = \frac{1}{2} - a \sinh\left(\frac{1}{a}\right) + \frac{1}{2} \cosh\left(\frac{1}{a}\right). \quad (15)$$

However, using the identities

$$\sinh(2\theta) = 2 \sinh \theta \cosh \theta \quad \text{and} \quad \cosh(2\theta) = 2 \cosh^2 \theta - 1,$$

we can simplify equation (15) to

$$\frac{dp}{da} = \cosh\left(\frac{1}{2a}\right) \left[ \cosh\left(\frac{1}{2a}\right) - 2a \sinh\left(\frac{1}{2a}\right) \right]. \quad (16)$$

Now, using equations (13), (14), and (16), we obtain after simplifying:

$$\frac{dp}{dl} = -a \cosh\left(\frac{1}{2a}\right). \quad (17)$$

This derivative approaches negative infinity in both the limits  $l \rightarrow 1$  (i.e.,  $a \rightarrow \infty$ ) and  $l \rightarrow \infty$  (i.e.,  $a \rightarrow 0$ ), as shown in the plots of  $p$  versus  $l$  in Figures 3 and 4, respectively. It can be shown that the functional dependence approaches  $p = -\frac{1}{4}l^2$  for large values of  $l$ .

The behavior seen in the plots in Figures 3 and 4 indicate that there must be an “inflection point” somewhere on the graph, where  $\frac{d^2p}{dl^2} = 0$ .

Deriving the expression for  $\left\{ \frac{d}{da} \left( \frac{dp}{dl} \right) \right\}$  from equation (17), resorting once more to equation (14), and then making use of

$$\frac{d^2p}{dl^2} = \left\{ \frac{d}{da} \left( \frac{dp}{dl} \right) \right\} \frac{da}{dl},$$

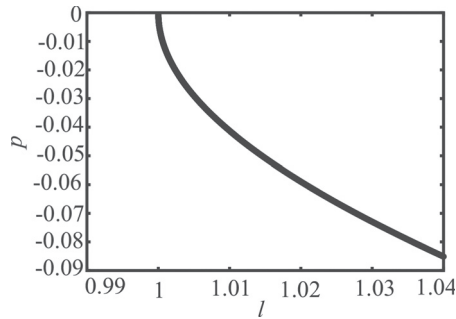


**Figure 3** The dimensionless gravitational potential energy  $p$  plotted against the dimensionless length  $l$  of the catenary for small values of  $l$ .

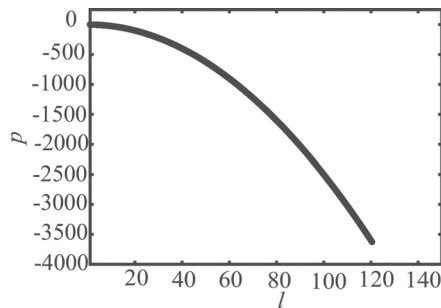


**Figure 4** The dimensionless gravitational potential energy  $p$  plotted against the dimensionless length  $l$  of the catenary for large values of  $l$ .

we obtain after simplifying:

$$\frac{d^2 p}{dl^2} = \frac{1}{2} \left( \frac{\sinh(1/2a) - 2a \cosh(1/2a)}{2a \sinh(1/2a) - \cosh(1/2a)} \right). \quad (18)$$

For the critical value of  $a$ , denoted by  $a_c$ , which corresponds to  $\frac{d^2 p}{dl^2} = 0$ , we get from equation (18), after some rearranging, that  $a_c$  is given by the transcendental equation:  $\frac{1}{2a_c} = \coth\left(\frac{1}{2a_c}\right)$ . Solving this equation numerically yields:  $a_c \approx 0.41678$ , which, in turn, with the use of equation (11), gives the dimensionless critical length  $l_c$  to be

$$l_c \approx \frac{\sinh(1.19967)}{1.19967} \approx 1.2577. \quad (19)$$

The significance of this notion of the critical length will be evident in our subsequent analysis.

Furthermore, using equation (18), it can be verified that

$$\left\{ \begin{array}{l} \frac{d^2 p}{dl^2} > 0, \text{ for } l < l_c, \text{ (i.e., } a > a_c), \\ \frac{d^2 p}{dl^2} < 0, \text{ for } l > l_c, \text{ (i.e., } a < a_c), \end{array} \right. \quad (20)$$

as suggested by the plots in Figures 3 and 4.

## The conditions for equilibrium of the whole chain forming a double catenary

For the whole chain of fixed length  $L^*$  (which must obviously satisfy  $L^* > 2D^*$ ) draped over the pins in the shape of the double catenary, let us denote the dimensionless lengths of the two catenaries by  $l_1$  and  $l_2$ , respectively. We have,

$$l_1 + l_2 = L. \quad (21)$$

where  $L$  is the dimensionless fixed length of the whole chain.

Now, if the dimensionless gravitational potential energies of the two catenaries are  $p_1$  and  $p_2$ , respectively, then the total dimensionless potential energy  $P$  of the whole chain is given by

$$P = p_1 + p_2. \quad (22)$$

Since the total length  $L$  is fixed, the constraint equation (21) deems the configuration a system with one degree of freedom. Treating  $l_1$  as the independent variable, we differentiate both sides of equation (22) to obtain:

$$\frac{dP}{dl_1} = \frac{dp_1}{dl_1} + \frac{dp_2}{dl_1}. \quad (23)$$

However, differentiating both sides of equation (21), we get, after rearranging,

$$\frac{dl_2}{dl_1} = -1, \quad (24)$$

which allows us to conclude, from equation (23):

$$\frac{dP}{dl_1} = \frac{dp_1}{dl_1} - \frac{dp_2}{dl_2}. \quad (25)$$

Recalling the principle that the potential energy must be an extremum (i.e.,  $\frac{dP}{dl_1} = 0$ ) at the equilibrium configuration, we can write from equation (25), that the condition

$$\frac{dp_1}{dl_1} = \frac{dp_2}{dl_2} \quad (26)$$

must hold at equilibrium.

Regarding stability, the equilibrium will be stable or unstable, depending on whether the potential energy will be a local minimum (i.e.,  $\frac{d^2P}{dl_1^2} > 0$ ) or a maximum (i.e.,  $\frac{d^2P}{dl_1^2} < 0$ ), respectively. Differentiating equation (25) one more time with respect to  $l_1$ , and using equation (24), we obtain:

$$\frac{d^2P}{dl_1^2} = \frac{d^2p_1}{dl_1^2} + \frac{d^2p_2}{dl_2^2}.$$

Hence, we can write:

$$\left\{ \begin{array}{ll} \frac{d^2p_1}{dl_1^2} + \frac{d^2p_2}{dl_2^2} > 0 & \text{for stable equilibrium,} \\ \frac{d^2p_1}{dl_1^2} + \frac{d^2p_2}{dl_2^2} < 0 & \text{for unstable equilibrium.} \end{array} \right. \quad (27)$$

Writing the equilibrium conditions for the whole chain in the forms as in equations (26) and (27) is helpful, since  $p_2$  has the same functional form in terms of  $l_2$  as  $p_1$  has in terms of  $l_1$ , namely the form given by equations (11) and (12) together, depicted in the plots in Figures 3 and 4.

## Investigating the configuration of two identical catenaries

For the configuration consisting of two identical catenaries, we will have:  $l_1 = l_2 = L/2$ . Hence, at that configuration,

$$\begin{aligned}\frac{dp_1}{dl_1} &= \left(\frac{dp}{dl}\right)_{l=L/2} \\ \frac{dp_2}{dl_2} &= \left(\frac{dp}{dl}\right)_{l=L/2},\end{aligned}$$

thus satisfying the equilibrium condition in equation (26). Hence, we can infer that: *The configuration of the two identical catenaries will always be an equilibrium configuration.*

Once again, since at this configuration we have  $l_1 = l_2 = L/2$ , what also holds for this configuration is

$$\frac{d^2 p_1}{dl_1^2} + \frac{d^2 p_2}{dl_2^2} = 2 \left(\frac{d^2 p}{dl^2}\right)_{l=L/2}.$$

Combining equation (27) with equations (19) and (20), we obtain the condition that dictates if the configuration under consideration is stable: *The configuration of the two identical catenaries is stable if  $L < L_c$  and unstable if  $L > L_c$ , where  $L_c = 2l_c \approx 2.5154$ .*

What about the transition point itself, namely when  $L = L_c$ ? Since both  $\left(\frac{dP}{dl_1}\right)_{l_1=L/2}$  and  $\left(\frac{d^2 P}{dl_1^2}\right)_{l_1=L/2}$  become zero at the transition point, we need to investigate the

higher-order derivatives. As we did for  $\left(\frac{dP}{dl_1}\right)$ , we can show in similar fashion that any odd-order derivative of  $P$  with respect to  $l_1$  will vanish at  $l_1 = L/2$ . Hence,  $\left(\frac{d^3 P}{dl_1^3}\right)_{l_1=L/2} = 0$ , including when  $L = L_c$ .

However, for any even-order derivative of  $P$  with respect to  $l_1$ , we can show in the same fashion as we did for  $\left(\frac{d^2 P}{dl_1^2}\right)$ , that its value at  $l_1 = L/2$  is twice the value of the corresponding derivative of  $p_1$  with respect to  $l_1$ . Hence,

$$\left(\frac{d^4 P}{dl_1^4}\right)_{l_1=L/2} = 2 \left(\frac{d^4 p_1}{dl_1^4}\right)_{l_1=L/2}. \quad (28)$$

Now, differentiating equation (18) twice, and using equation (14) as needed, we obtain after simplifying:

$$\frac{d^4 p}{dl^4} = \frac{1}{8a^2} \left( \frac{16a^2 \sinh(1/2a) + 3 \sinh(1/2a) - 8a \cosh(1/2a)}{(\cosh(1/2a) - 2a \sinh(1/2a))^5} \right).$$



Through direct enumeration at  $l = l_c \approx 1.2577$  (i.e.,  $a = a_c \approx 0.41678$ ), we get  $\left(\frac{d^4 P}{dl^4}\right)_{l=l_c} \approx 38.0$ . Hence, using equation (28), we obtain that at the transition point

of  $L = L_c = 2l_c$ , we have that  $\left(\frac{d^4 P}{dl_1^4}\right)_{l_1=L/2=L_c/2} \approx 76.0$ . Since the above value is

positive, and all lower order derivatives are zero at this point, we infer that: *At the transition point itself, the configuration of two similar catenaries still corresponds to a local minimum of the gravitational potential energy, and hence that configuration is still a stable equilibrium.*

Figure 5 shows the plot of the dimensionless gravitational potential energy  $P$  of the whole chain against  $l_1$ , for values of  $L$  less than (Figure 5a), equal to (Figure 5b), and greater than  $L_c$  (Figure 5c), capturing the nature of the extremum at the configuration of the two similar catenaries, i.e.,  $l_1 = L/2$ .

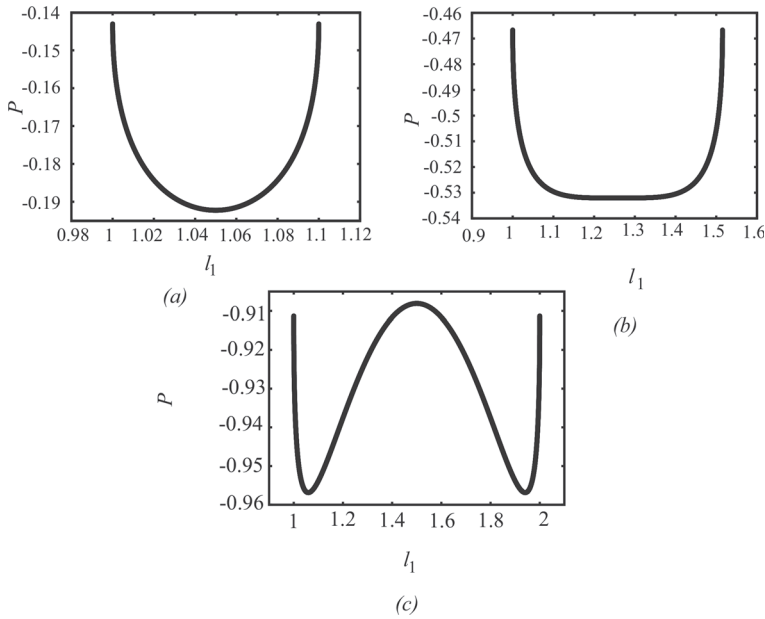


**Figure 5** The total gravitational potential energy  $P$  plotted against  $l_1$  for: (a)  $L = 2.1$ , showing a local minimum at the midpoint  $l_1 = L/2$ ; (b) the transition point of  $L = L_c = 2.5154$ , showing a flat minimum at the midpoint  $l_1 = L/2$ ; (c)  $L = 3.0$ , showing a local maximum at the midpoint  $l_1 = L/2$ , along with two newly emerged local minima symmetrically situated about the midpoint on the two sides.

## The general solution for equilibrium

Combining equations (17) and (26), the general equilibrium condition can be written as

$$a_1 \cosh\left(\frac{1}{2a_1}\right) = a_2 \cosh\left(\frac{1}{2a_2}\right), \quad (29)$$

while using equation (11) and (21) we retain the constraint of fixed total length of the chain:

$$2a_1 \sinh\left(\frac{1}{2a_1}\right) + 2a_2 \sinh\left(\frac{1}{2a_2}\right) = L. \quad (30)$$

Solving the transcendental equations (29) and (30) yield the values of  $a_1$  and  $a_2$  that correspond to equilibrium, from which we can determine  $l_1$  and  $l_2$  using equation (11).

It is worth noting that the trivial solution of  $l_1 = L/2$  and  $l_2 = L/2$  (i.e., the solution of two similar catenaries) is always a solution for any given length  $L$  of the chain (which must, of course, satisfy  $L > 2$ ).

However, it can be shown that when  $L \leq L_c$ , the above solution is the only solution, which, as shown already, happens to correspond to a stable equilibrium. When  $L > L_c$  however (when the solution of the two similar catenaries becomes unstable, as shown already), it can be shown that exactly two more degenerate solutions emerge (as manifested in the potential energy diagram, Figure 5c) symmetrically about the  $l_1 = L/2$  mark, both of which correspond to stable equilibrium configurations.

For example, when  $L = 3.0$ , a numerical solution gives us  $a_1 \approx 0.847$ ;  $a_2 \approx 0.235$ , which, in turn, yields  $l_1 \approx 1.059$ ;  $l_2 \approx 1.941$ , along with the degenerate solutions  $a_1 \approx 0.235$ ;  $a_2 \approx 0.847$ , implying  $l_1 \approx 1.941$ ;  $l_2 \approx 1.059$ . These are the two stable equilibrium points symmetrically located around the  $l_1 = L/2$  mark, as captured in Figure 5c. The corresponding catenary segments are plotted in Figure 6.

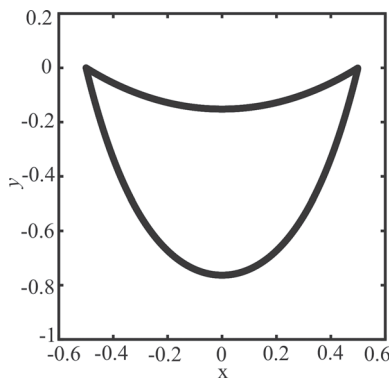


**Figure 6** The two catenaries formed at the stable equilibrium configuration for  $L = 3.0$ . The endpoints (pins) have coordinates  $(-\frac{1}{2}, 0)$  and  $(\frac{1}{2}, 0)$ .

## Further physical insight

It turns out that there is another physical interpretation of the conditions for equilibrium of the double catenary and the nature of the equilibrium, besides the one involving the extremum of the total gravitational potential energy. If  $T$  is the tension at either endpoint of a single catenary (i.e., in this paper, the tension in the chain where it meets either pin), then the condition for equilibrium can also be written as  $T_1 = T_2$ , implying that, at equilibrium, the endpoint-tensions in the two catenaries must be the same!

In addition, the following relations govern the nature of the equilibrium:

$$\left\{ \begin{array}{ll} \frac{dT_1}{dl_1} + \frac{dT_2}{dl_2} < 0 & \text{for stable equilibrium,} \\ \frac{dT_1}{dl_1} + \frac{dT_2}{dl_2} > 0 & \text{for unstable equilibrium.} \end{array} \right. \quad (31)$$

## Concluding remarks

It so happens that there is a subtle connection between the solutions obtained for the double catenary in the present problem and the two catenaries referred to as the “flat

catenary” and the “deep catenary” (see Arfken [1]) in the context of the classic problem of the minimization of a surface area of revolution. I intend to present that finding separately in a future communication.

## REFERENCES

- [1] Arfken, G. B., Weber, H. J. (2005). *Mathematical Methods of Physicists*, 6th ed. Amsterdam: Elsevier.
- [2] Douglas, D. A. (1986). *Classical Mechanics*. New York: Academic.
- [3] Serway, R. A., Jewett Jr., J. W. (2004). *Physics for Scientists and Engineers*, 9th ed. Belmont, CA: Brooks/Cole Publishing.
- [4] Taylor, J. (2005). *Classical Mechanics*. Sausalito, CA: University Science Books.
- [5] Weisstein, E. W. (2022). “Hyperbolic Functions.” From MathWorld—A Wolfram Web Resource. <http://mathworld.wolfram.com/HyperbolicFunctions.html>
- [6] Weisstein, E. W. (2022). “Hyperbolic Cosine.” From MathWorld—A Wolfram Web Resource. <http://mathworld.wolfram.com/HyperbolicCosine.html>

**Summary.** In this paper, we study the static equilibrium of a double catenary formed when a closed, ideal chain of length  $L^*$  is draped over two frictionless pins at the same vertical height and separated by horizontal distance  $D^*$ . Each of the two segments forms a catenary at equilibrium. At issue is whether or not a given equilibrium solution is stable. First, we show that the trivial solution of two identical catenaries is always an equilibrium configuration. However, it is not always stable. There exists a critical length  $L_c^*$  such that the trivial solution becomes unstable for  $L^* > L_c^*$ . In such cases, the system is stable only for catenaries of differing lengths.

**SUBHRANIL DE** (MR Author ID: [1179343](#)) earned a Ph.D. in physics from the University of Rochester in 2003. He has a theoretical background in statistical physics and fluid mechanics. He is also fascinated with how various aspects of calculus and geometry play a role in classical mechanics. He has been teaching physics at Indiana University Southeast since 2008. Among his interests outside the realm of physics, writing happens to be a fond avocation. He also enjoys soccer and classical music, and loves to throw a Frisbee on a sunny day.

# Why Curves Curve: The Geodesics on the Torus

KYLE CELANO

University of Miami  
Coral Gables, FL 33146  
[celano@math.miami.edu](mailto:celano@math.miami.edu)

VINCENT E. COLL

Lehigh University  
Bethlehem, PA 18015  
[vec208@lehigh.edu](mailto:vec208@lehigh.edu)

JEFF DODD

Jacksonville State University  
Jacksonville, AL 36265  
[jdodd@jsu.edu](mailto:jdodd@jsu.edu)

Curves on surfaces curve for two reasons:

- (1) They must—the surface on which they reside is itself curved.
- (2) They feel like it—they curve more than the surface forces them to.

Curves that curve as little as possible, and therefore curve only because they must, are called *geodesics*. These are the analogues of straight lines in the plane, and they minimize the distance between two sufficiently close points.

Finding the geodesics on a given surface is a central problem in the differential geometry of curves and surfaces. After the plane, the sphere provides an example where the geodesics are as simple as can be: they are all great circles. To seek a surface with more interesting and varied geodesics, it is natural to consider the torus, which indeed yields a much richer collection of geodesics. The first complete classification of the geodesics on the torus was given by G. A. Bliss in his article “The geodesics on the anchor ring” [2] which appeared in 1902 in the *Annals of Mathematics*. Bliss’s treatment, which is based on a calculus of variations argument, is not an easy read, and it is hardly self-contained, referencing a number of nineteenth century sources that now would be difficult to find.

Over time, the simpler aspects of this classification have been distilled to the point where they appear as exercises in modern differential geometry textbooks [3, 8] and are sometimes used as qualifying examination problems for graduate students in mathematics. But still this beautiful classical material, which so well illustrates the beauty, power, and perspective of differential geometry, is not easily accessible to most undergraduates. This is due, in part, to the formalities of Riemannian geometry that are normally used to explain it. Here, we arrive at a classification of the geodesics on a torus using only simple tools from standard introductory courses in single and multivariable calculus, without any specialized language or notation from differential geometry. In particular, we discern the subtle long-term behavior of a geodesic on a torus based on the angle it makes as it crosses the equator of the torus. (See Figure 1.\*) Our version of this story has been used numerous times as the basis of a single, self-contained lecture on this material, successfully delivered to a multivariable calculus class. We hope that others can make similar use of these “lecture notes.” More generally, we hope our

---

\*Note that the online version of this article has color diagrams.

study can serve as a model for clarifying and simplifying other great stories so that they also can be told effectively to students in our introductory calculus sequences.

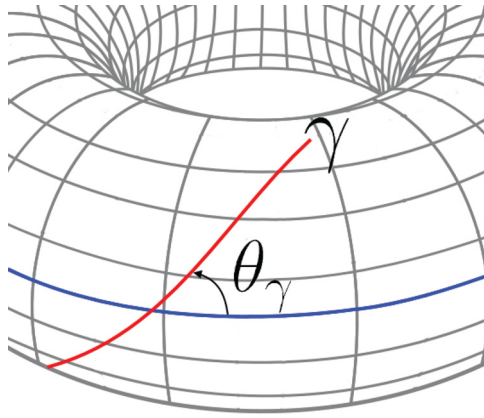


**Figure 1** A geodesic  $\gamma$  (red) crossing the outer parallel (blue)

## Surfaces of revolution

A *surface of revolution* is a surface  $S$  obtained by rotating a ( $C^2$  smooth) curve  $C$  that lies in some plane around an axis that lies in that same plane. The curve  $C$  is called the *profile curve* of  $S$ . We take the  $xz$ -plane as the plane of the profile curve and the  $z$ -axis as the axis of rotation. (See Figure 2.)

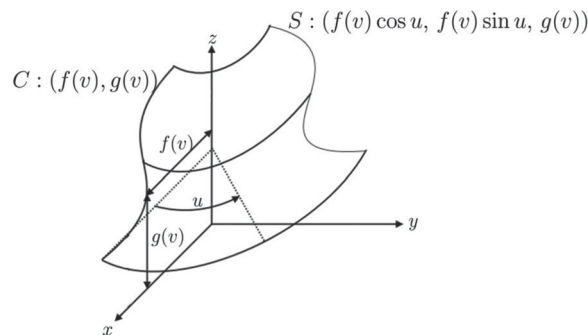


**Figure 2** A surface of revolution

We parametrize the profile curve  $C$  by

$$(x, z) = (f(v), g(v))$$

for a real variable  $v$ . To ease calculations, we assume that the parameterization is unit speed. The resulting surface of revolution  $S$  is parameterized by

$$\mathbf{X}(u, v) = (f(v) \cos u, f(v) \sin u, g(v)), \quad 0 \leq u < 2\pi, \quad (1)$$

where  $\|\mathbf{X}_v\| = (f')^2 + (g')^2 = 1$ . The unit speed condition also implies that  $\mathbf{X}_{vv} \cdot \mathbf{X}_v = 0$ , as the reader can easily verify. Also note that for a surface of revolution parameterized as above,  $\mathbf{X}_u \cdot \mathbf{X}_v = 0$ .

The horizontal circles described by equations of the form  $v \equiv \text{constant}$  are the *parallels* of  $S$ . The rotated copies of the profile curve described by equations of the form  $u \equiv \text{constant}$  are the *meridians* of  $S$ .

**Example 2.1.** A sphere of radius  $r$ ,  $S^2(r)$ , is a surface of revolution whose profile curve  $C$  is a semicircle of radius  $r$  in the  $xz$ -plane centered at  $(x, z) = (0, 0)$ . (See Figure 3a.) We parameterize  $C$  by

$$(x, z) = (f(v), g(v)) = (r \cos v, r \sin v), \quad -\frac{\pi}{2} \leq v \leq \frac{\pi}{2},$$

resulting in the parameterization of  $S^2(r)$ :

$$\mathbf{X}(u, v) = (r \cos v \cos u, r \sin v \sin u, r \sin v), \quad 0 \leq u < 2\pi.$$

**Example 2.2.** A torus  $T^2(r_1, r_2)$ , with *inner* and *outer* radii  $r_1$  and  $r_2$ , respectively, is a surface of revolution whose profile curve  $C$  is a circle of radius  $\frac{r_2 - r_1}{2}$  in the  $xz$ -plane centered at  $(x, z) = (\frac{r_1 + r_2}{2}, 0)$ . (See Figure 3b.) We parametrize  $C$  by

$$(x, z) = (f(v), g(v)) = \left( \frac{r_1 + r_2}{2} + \frac{r_2 - r_1}{2} \cos v, \frac{r_2 - r_1}{2} \sin v \right), \quad 0 \leq v < 2\pi,$$

and for  $u \in [0, 2\pi)$ , we have the resulting parametrization of  $T^2(r_1, r_2)$ :

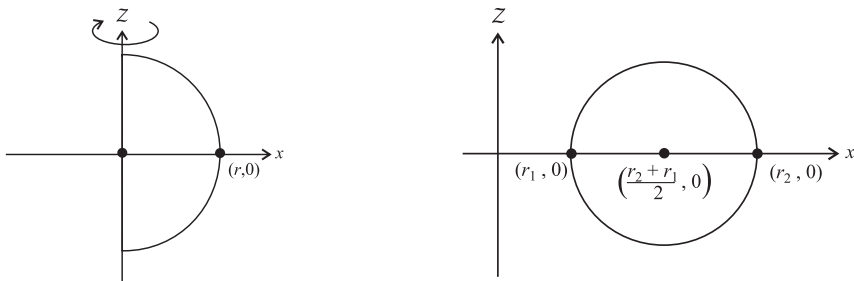
$$\mathbf{X}(u, v) = (x, y, z),$$

where

$$x = \left( \frac{r_1 + r_2}{2} + \frac{r_2 - r_1}{2} \cos v \right) \cos u,$$

$$y = \left( \frac{r_1 + r_2}{2} + \frac{r_2 - r_1}{2} \cos v \right) \sin u$$

$$z = \frac{r_2 - r_1}{2} \sin v.$$



(a) The profile curve of  $S^2(r)$

(b) The profile curve of  $T^2(r_1, r_2)$

**Figure 3** Profile curves

## Geodesics on a surface of revolution

Intuitively, a geodesic on a surface  $S$  is a ( $C^2$  smooth) curve  $\gamma : (a, b) \rightarrow \mathbb{R}^3$  that curves only as much as it needs to in order to stay on  $S$ . If such a curve  $\gamma$  lies on  $S$ , then for each  $s \in (a, b)$ , the vector  $\ddot{\gamma}(s)$  breaks into components normal and tangent to  $S$ ,

$$\ddot{\gamma}(s) = \ddot{\gamma}(s)^\perp + \ddot{\gamma}(s)^{\text{tan}}.$$

The normal component is the curvature of  $\gamma$  imposed on it by the shape of  $S$ , and  $\kappa_n = \|\ddot{\gamma}(s)^\perp\|$  is called the *normal curvature*. The tangential component measures any “extra” curvature of  $\gamma$  relative to  $S$ , and  $\kappa_g = \|\ddot{\gamma}(s)^{\text{tan}}\|$  is called the *geodesic curvature*. Recall that the *spacial curvature* of a unit-speed  $\gamma$  is given by  $\kappa(s) = \|\ddot{\gamma}(s)\|$ . The three curvatures associated with  $\gamma$  have a nice Pythagorean relationship given by

$$\kappa^2 = \kappa_n^2 + \kappa_g^2,$$

and  $\gamma$  is a *geodesic* when  $\kappa_g = 0$ . For a surface of revolution parameterized as in equation (1):

$$\ddot{\gamma}(s)^{\text{tan}} = \ddot{\gamma} \cdot \mathbf{X}_v + \ddot{\gamma} \cdot \mathbf{X}_u.$$

It follows that  $\gamma$  is a geodesic precisely when

$$\ddot{\gamma} \cdot \mathbf{X}_v = 0 \quad \text{and} \quad \ddot{\gamma} \cdot \mathbf{X}_u = 0. \quad (2)$$

The geometric conditions in equation (2) can be rewritten as two second-order differential equations for the functions  $u(s)$  and  $v(s)$  that define  $\gamma$ . We assume the parametrization in equation (1) so that

$$\gamma(s) = \mathbf{X}(u(s), v(s)).$$

Careful application of the chain rule yields expressions for velocity and acceleration:

$$\dot{\gamma}(s) = \mathbf{X}_u \dot{u}(s) + \mathbf{X}_v \dot{v}(s),$$

and

$$\begin{aligned} \ddot{\gamma} &= (\mathbf{X}_u)' \dot{u} + \mathbf{X}_u \ddot{u} + (\mathbf{X}_v)' \dot{v} + \mathbf{X}_v \ddot{v} \\ &= (\mathbf{X}_{uu} \dot{u} + \mathbf{X}_{uv} \dot{v}) \dot{u} + \mathbf{X}_u \ddot{u} + (\mathbf{X}_{vu} \dot{u} + \mathbf{X}_{vv} \dot{v}) \dot{v} + \mathbf{X}_v \ddot{v} \\ &= \mathbf{X}_{uu} \dot{u}^2 + 2\mathbf{X}_{uv} \dot{u} \dot{v} + \mathbf{X}_u \ddot{u} + \mathbf{X}_v \ddot{v} + \mathbf{X}_{vv} \dot{v}^2. \end{aligned} \quad (3)$$

In these expressions, the vectors  $\mathbf{X}_u$ ,  $\mathbf{X}_v$ ,  $\mathbf{X}_{uu}$ ,  $\mathbf{X}_{vv}$ , and  $\mathbf{X}_{uv}$  describe the geometry of the surface at the point  $\mathbf{X}(u, v)$ , whereas the scalars  $\dot{u}(s)$ ,  $\dot{v}(s)$ ,  $\ddot{u}(s)$ , and  $\ddot{v}(s)$  describe what  $\gamma$  looks like as it passes through the point  $\mathbf{X}(u(s), v(s))$ .

To compute the inner products in equation (2) we require the following data. First, the necessary derivatives:

$$\begin{aligned} \mathbf{X}_u &= (-f(v) \sin u, f(v) \cos u, 0) \\ \mathbf{X}_v &= (f'(v) \cos u, f'(v) \sin u, g'(v)) \\ \mathbf{X}_{uu} &= (-f(v) \cos u, -f(v) \sin u, 0) \\ \mathbf{X}_{vv} &= (f''(v) \cos u, f''(v) \sin u, g''(v)) \\ \mathbf{X}_{uv} &= \mathbf{X}_{vu} = (-f'(v) \sin u, f'(v) \cos u, 0); \end{aligned}$$

And now the necessary inner products:

$$\begin{array}{lll} \mathbf{X}_u \cdot \mathbf{X}_u & = & f^2 \\ \mathbf{X}_{uu} \cdot \mathbf{X}_u & = & 0 \\ \mathbf{X}_{uu} \cdot \mathbf{X}_v & = & -ff' \end{array} \quad \begin{array}{lll} \mathbf{X}_v \cdot \mathbf{X}_v & = & 1 \\ \mathbf{X}_{vv} \cdot \mathbf{X}_u & = & 0 \\ \mathbf{X}_{vv} \cdot \mathbf{X}_v & = & 0 \end{array} \quad \begin{array}{lll} \mathbf{X}_u \cdot \mathbf{X}_v & = & 0 \\ \mathbf{X}_{uv} \cdot \mathbf{X}_u & = & ff' \\ \mathbf{X}_{uv} \cdot \mathbf{X}_v & = & 0. \end{array} \quad (4)$$

Putting equations (2)–(4) together yields the *geodesic equations* for a surface of revolution:

$$2ff'\dot{u}\dot{v} + f^2\ddot{u} = 0 \quad (5)$$

and

$$\ddot{v} - ff'\dot{u}^2 = 0. \quad (6)$$

We also maintain the tacit assumption that  $\gamma$  is unit speed<sup>1</sup>, which gives

$$1 = f^2\dot{u}^2 + \dot{v}^2. \quad (7)$$

Armed with the geodesic equations (5) and (6), and the *unit speed condition* (7), we can begin our search for geodesics in earnest. The natural first question emerges: which, if any, among the meridians and parallels are geodesics? We address this question in the next two subsections.

**Meridians** Recall that on a surface of revolution parameterized as in equation (1), a meridian is a curve  $\gamma(s) = \mathbf{X}(u(s), v(s))$  where  $u$  is constant. But  $u$  being constant implies that both  $\dot{u}$  and  $\ddot{u}$  are identically zero and the first geodesic equation (5) is trivially satisfied. The second geodesic equation (6) now follows from equation (7). We conclude that all meridians are geodesics.

**Parallels** On a surface of revolution, parameterized as in (1), a parallel is a curve  $\gamma(s) = \mathbf{X}(u(s), v(s))$ , where  $v$  is constant. But if  $v$  is constant, the unit speed condition (7) implies that  $f\dot{u} = 1$  and so,  $f \neq 0$  and  $\dot{u} \neq 0$ . It follows that the two geodesic equations (5) and (6) are equivalent and that  $\gamma$  is a geodesic if and only if the constant  $v$  is such that  $f'(v) = 0$ . That is, the only parallels that are geodesics are generated by critical points of the radial distance function  $f$ .

**Example 3.1.** On  $S^2(r)$ ,  $f(v) = r \cos v$ ,  $-\frac{\pi}{2} < v < \frac{\pi}{2}$ . Here,  $f'(v) = 0$  precisely when  $v = 0$ . So, the only parallel that is a geodesic is the outer parallel, which is the orbit of the point  $(r, 0)$ .

**Example 3.2.** On  $T^2(r_1, r_2)$ ,

$$f(v) = \frac{r_2 + r_1}{2} + \frac{r_2 - r_1}{2} \cos v \quad (0 \leq v < 2\pi).$$

Here,  $f'(v) = 0$  precisely when  $v = 0$  or  $v = \pi$ . So, the only parallels that are geodesics are the inner and outer ones. That is, the orbits of the points  $(r_1, 0)$  and  $(r_2, 0)$ , respectively.

---

<sup>1</sup>This can always be arranged when  $\gamma$  is nonconstant. Throughout this article, “geodesic” will always mean “nonconstant geodesic.”



To identify other geodesics on surfaces of revolution, we will tease more information out of the first geodesic equation (5). Since this equation can be written as the exact differential

$$2ff'\dot{u}\dot{v} + f^2\ddot{u} = \frac{d}{dt}(f^2\dot{u}) = 0,$$

we see that a necessary condition for a curve to be a geodesic is that its parameterizing function  $u$  must satisfy  $f^2\dot{u} = c$ , for some constant  $c$ . On the other hand, let  $\gamma$  be any unit speed curve on the surface of revolution that crosses a parallel at an angle  $\theta \in [-\frac{\pi}{2}, \frac{\pi}{2}]$ . We know from vector calculus that

$$\cos \theta = \frac{|\dot{\gamma} \cdot \mathbf{X}_u|}{\|\dot{\gamma}\| \|\mathbf{X}_u\|} = \frac{|(\mathbf{X}_u\dot{u} + \mathbf{X}_v\dot{v}) \cdot \mathbf{X}_u|}{\|\mathbf{X}_u\|} = \left| \frac{f^2\dot{u}}{f} \right| = |f\dot{u}|. \quad (8)$$

Multiplying both sides of equation (8) by  $f$  gives  $f \cos \theta = f^2|\dot{u}|$  and so  $f \cos \theta = |c|$ . We have established the following theorem.

**Theorem 1** (Clairaut's relation [5]<sup>2</sup>). *Let  $\gamma$  be a geodesic on a surface of revolution  $S$  parameterized as in (1). If  $\gamma(s)$  intersects a parallel of  $S$ , let  $\theta$  be the angle between  $\gamma$  and that parallel, i.e., between  $\dot{\gamma}$  and  $\mathbf{X}_u$ , and let  $f$  be the radial distance the point of intersection is from the axis of revolution. Along  $\gamma$ , we then have the constant relationship*

$$c = f \cos \theta. \quad (9)$$

Theorem 9 implies that for each geodesic  $\gamma$  on a surface of revolution, there is a *critical distance*,  $c = f \cos \theta$ , which can be computed at any parallel that  $\gamma$  intersects. This allows us to construct surfaces of revolution with geodesics that have prescribed behaviors. For example, suppose  $\gamma$ 's critical distance is  $c$  and that  $\gamma$  is approaching a parallel  $P$  whose distance from the axis of rotation is also  $c$ . Can  $\gamma$  intersect  $P$ ? The answer depends on whether or not  $P$  is a geodesic. More specifically, if  $\gamma$  does intersect  $P$ , then Theorem 9 implies that it must do so tangentially ( $c = c \cos \theta \implies \theta = 0$ ). If it happens that  $P$  is a geodesic, then at the presumed point of intersection of  $\gamma$  and  $P$ , two different geodesics would have the same tangent vector. This is not possible since a geodesic is locally uniquely determined by a point and a direction. In this situation,  $\gamma$  spirals asymptotically toward  $P$ . For this reason, such  $P$ 's have elsewhere been called *barrier curves* [4, 6]. (See Figure 4(a)). If on the other hand,  $P$  is not a geodesic, then  $\gamma$  has reached its critical distance at this parallel and then moves in the direction of increasing radial distance from the axis of rotation. Effectively,  $\gamma$  “bounces off” of  $P$ ; see Figure 4(b), where the red geodesic is forever trapped, bouncing between the two green barrier curves. (We often call the parallel with the largest radial distance the “equator” of a surface of revolution—as noted in Figure 4.)

## Geodesics on the torus

The results of the previous section establish that all the meridians on a surface of revolution are geodesics. But for parallels the story is quite different. If  $f$  is the function that records the radial distance from a point on the surface of revolution to the axis of revolution, then only those parallels which are orbits of local extrema of  $f$  are

<sup>2</sup>Named after the French mathematician and geophysicist Alexis Claude Clairaut (1713–1765) who helped to establish the Newtonian claim that the earth was not a perfect sphere. Pressley [8, p. 185] explains Theorem 1 as an expression of the conservation of angular momentum about the axis of revolution when a particle slides along a geodesic under no forces other than those that keep it on the surface. See also Oprea [7, pp. 223–224].

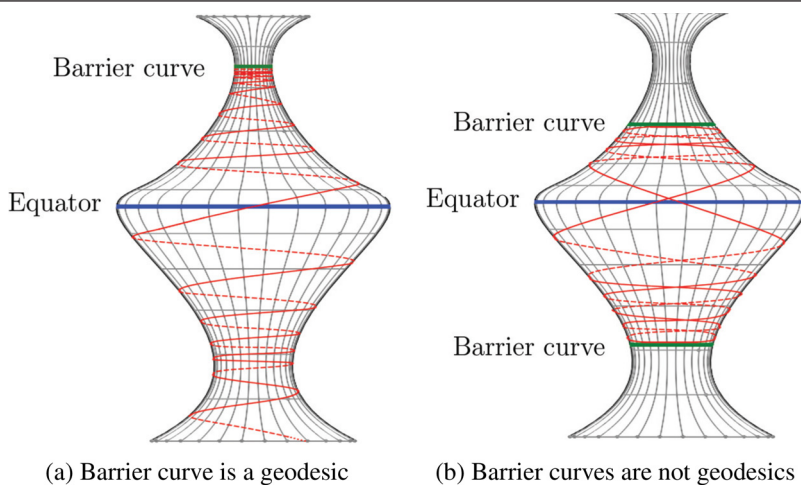


**Figure 4** Barrier curves

geodesics. For the torus, this means that the only parallels which are geodesics are the inner and outer ones. To find other geodesics on the torus, the following theorem is fundamental.

**Theorem 2.** *Except for the inner parallel, every geodesic on the torus must intersect the outer parallel.*

*Proof.* All meridians intersect the outer parallel at right angles. We therefore assume that a geodesic  $\gamma$  intersects the parallels of  $T^2$  with a radial distance function  $f$  and an angular function  $\theta \neq \frac{\pi}{2}$ . Now follow  $\gamma$  in the direction of increasing  $f$ —which is monotonically increasing and bounded above by  $r_2$ . We need only show that  $\gamma$  cannot asymptotically approach the outer parallel. If that were to happen, we would have  $\lim_{f \rightarrow r_2} \theta = 0$ . But, by equation (9),  $f$  and  $\theta$  increase together. So,  $\gamma$  must intersect the outer parallel. ■

Proceeding to the classification of the geodesics on  $T^2(r_1, r_2)$ , we first define the *critical angle* of the torus:

$$\theta_C = \cos^{-1} \left( \frac{r_1}{r_2} \right).$$

We can now classify the geodesics on the torus according to the relationship between the geodesic's crossing angle and the critical angle of the torus. We do this in the following subsections, where we also note the long-term behavior of the geodesics.

**Classification of geodesics on the Torus** Let  $T^2(r_1, r_2)$  be a torus with inner and outer radii,  $r_1$  and  $r_2$ , respectively. All meridians are geodesics and of the parallels, only the inner and outer parallel are geodesics. If  $\gamma$  a geodesic which crosses the outer parallel at an angle,  $\theta_\gamma \in (0, \frac{\pi}{2})$ , we are reduced to the following three cases treated in the following subsections.

*Case 1.*  $0 < \theta_\gamma < \theta_C$  Since cosine is a decreasing function,  $\cos \theta_\gamma > \cos \theta_C = \frac{r_1}{r_2}$  and so  $r_2 \cos \theta_\gamma > r_1$ . But since  $r_2$  is the distance where  $\gamma$  crosses the outer parallel, Theorem 1 implies that  $\gamma$ 's critical distance  $c$  is greater than  $r_1$ . (See Figure 5.)

*Case 2.*  $\theta_\gamma = \theta_C$  This case leads to  $\cos \theta_\gamma = \cos \theta_C = \frac{r_1}{r_2}$ . Theorem 1 implies that

$$c = r_2 \cos \theta_\gamma = r_2 \frac{r_1}{r_2} = r_1.$$

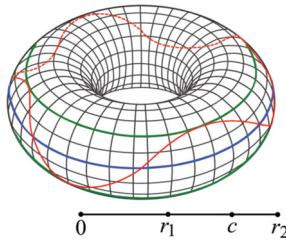


**Figure 5** Case 1 geodesic oscillating between two barrier curves

So,  $c = r_1$  and since the inner parallel is a geodesic,  $\gamma$  spirals asymptotically toward it. (See Figure 6.)

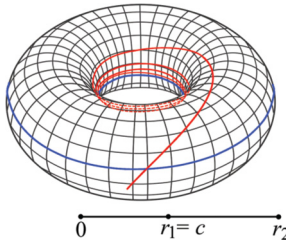


**Figure 6** Case 2 geodesic asymptotically approaching the inner parallel

*Case 3.*  $\theta_C < \theta_\gamma < \frac{\pi}{2}$  This case leads to  $\cos \theta_\gamma < \cos \theta_C$ . Theorem 1 implies that

$$c = r_2 \cos \theta_\gamma < r_2 \cos \theta_C = r_1.$$

So,  $c < r_1$ , and  $\gamma$  can never realize its critical distance by either intersection or asymptotic approach. (See Figure 7.)

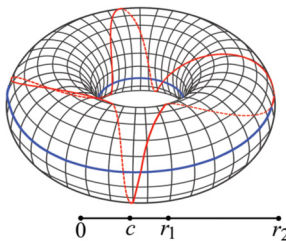


**Figure 7** Case 3 geodesic with no barrier curve

## Afterword and looking ahead

Except for the meridians and the inner and outer parallels of a torus  $T^2(r_1, r_2)$ , each geodesic  $\gamma$  must intersect the equator of the torus at the geodesic's crossing angle  $0 < \theta_\gamma < \frac{\pi}{2}$ , and  $\gamma$ 's eventual behavior is determined by the relationship between  $\theta_\gamma$  and the critical angle of the torus defined by  $\theta_C = \cos^{-1}(\frac{r_1}{r_2})$ . We are left with the three cases of the previous section. We will examine Case 1 and Case 3 more closely.

In Case 1 ( $\theta_\gamma < \theta_C$ ), the geodesic does not have enough “energy” (see Jantzen [6]) to encircle the outer parallel, but oscillates back and forth across the equator and between its barrier curves as it encircles the  $z$ -axis. In Case 3 ( $\theta_\gamma > \theta_C$ ), the geodesic’s crossing angle is steep enough, and so its energy sufficient, that it can repeatedly encircle the outer parallel as it winds around the  $z$ -axis. In some instances, these geodesics may be *closed*. That is, there is an  $s_0 \in \mathbb{R}$  such that  $\gamma(s_0 + s) = \gamma(s)$ , for all values of  $s$ . Here, such a closed geodesic winds  $p$  times around the  $z$ -axis while making  $q$ -oscillations ( $2q$  crossings) across the equatorial geodesic, before returning to its “starting point,” which we take to be an arbitrary point where  $\gamma$  intersects the equator. In this way, closed geodesics on the torus are indexed by pairs of coprime integers  $p$  and  $q$ . We call the ordered pair  $(p, q)$  the *index* of the closed geodesic.

In a follow-up note, and again using elementary means, we determine the permissible index of a geodesic on  $T^2(r_1, r_2)$ , by examining allowable quotients  $p/q$  in terms of the tori’s defining parameters  $r_1$  and  $r_2$  (see Alexander [1]). Here, another angle takes center stage—the *return angle* of a closed geodesic. More specifically, and to illustrate, let  $\gamma$  be a closed Case 1 geodesic, which intersects the equator at two points  $p_1$  and  $p_2$ . The return angle of  $\gamma$  is denoted by  $\gamma_r$  and is defined as the central angle subtended by the rays defined by the origin and the points  $p_1$  and  $p_2$ ; see Figure 8, where a portion of a Case 1 geodesic is depicted in red.

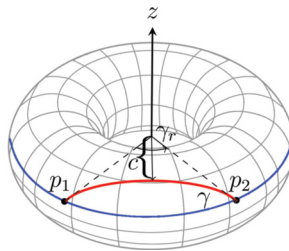


**Figure 8** The return angle  $\gamma_r$

We find, in particular, that  $T^2(r_1, r_2)$  has a closed Case 1 geodesic  $\gamma$  of index  $(p, q)$  precisely when the quotient  $\frac{p}{q}$  is bounded below (and related to  $\gamma$ ’s return angle  $\gamma_r$ ) as follows:

$$\sqrt{\frac{r_2 - r_1}{2r_2}} < \frac{p}{q} = \frac{\gamma_r}{\pi}.$$

**Remark.** *The details of this section are beyond the scope of this paper and will appear elsewhere.*

**Acknowledgments** The authors would like to thank two anonymous referees whose suggestions and commentary significantly streamlined the exposition in this article.

## REFERENCES

- [1] Alexander, J. (2006). Closed geodesics on certain surfaces of revolution. *J. Geom. Symmetry Phys.* 8: 1–16. [doi.org/10.7546/jgsp-8-2006-1-16](https://doi.org/10.7546/jgsp-8-2006-1-16)
- [2] Bliss, G. A. (1902). The geodesic lines on the anchor ring. *Ann. Math.* 4(1): 1–21. [doi.org/10.2307/1967147](https://doi.org/10.2307/1967147)
- [3] DoCarmo, M. (1976). *Differential Geometry of Curves and Surfaces*. Englewood Cliffs: Prentice-Hall.
- [4] Irons, M. (2005). The curvature and geodesics of the torus. [www.rdrop.com/~half/math/torus/torus.geodesics.pdf](http://www.rdrop.com/~half/math/torus/torus.geodesics.pdf). Last accessed February 2022.

- [5] Clairaut, A. (1735). Détermination géométrique de la perpendiculaire à la méridienne tracée par M. Cassini, *Ib.* 1733, 406.
- [6] Jantzen, R. T. Geodesics on the Torus and other Surfaces of Revolution Clarified Using Undergraduate Physics Tricks with Bonus: Nonrelativistic and Relativistic Kepler Problems. <http://www.homepage.villanova.edu/robert.jantzen/notes/torus/>, and <http://arxiv.org/abs/1212.6206>.
- [7] Oprea, J. (2007). *Differential Geometry and Its Applications*, 2nd ed. Washington, DC: Mathematical Association of America
- [8] Pressley, A. N. (2010). *Elementary Differential Geometry*, 2nd ed. London: Springer.

**Summary.** Based on an intuitively appealing way of defining what is meant by a geodesic on a two-dimensional surface in three-dimensional Euclidean space, we describe the general behavior of the geodesics on surfaces of revolution and give a simple yet precise characterization of the geodesics on a torus. We use only simple tools from the standard introductory courses in single and multivariable calculus, and no specialized language or notation from differential geometry, so our presentation is self-contained for anyone who is familiar with the contents of these courses. In particular, we are able to develop Clairaut's relation with relative ease.

**KYLE CELANO** received his B.S. in mathematics from Lehigh University in 2016. He is currently working on his Ph.D. in mathematics at the University of Miami. His research concerns the representation theory of the chromatic symmetric function. When he is not coloring graphs, he enjoys playing board games and other tabletop experiences.

**VINCENT E. COLL, JR.** received his Ph.D. in mathematics from the University of Pennsylvania in 1990 under the direction of Murray Gerstenhaber. He enjoys tinkering with classical geometry problems although his main work is in algebraic combinatorics. His pastimes include golf and bridge, where in the latter he has just made bronze life-master – YAY!

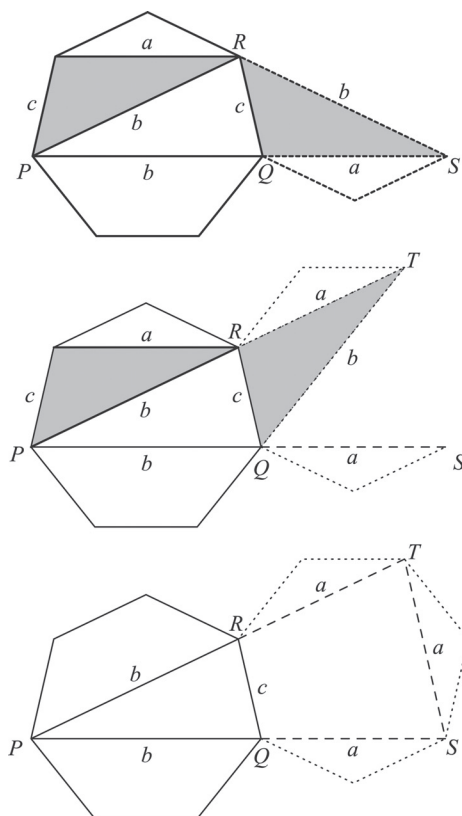
**JEFF DODD** received his Ph.D. in mathematics from the University of Maryland in 1996 under the direction of Robert L. Pego. Since then, he has been on the faculty at Jacksonville State University.

# PROOFS WITHOUT WORDS

## Diagonals on a Regular Heptagon

POO-SUNG PARK

Kyungnam University  
Changwon, Republic of Korea 51767  
[pspark@kyungnam.ac.kr](mailto:pspark@kyungnam.ac.kr)



$$\triangle PQR \sim \triangle PST$$

$$b : b + a = c : a$$

$$\frac{1}{c} = \frac{1}{a} + \frac{1}{b}$$

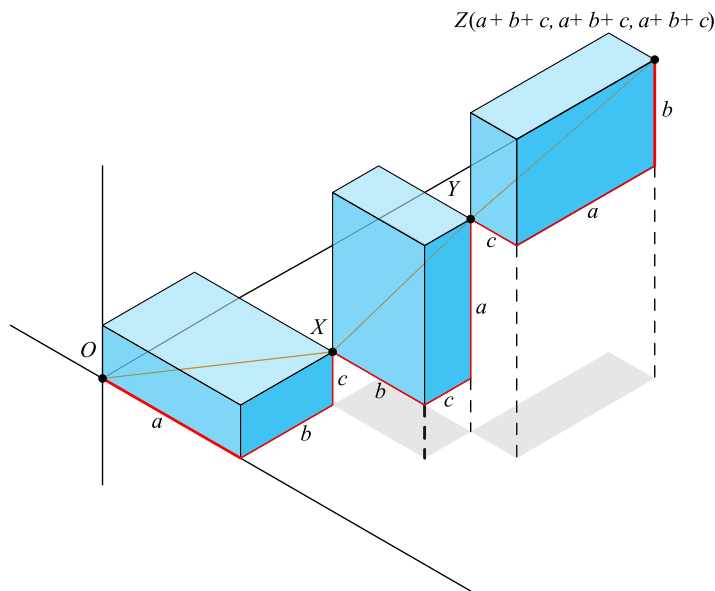
**Summary.** We provide a visual proof for a relationship among the diagonals of a regular heptagon.

**POO-SUNG PARK** (MR Author ID: 803154) obtained a Ph.D. in mathematics from Seoul National University in 2005. He is a professor in the Department of Mathematics Education at Kyungnam University, South Korea. His research focuses on the arithmetic theory of quadratic forms. He is also interested in recreational mathematics.

*Math. Mag.* **95** (2022) 240. doi:10.1080/0025570X.2022.2054637 © Mathematical Association of America

**AM ≤ QM**

DAVID TREEBY

Monash University  
Melbourne, Australia  
[david.treeby@gmail.com](mailto:david.treeby@gmail.com)

$$OZ \leq OX + XY + YZ \leq 3(a + b + c)$$

$$\iff \sqrt{3}(a + b + c) \leq 3\sqrt{a^2 + b^2 + c^2} \leq 3(a + b + c)$$

$$\iff \frac{a + b + c}{3} \leq \sqrt{\frac{a^2 + b^2 + c^2}{3}} \leq \frac{a + b + c}{\sqrt{3}}$$

## REFERENCES

- [1] Alsina, C., Nelsen, R. B. (2009). *When Less is More: Visualizing Basic Inequalities*. Washington, DC: Mathematical Association of America, p. 3.
- [2] Bullen, P. S., Mitrinovic, D. S., Vasic, P. M. (1988). *Means and their Inequalities*. Dordrecht: D. Reidel.
- [3] Gwanyama, P. W. (2004). The HM-GM-AM-QM Inequalities. *College Math. J.* 35(1): 47–50. doi.org/10.1080/07468342.2004.11922051
- [4] Kung, S. (1990). Harmonic, geometric, arithmetic, root mean inequality. *College Math. J.* 21(3): 227.
- [5] Nelsen, R. B. (1993). *Proofs Without Words I: Exercises in Visual Thinking*. Washington, DC: Mathematical Association of America.

**Summary.** We present a wordless proof of the arithmetic mean-quadratic mean inequality.

**DAVID TREEBY** teaches mathematics at Scotch College, Melbourne, and is a Research Associate at Monash University, Australia.

---

# PROBLEMS

---

LES REID, *Editor*

Missouri State University

EUGEN J. IONAȘCU, *Proposals Editor*

Columbus State University

RICHARD BELSHOFF, Missouri State University; MAHYA GHANDEHARI, University of Delaware; EYVINDUR ARI PALSSON, Virginia Tech; GAIL RATCLIFF, East Carolina University; ROGELIO VALDEZ, Centro de Investigación en Ciencias, UAEM, Mexico; *Assistant Editors*

## Proposals

*To be considered for publication, solutions should be received by November 1, 2022.*

**2146.** *Proposed by Kenneth Fogarty, Bronx Community College (emeritus), Bronx, NY.*

Let  $a$  and  $d$  be integers with  $d > 0$ . We say that  $(a, d)$  is *good* if there is an arithmetic sequence with initial term  $a$  and difference  $d$  that can be split into two sequences of consecutive terms with the same sum. In other words, there exist integers  $k$  and  $n$  with  $0 < k < n$  such that

$$\sum_{i=0}^{k-1} (a + di) = \sum_{i=k}^{n-1} (a + di).$$

If there is no such arithmetic sequence, we say that  $(a, d)$  is *bad*.

- (a) Show that if  $2a > d$ , then  $(a, d)$  is good.
- (b) Show that if  $2a = d$ , then  $(a, d)$  is bad.
- (c) Show that if  $a = 0$  (and hence  $2a < d$ ), then  $(a, d)$  is good.
- (d) Show that if  $2a < d$  and  $a \neq 0$ , then there is a  $d$  such that  $(a, d)$  is good and a  $d$  such that  $(a, d)$  is bad.

**2147.** *Proposed by Lokman Gökçe, Istanbul, Turkey.*

Evaluate

$$\prod_{n=2}^{\infty} \frac{n^4 + 4}{n^4 - 1}.$$

---

*Math. Mag.* **95** (2022) 242–250. doi:10.1080/0025570X.2022.2061246 © Mathematical Association of America

We invite readers to submit original problems appealing to students and teachers of advanced undergraduate mathematics. Proposals must always be accompanied by a solution and any relevant bibliographical information that will assist the editors and referees. A problem submitted as a Quickie should have an unexpected, succinct solution. Submitted problems should not be under consideration for publication elsewhere.

Proposals and solutions should be written in a style appropriate for this MAGAZINE.

Authors of proposals and solutions should send their contributions using the Magazine's submissions system hosted at <http://mathematicsmagazine.submittable.com>. More detailed instructions are available there. We encourage submissions in PDF format, ideally accompanied by L<sup>A</sup>T<sub>E</sub>X source. General inquiries to the editors should be sent to [mathmagproblems@maa.org](mailto:mathmagproblems@maa.org).

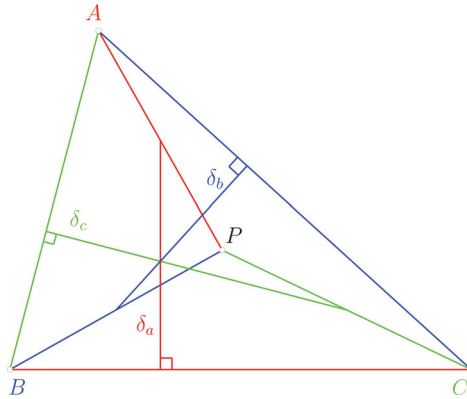


**2148.** *Proposed by Tran Quang Hung, Hanoi, Vietnam.*

Let  $P$  be an interior point of triangle  $ABC$ . Denote by  $\delta_a$ ,  $\delta_b$ , and  $\delta_c$  the distances from midpoints of segments  $PA$ ,  $PB$ , and  $PC$  to the lines  $BC$ ,  $CA$ , and  $AB$ . Prove that

$$PA + PB + PC \geq \delta_a + \delta_b + \delta_c.$$

Show that equality holds if and only if triangle  $ABC$  is equilateral and  $P$  is its center.



**2149.** *Proposed by Ioan Băetu, Botoșani, Romania.*

Let  $a_1, a_2, \dots$  be a sequence of integers greater than 1. The series

$$\sum_{k=0}^{\infty} \frac{(-1)^k}{\prod_{i=1}^k a_i} = 1 - \frac{1}{a_1} + \frac{1}{a_1 a_2} - \frac{1}{a_1 a_2 a_3} + \dots$$

converges by the alternating series test.

- If the sequence  $a_1, a_2, \dots$  is unbounded, show that the sum of the series is irrational.
- Give an example of a bounded sequence of  $a_i$ 's such that the sum of the series is irrational.

**2150.** *Proposed by Matthew McMullen, Otterbein University, Westerville, OH.*

Find the maximum area of a triangle whose vertices lie on the cardioid  $r = 1 + \cos \theta$ .

## Quickies

**1121.** *Proposed by Salem Malikic, Bethesda, MD.*

For integers  $n \geq 0$ , let  $a_n$  and  $b_n$  be the unique real numbers such that

$$a_n + b_n i = (2 + i)^n.$$

Evaluate

$$\sum_{n=0}^{\infty} \frac{a_n b_n}{2^n (a_n^2 + b_n^2)}.$$

**1122.** *Proposed by the Columbus State University Problem Solving Group, Columbus State University, Columbus, GA.*

Show that there are infinitely many nonsimilar triangles having integer side lengths such that the angle measures are in arithmetic progression.

## Solutions

### Evaluate the definite integral

June 2021

**2121.** *Proposed by Seán M. Stewart, Bomaderry, Australia.*

Evaluate

$$\int_0^{\frac{1}{2}} \frac{\arctan x}{x^2 - x - 1} dx.$$

*Solution by Lixing Han, University of Michigan-Flint, Flint, MI and Xinjia Tang, Changzhou University, Changzhou, China.*

Using the substitution

$$x = \frac{\frac{1}{2} - t}{1 + \frac{1}{2}t} = \frac{1 - 2t}{2 + t},$$

we obtain

$$\begin{aligned} \int_0^{\frac{1}{2}} \frac{\arctan x}{x^2 - x - 1} dx &= \int_{\frac{1}{2}}^0 \frac{\arctan\left(\frac{\frac{1}{2}-t}{1+\frac{1}{2}t}\right)}{\left(\frac{1-2t}{2+t}\right)^2 - \frac{1-2t}{2+t} - 1} \cdot \frac{-5}{(2+t)^2} dt \\ &= \int_0^{\frac{1}{2}} \frac{\arctan\left(\frac{1}{2}\right) - \arctan t}{t^2 - t - 1} dt \\ &= \int_0^{\frac{1}{2}} \frac{\arctan\left(\frac{1}{2}\right)}{t^2 - t - 1} dt - \int_0^{\frac{1}{2}} \frac{\arctan t}{t^2 - t - 1} dt. \end{aligned}$$

Thus, we have

$$\begin{aligned} \int_0^{\frac{1}{2}} \frac{\arctan x}{x^2 - x - 1} dx &= \frac{1}{2} \arctan\left(\frac{1}{2}\right) \int_0^{\frac{1}{2}} \frac{dt}{t^2 - t - 1} \\ &= \frac{1}{2} \arctan\left(\frac{1}{2}\right) \frac{1}{\sqrt{5}} \ln \left( \left| \frac{2t - \sqrt{5} - 1}{2t + \sqrt{5} - 1} \right| \right) \Big|_0^{\frac{1}{2}} \\ &= -\frac{1}{2\sqrt{5}} \arctan\left(\frac{1}{2}\right) \ln \left( \frac{\sqrt{5} + 1}{\sqrt{5} - 1} \right) \\ &= -\frac{1}{\sqrt{5}} \arctan\left(\frac{1}{2}\right) \ln \left( \frac{\sqrt{5} + 1}{2} \right). \end{aligned}$$

*Also solved by Brian Bradie, Hongwei Chen, Hervé Grandmontagne (France), Eugene A. Herman, Omran Kouba (Syria), Kee-Wai Lau (China), Albert Natian, Moobinoor Omarjee (France), Didier Pichon (France), Albert Stadler (Switzerland), Fejéntaláltuka Szöged (Hungary), and the proposer. There were four incomplete or incorrect solutions.*

**Find the maximum gcd****June 2021****2122.** *Proposed by Ahmad Sabihi, Isfahan, Iran.*

Let

$$G(m, k) = \max\{\gcd((n+1)^m + k, n^m + k) | n \in \mathbb{N}\}.$$

Compute  $G(2, k)$  and  $G(3, k)$ .*Solution by Michael Reid, University of Central Florida, Orlando, FL.*We show that for  $k \in \mathbb{Z}$ ,  $G(2, k) = |4k + 1|$ , and

$$G(3, k) = \begin{cases} 27k^2 + 1 & \text{if } k \text{ is even,} \\ (27k^2 + 1)/4 & \text{if } k \text{ is odd.} \end{cases}$$

The polynomial identity

$$(2n+3)(n^2+k) - (2n-1)((n+1)^2+k) = 4k+1$$

shows that

$$\gcd((n+1)^2+k, n^2+k) \text{ divides } 4k+1,$$

and thus is at most  $|4k+1|$ . Hence,  $G(2, k) \leq |4k+1|$ .Suppose  $k > 0$ , and let  $n = 2k \in \mathbb{N}$ . We have

$$n^2+k = k(4k+1) \text{ and } (n+1)^2+k = (k+1)(4k+1),$$

both of which are divisible by  $4k+1$ . Thus

$$\gcd((n+1)^2+k, n^2+k) = 4k+1 = |4k+1|,$$

so  $G(2, k) = |4k+1|$  in this case.For  $k = 0$ , we have  $\gcd((n+1)^2, n^2) = 1$  for all  $n \in \mathbb{N}$ , so  $G(2, 0) = 1 = |4k+1|$  in this case.Suppose  $k < 0$ , and consider  $n = -(2k+1) \in \mathbb{N}$ . Then

$$n^2+k = (k+1)(4k+1) \text{ and } (n+1)^2+k = k(4k+1)$$

are each divisible by  $4k+1$ . Thus

$$\gcd((n+1)^2+k, n^2+k) = |4k+1|,$$

so  $G(2, k) = |4k+1|$  in this case as well.Now we consider  $G(3, k)$ . The polynomial identity

$$\begin{aligned} & (6n^2 - 9nk - 3n + 9k + 1)((n+1)^3+k) \\ & - (6n^2 - 9nk + 15n - 18k + 10)(n^3+k) = 27k^2 + 1 \end{aligned}$$

shows that

$$\gcd((n+1)^3+k, n^3+k) \text{ divides } 27k^2+1. \quad (1)$$

For all  $n$ ,  $(n+1)^3 + k$  and  $n^3 + k$  have opposite parity, so their greatest common divisor is odd. If  $k$  is odd, then  $27k^2 + 1 = 4((27k^2 + 1)/4)$  is a product of two integers. Since the greatest common divisor is odd, and divides this product,

$$\gcd((n+1)^3 + k, n^3 + k) \text{ divides } \frac{27k^2 + 1}{4}. \quad (2)$$

For  $k = 0$ , we have  $\gcd((n+1)^3, n^3) = 1$  for all  $n$ , so  $G(3, 0) = 27k^2 + 1 = 1$ .

For nonzero  $k$ , take  $n = 3k(9k - 1)/2$ , which is a positive integer. We calculate

$$n^3 + k = (27k^2 + 1) \left( \frac{(729k^3 - 243k^2 + 8)k}{8} \right)$$

and

$$(n+1)^3 + k = (27k^2 + 1) \left( \frac{729k^4 - 243k^3 + 162k^2 - 28k + 8}{8} \right).$$

If  $k$  is even, each factor above is an integer, which shows that

$$27k^2 + 1 \text{ divides } \gcd((n+1)^3 + k, n^3 + k).$$

With (1), we have

$$\gcd((n+1)^3 + k, n^3 + k) = 27k^2 + 1,$$

so  $G(3, k) = 27k^2 + 1$  when  $k$  is even.

If  $k$  is odd, rewrite the above factorizations as

$$n^3 + k = \left( \frac{27k^2 + 1}{4} \right) \left( \frac{(729k^3 - 243k^2 + 8)k}{2} \right)$$

and

$$(n+1)^3 + k = \left( \frac{27k^2 + 1}{4} \right) \left( \frac{729k^4 - 243k^3 + 162k^2 - 28k + 8}{2} \right),$$

again, all factors being integers. Therefore

$$\frac{27k^2 + 1}{4} \text{ divides } \gcd((n+1)^3 + k, n^3 + k).$$

With (2), we conclude that

$$\gcd((n+1)^3 + k, n^3 + k) = \frac{27k^2 + 1}{4},$$

so  $G(3, k) = (27k^2 + 1)/4$  when  $k$  is odd.

*Also solved by Hongwei Chen, Eagle Problem Solvers (Georgia Southern University), Dmitry Fleischman, George Washington University Math Problem Solving Group, Eugene A. Herman, Walther Janous (Austria), Didier Pinchon (France), Albert Stadler (Switzerland), Enrique Treviño, and the proposer. There were two incomplete or incorrect solutions.*

**Find the expected winnings****June 2021****2123.** *Proposed by Albert Natian, Los Angeles Valley College, Valley Glen, CA.*

An urn contains  $n$  balls. Each ball is labeled with exactly one number from the set

$$\{a_1, a_2, \dots, a_n\}, a_1 > a_2 > \dots > a_n$$

(so no two balls have the same number). Balls are randomly selected from the urn and discarded. At each turn, if the number on the ball drawn was the largest number remaining in the urn, you win the dollar amount of that ball. Otherwise, you win nothing. Find the expected value of your total winnings after  $n$  draws.

*Solution by Enrique Treviño, Lake Forest College, Lake Forest, IL.*

Let  $X$  be the random variable described. Then  $X = a_{i_1} + a_{i_2} + \dots + a_{i_j}$  with  $1 = i_1 < i_2 < \dots < i_j \leq n$ . Therefore, the expected value will be

$$\mathbb{E}[X] = \sum_{k=1}^n c_k a_k,$$

where  $c_k$  is the probability that the summand  $a_k$  appears in  $X$ . For  $a_k$  to appear, the ball labeled  $a_k$  must be drawn after those labeled  $a_1, a_2, \dots, a_{k-1}$ , but this only happens if the permutation of  $\{a_1, \dots, a_k\}$  ends in  $a_k$ . This occurs with probability  $1/k$ . Therefore

$$\mathbb{E}[X] = a_1 + \frac{1}{2}a_2 + \frac{1}{3}a_3 + \dots + \frac{1}{n}a_n.$$

Also solved by Robert A. Agnew, Alan E. Berger, Brian Bradie, Elton Bojaxhiu (Germany) & Enkel Hysnelaj (Australia), Paul Budney, Michael P. Cohen, Eagle Problem Solvers (Georgia Southern University), John Fitch, Dmitry Fleischman, Fresno State Journal Problem Solving Group, GWstat Problem Solving Group, George Washington University Problems Group, Victoria Gudkova (student) (Russia), Stephen Herschkorn, Shing Hin Jimmy Pa (Canada), David Huckaby, Walther Janous (Austria), Omran Kouba (Syria), Ken Levasseur, Reiner Martin (Germany), Kelly D. McLenithan, José Nieto (Venezuela), Didier Pinchon (France), Michael Reid, Edward Schmeichel, Albert Stadler (Switzerland), Fejéntaláltuka Szöged, and the proposer. There were two incomplete or incorrect solutions.

**A sum over the partitions of  $n$** **June 2021****2124.** *Proposed by Mircea Merca, University of Craiova, Craiova, Romania.*

For a positive integer  $n$ , prove that

$$\sum_{\substack{\lambda_1 + \lambda_2 + \dots + \lambda_k = n \\ \lambda_1 \geq \lambda_2 \geq \dots \geq \lambda_k > 0}} (-1)^{n-\lambda_1} \frac{\binom{\lambda_1}{\lambda_2} \binom{\lambda_2}{\lambda_3} \dots \binom{\lambda_k}{0}}{1^{\lambda_1} 2^{\lambda_2} \dots k^{\lambda_k}} = \frac{1}{n!},$$

where the sum runs over all the partitions of  $n$ .

*Solution by José Heber Nieto, Universidad del Zulia, Maracaibo, Venezuela.*

Put  $s_1 = \lambda_1 - \lambda_2$ ,  $s_2 = \lambda_2 - \lambda_3, \dots, s_{k-1} = \lambda_{k-1} - \lambda_k$ ,  $s_k = \lambda_k$ . Clearly, we have  $s_i \geq 0$ ,  $s_1 + s_2 + \dots + s_k = \lambda_1$ , and  $s_1 + 2s_2 + 3s_3 + \dots + ks_k = n$ . Moreover, for fixed  $\lambda_1$ , if we vary  $k$  and  $\lambda_2, \lambda_3, \dots, \lambda_k$  satisfying the conditions  $\lambda_1 \geq \lambda_2 \geq \dots \geq \lambda_k > 0$

and  $\lambda_1 + \lambda_2 + \cdots + \lambda_k = n$ , we obtain all the sequences of  $s_i$ 's satisfying  $s_i \geq 0$ ,  $s_1 + s_2 + \cdots + s_k = \lambda_1$  and  $s_1 + 2s_2 + 3s_3 + \cdots + ks_k = n$ .

Now

$$\frac{\binom{\lambda_1}{\lambda_2} \binom{\lambda_2}{\lambda_3} \cdots \binom{\lambda_k}{0}}{1^{\lambda_1} 2^{\lambda_2} \cdots k^{\lambda_k}} = \frac{\lambda_1!}{s_1! s_2! \cdots s_k! (1!)^{s_1} (2!)^{s_2} \cdots (k!)^{s_k}}.$$

We note that

$$\frac{n!}{s_1! s_2! \cdots s_k! (1!)^{s_1} (2!)^{s_2} \cdots (k!)^{s_k}}$$

is the number of partitions of the set  $\{1, 2, \dots, n\}$  into  $s_i$  blocks of size  $i$ , for  $i = 1, 2, \dots, k$ . For fixed  $\lambda_1$ , if we sum these expressions for all values of the  $s_i$ 's and  $k$  such that  $s_i \geq 0$ ,  $s_1 + s_2 + \cdots + s_k = \lambda_1$  and  $s_1 + 2s_2 + 3s_3 + \cdots + ks_k = n$ , we obtain the number of partitions of the set  $\{1, 2, \dots, n\}$  into  $\lambda_1$  blocks, that is the Stirling number of second kind  $\left\{ \begin{smallmatrix} n \\ \lambda_1 \end{smallmatrix} \right\}$ . Therefore

$$\sum_{\substack{\lambda_1 + \lambda_2 + \cdots + \lambda_k = n \\ \lambda_1 \geq \lambda_2 \geq \cdots \geq \lambda_k > 0}} (-1)^{n-\lambda_1} \frac{\binom{\lambda_1}{\lambda_2} \binom{\lambda_2}{\lambda_3} \cdots \binom{\lambda_k}{0}}{1^{\lambda_1} 2^{\lambda_2} \cdots k^{\lambda_k}} = \frac{1}{n!} \sum_{\lambda_1=1}^n (-1)^{n-\lambda_1} \lambda_1! \left\{ \begin{smallmatrix} n \\ \lambda_1 \end{smallmatrix} \right\}. \quad (1)$$

It is well known that

$$\sum_{\lambda_1=1}^n \left\{ \begin{smallmatrix} n \\ \lambda_1 \end{smallmatrix} \right\} x(x-1)(x-2) \cdots (x-\lambda_1+1) = x^n.$$

Substituting  $-x$  for  $x$  we obtain

$$\sum_{\lambda_1=1}^n (-1)^{n-\lambda_1} \left\{ \begin{smallmatrix} n \\ \lambda_1 \end{smallmatrix} \right\} x(x+1)(x+2) \cdots (x+\lambda_1-1) = x^n.$$

For  $x = 1$ , we have

$$\sum_{\lambda_1=1}^n (-1)^{n-\lambda_1} \left\{ \begin{smallmatrix} n \\ \lambda_1 \end{smallmatrix} \right\} \lambda_1! = 1,$$

hence the right-hand side of (1) is  $1/n!$  and we are done.

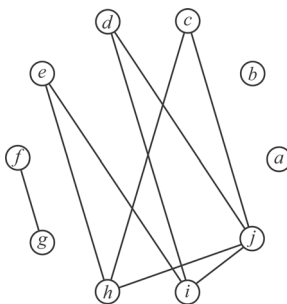
*Also solved by Albert Stadler (Switzerland) and the proposer.*

## A graph involving a partition of 100 into ten parts

June 2021

**2125.** *Proposed by Freddy Barrera, Colombia Aprendiendo, and Bernardo Recamán, Universidad Sergio Arboleda, Bogotá, Colombia.*

Given a collection of positive integers, not necessarily distinct, a graph is formed as follows. The vertices are these integers and two vertices are connected if and only if they have a common divisor greater than 1. Find an assignment of ten positive integers totaling 100 that results in the graph shown below.



*Solution by Eagle Problem Solvers, Georgia Southern University, Statesboro, GA and Savannah, GA.*

With the labeling above,

$$(a, b, c, d, e, f, g, h, i, j) = (1, 1, 7, 9, 10, 11, 11, 14, 15, 21)$$

is a solution. Note that each of  $e$ ,  $h$ ,  $i$ , and  $j$  must have at least two prime divisors, since each is adjacent to two vertices that are not adjacent to each other. The simplest option is  $e = pq$ ,  $h = qr$ ,  $i = rs$ , and  $j = ps$  with  $p, q, r$ , and  $s$  prime. Assuming  $\{p, q, r, s\} = \{2, 3, 5, 7\}$ , the vertices  $e$ ,  $h$ ,  $i$ , and  $j$  must consist of two of the three pairs  $(6, 35)$ ,  $(10, 21)$ , and  $(14, 15)$ . The possibility with the smallest sum is  $\{e, h, i, j\} = \{10, 14, 15, 21\}$ . If we take  $a = b = 1$  and  $f = g = 11$ , this forces  $c + d = 16$ . Assuming that  $c$  and  $d$  are powers of distinct primes from  $\{2, 3, 5, 7\}$ , we must have  $(c, d) = (7, 9)$  or  $(c, d) = (9, 7)$ . The former forces  $(e, h, i, j) = (10, 14, 15, 21)$ , which yields the solution above. The latter gives a solution with  $(e, h, i, j) = (10, 15, 14, 21)$ .

A more detailed analysis shows that, in fact, these are the only solutions.

*Also solved by Brian D. Beasley, Elton Bojaxhiu (Germany) & Enkel Hysnelaj (Australia), Dmitry Fleischman, George Washington University Problems Group, Kelly D. McLenithan & Stephen C. Mortenson, Lane Nielsen, José Heber Nieto (Venezuela), Didier Pinchon (France), Randy K. Schwartz, Albert Stadler (Switzerland), and the proposers.*

## Answers

*Solutions to the Quickies from page 243.*

**A1121.** More generally, we will evaluate

$$\sum_{n=0}^{\infty} \frac{a_n b_n}{c^n (a_n^2 + b_n^2)},$$

where  $a_n, b_n, c, \alpha$ , and  $\beta$  are real,  $|c| > 1$ , and

$$a_n + b_n i = (\alpha + \beta i)^n.$$

Note that

$$a_n^2 + b_n^2 = (a_n + b_n i)(a_n - b_n i) = (\alpha + \beta i)^n (\alpha - \beta i)^n = (\alpha^2 + \beta^2)^n,$$

and

$$a_n b_n = \frac{1}{2} \operatorname{Im}((a_n + b_n i)^2) = \frac{1}{2} \operatorname{Im}((\alpha + \beta i)^{2n}).$$

Since

$$\left| \frac{(\alpha + \beta i)^2}{c(\alpha^2 + \beta^2)} \right| = \frac{1}{|c|} < 1,$$

we have

$$\begin{aligned} \sum_{n=0}^{\infty} \frac{a_n b_n}{c^n (a_n^2 + b_n^2)} &= \frac{1}{2} \operatorname{Im} \left( \sum_{n=0}^{\infty} \left( \frac{(\alpha + \beta i)^2}{c(\alpha^2 + \beta^2)} \right)^n \right) \\ &= \frac{1}{2} \operatorname{Im} \left( \frac{1}{1 - \frac{(\alpha + \beta i)^2}{c(\alpha^2 + \beta^2)}} \right) \text{ (geometric series)} \\ &= \frac{1}{2} \operatorname{Im} \left( \frac{c(\alpha^2 + \beta^2)}{c(\alpha^2 + \beta^2) - (\alpha^2 - \beta^2) - 2\alpha\beta i} \right) \\ &= \frac{1}{2} \left( \frac{c(\alpha^2 + \beta^2)2\alpha\beta}{(c(\alpha^2 + \beta^2) - (\alpha^2 - \beta^2))^2 + 4\alpha^2\beta^2} \right) \\ &= \frac{c(\alpha^2 + \beta^2)\alpha\beta}{c^2(\alpha^2 + \beta^2)^2 - 2c(\alpha^2 + \beta^2)(\alpha^2 - \beta^2) + (\alpha^2 + \beta^2)^2} \\ &= \frac{c\alpha\beta}{c^2(\alpha^2 + \beta^2) - 2c(\alpha^2 - \beta^2) + (\alpha^2 + \beta^2)} \\ &= \frac{c\alpha\beta}{(c-1)^2\alpha^2 + (c+1)^2\beta^2} \end{aligned}$$

For the original problem,  $(\alpha, \beta, c) = (2, 1, 2)$  and the series sums to  $4/13$ .

**A1122.** Since the angle sum of a triangle is  $180^\circ$ , the middle angle must have measure  $60^\circ$ . By the law of cosines, we have

$$a^2 + b^2 - ab = c^2.$$

Dividing by  $c^2$ , we have

$$x^2 - xy + y^2 = 1$$

with  $x, y \in \mathbb{Q}$ . The point  $(1, 0)$  is clearly on this curve. The equation of a line with slope  $m$  passing through the point is  $y = mx + 1$ . We know that this line meets the conic section above in  $(1, 0)$  and find that the other point of intersection is

$$(x, y) = \left( \frac{1 - 2m}{1 - m + m^2}, \frac{1 - m^2}{1 - m + m^2} \right).$$

Taking relatively prime positive integers  $p$  and  $q$  with  $2p < q$ , letting  $m = p/q$ , and clearing denominators gives

$$a = q(q - 2p), b = q^2 - p^2, c = p^2 - pq + q^2$$

as solutions.



---

# REVIEWS

---

PAUL J. CAMPBELL, *Editor*  
Beloit College

*Assistant Editor: Eric S. Rosenthal, West Orange, NJ. Articles, books, and other materials are selected for this section to call attention to interesting mathematical exposition that occurs outside the mainstream of mathematics literature. Readers are invited to suggest items for review to the editors.*

Popko, Edward S., and Christopher J. Kitrick, *Divided Spheres: Geodesics & the Orderly Subdivision of the Sphere*, 2nd ed., CRC Press, 2021; xxx + 454 pp, \$120, \$102(E). ISBN 978-0-367-68003-9, 978-1-00313411-4

This is a fascinating and beautiful book on a narrow topic (spherical geometry) of widespread appeal and application. Naturally, the book harks back to R. Buckminster Fuller's geodesic domes and the 31 great circles of a spherical icosahedron; the main author is an architect. But spherical design occurs also in pollen grains, viruses, maps, fish pens, and implementations of puzzles similar to Rubik's Cube. It turns out that it is not easy to distribute points evenly on a sphere! Applications include locations of cellphone towers, orbits of satellites, golf balls (there is a whole chapter on them), and pharmaceuticals. The book develops six schemas for subdividing a sphere and offers comparisons for different purposes. Other chapters present basic spherical geometry and grids on spheres. Appendices treat at length stereographic projection, coordinate rotations via matrices, and geodesic math. Almost every page contains a figure or illustration, many of them in color.

Brooks, Michael, *The Art of More: How Mathematics Created Civilization*, Pantheon, 2021; vii + 321 pp, \$28. ISBN 978-1-5247-4899-9.

The title is uninspiring, but the subtitle is arresting! Some will scoff at the latter, as well as at author Brooks's assertion that "our skill with numbers is the greatest human achievement of all." Nevertheless, Brooks makes cases for many branches of mathematics: arithmetic (bookkeeping and accounting as a key to government, finance, and trade); geometry (navigation, cartography, architecture, perspective drawing); algebra (gunnery, particle physics, the PageRank algorithm); calculus (optimization, engineering, aviation, models for diseases); logarithms (calculation, exponential growth); imaginary numbers (AC circuits, quantum theory); statistics (separating out causes, quantifying uncertainty, streaming videos and music); and information theory (error correction in communications, encryption, 5G phone signals). Even a reader who is not convinced of the claim of the subtitle will agree with Brooks's conclusion that mathematics is a "many-splendored thing."

Rosenthal, Daniel, and Jeffrey S. Rosenthal, Optimal strategies and the game of Horse, *Notices of the American Mathematical Society* (to appear June/July 2022), <https://arxiv.org/abs/2201.06560>.

In the game of Horse, two players alternate taking basketball shots, each trying a shot attempted by the other. The authors point out that traditional rules give a further advantage to the better player, if that player plays first and attempts an easy shot. The authors suggest a slight change in the rules that should result in attempting more-difficult shots.

Bollman, Mark, *Mathematics of the Big Four Casino Table Games: Blackjack, Baccarat, Craps, & Roulette*, CRC Press, 2022; xi 352 pp, \$89.95, \$34.95(P), \$29.70(E). ISBN 978-0-367-74229-4, 978-0-367-74090-0, 978-1-00315668-0.

After a brief introduction to elementary probability, this book explores many more variations on the "big four" than I could have imagined to exist, plus numerous side bets. Examples and exercises abound throughout.

Kalajdzievski, Sasho, *Math and Art*, 2nd ed., CRC Press, 2022; xii + 386 pp, \$170, \$69.95(P), \$59.45(E). ISBN 978-0-367-07613-9, 978-0-367-07611-5, 978-0-429-02160-2.

There are many books about mathematics and art; this one distinguishes itself as an “unorthodox geometry textbook,” with exercises and fun art projects. The book is based on 20 years of offering a course to more than 10,000 students. It stops short of covering some of the mathematics (groups are mentioned but not defined), though one theorem (classification of similarities) is proved in an appendix. Topics are Euclidean geometry, transformations of the plane, similarities and fractals, hyperbolic geometry, perspective, three-dimensional objects, and topology. The book averages two figures per page, with many utterly beautiful in color. You might be surprised at the sophisticated mathematical content of some crop circles (no doubt made by aliens!), and amazed by some of the illustrations of artworks.

Chartier, Tim, *X-Games in Mathematics: Sports Training that Counts!*, World Scientific, 2021; xviii + 234 pp, \$78, \$38(P), \$30(E). ISBN 978-981-122-383-9 978-981-122-487-4, 978-981-122-385-3.

Sports analytics is the rage among fans, players, coaches, and managers. Author Chartier surveys instances of use of analytics in various sports, with a light touch. He uses the occasions to bring up various topics in mathematics itself, such as puzzles, the birthday paradox, math mosaics, and cryptology. There are lots of interesting sports tidbits. However, there is actually more mathematics in the book than sports analytics; but don’t let prospective readers know!

Poirrer, Laurent, Wordle-solving state of the art: All optimality results so far, <https://www.poirrer.ca/notes/wordle-optimal/>.

Wordle is a game in which you try to guess a five-letter “English” word, using feedback hints (the dictionaries of target words and possible guesses can vary, hence the quotation marks). In spirit, it resembles the older puzzle Mastermind. Author Poirrer summarizes, for the standard dictionaries, what is known about the minimal number of guesses. Other authors have suggested optimal starting guesses (e.g., “stern” or “tares”) and particular strategies that can vary with the dictionaries used.

Broad, William J., The Texas oil heir who took on math’s impossible dare, *New York Times* (1 February 2022) D1. <https://www.nytimes.com/2022/01/31/science/james-vaughn-fermat-theorem.html>.

This article details the role of James M. Vaughn, Jr., in bankrolling efforts to prove Fermat’s Last Theorem. That successful campaign raises the question: Would the million dollars offered by the Clay Mathematics Institute for solving one of its Millennium Prize Problems be more likely to promote success if it were invested beforehand—funding researchers and conferences—instead of rewarding the final winner?

Roberts, Siobhan, The godmother of the digital image, *New York Times Magazine* (14 September 2021), <https://www.nytimes.com/2021/09/14/magazine/ingrid-daubechies.html>.

This article is a tribute to Ingrid Daubechies, a pioneer of wavelets. It recounts her history and her recent involvement in the conservation of the Ghent Altarpiece panels. It characterizes her major contribution as finding a way to make wavelets practical and easy to implement on a computer, but it also explores her insecurities and chronic depression (which she openly discusses).

Nolan, Deborah, and Sara Stoudt, *Communicating with Data: The Art of Writing for Data Science*, Oxford University Press, 2021; ix + 331 pp, \$45.95(P). ISBN 978-0-19-886275-8.

College departments of mathematics and computer science have been feverishly developing tracks in data science. This book about technical writing is particularly suitable (and necessary) for students in data science, or in any mathematical science. It begins with chapters on how to read technical articles, science news stories, and press releases (“examine the argument”); continues with chapters on how to describe and present data and code; advises how to get started writing (“who is the audience?”); and emphasizes the importance of editing and revising. A concluding chapter offers 22 imaginative exercises.